//

BNWL-2058
UC-80

Impact of a Hanford Nuclear Energy Center on Ground Level Fog and Humidity

by
J. V. Ramsdell
Atmospheric Sciences Department

March 1977

Prepared for the Energy Research and Development Administration under Contract EY-76-C-06-1830

Battelle
Pacific Northwest Laboratories

BNWL-2058

NOTICE

This report was prepared as an account of work sponsored by the United States Government. Neither the United States nor the Energy Research and Development Administration, nor any of their employees, nor any of their contractors, subcontractors, or their employees, makes any warranty, express or implied, or assumes any legal liability or responsibility for the accuracy, completeness or usefulness of any information, apparatus, product or process disclosed, or represents that its use would not infringe privately owned rights.

PACIFIC NORTHWEST LABORATORY
operated by
BATTELLE
for the
ENERGY RESEARCH AND DEVELOPMENT ADMINISTRATION
Under Contract EY-76-C-06-1830

Printed in the United States of America
Available from
National Technical Information Service
U.S. Department of Commerce
5285 Port Royal Road
Springfield, Virginia 22151
Price: Printed Copy $_____*; Microfiche $3.00

*Pages	NTIS Selling Price
001-025	$4.50
026-050	$5.00
051-075	$5.50
076-100	$6.00
101-125	$6.50
126-150	$7.00
151-175	$7.75
176-200	$8.50
201-225	$8.75
226-250	$9.00
251-275	$10.00
276-300	$10.25

ERDA-RL RICHLAND, WA

BNWL-2058

3 3679 00062 4884

IMPACT OF A HANFORD NUCLEAR ENERGY CENTER ON GROUND LEVEL FOG AND HUMIDITY

by
J. V. Ramsdell
Atmospheric Sciences Department

March 1977

BATTELLE
Pacific Northwest Laboratories
Richland, Washington 99352

CONTENTS

TABLES iii
FIGURES iv
INTRODUCTION 1
ATMOSPHERIC MODEL 6
Main Program BATMAN 8
Subroutine PRISE 11
Subroutine RCPTOR 12
Subroutine SIGMAZ 14
Subroutine DIFFUSE 16
Model Output 19
Output Interpretation 24
THE HNEC MODEL 27
Cluster Locations 28
Cooling System Models 30
Heat Sink Management Simulations 32
THE HANFORD CLIMATE 36
General Climatology 36
Diffusion Climatology 49
HNEC SIMULATION RESULTS 52
The Predicted Increase in Hours of Fog 55
The Influence of Site Location on Fog Increases 57
The Influence of Cooling System Type on Fog Increases . 58
The Reduction of Visibility in the Tri-Cities 61
The Statistical Significance of the Predicted Increases 62
The Impact on Summer Humidity 66
CONCLUSIONS 70
REFERENCES 72
APPENDIX A - BATMAN USER'S GUIDE AND COMPUTER CODE A-1

TABLES

1 Relationships Between σ_z, Atmospheric Stability and Distance Between the Receptor and Virtual Point Source. 16

2 Positions of the 4 Reactor Clusters for the HNEC Simulations. 30

3 Characteristic Cooling System Dimensions. 33

4 Cooling System Thermal Characteristics. 33

5 Site and Cooling System Combinations Simulated. . . . 35

6 Averages and Extremes of Climatic Elements at Hanford. 38

7 Total Duration and Maximum Persistence of Fog Tabulated in Hours for Hanford for the Period 1945-1970 46

8 Joint Probability of Wind Direction, Wind Speed and Atmospheric Stability at 200' for Hanford 51

9 Predicted Increases in Hours of Fog in Selected Areas 56

10 Predicted Increases in Hours of Reduced Visibility in the Tri-Cities 63

11 Predicted Fog Conditions in the Tri-Cities with an HNEC (Current Conditions + Predicted Increases). . 64

12 Minimum Statistically Significant Increases in Fog in the Tri-Cities 66

FIGURES

1 The Hanford Reservation Location. 3

2 Plume Source and Receptor Geometry. 13

3 Sigma Z Curves. 15

4 Sample Computer Output of Increased Water Vapor Density (1 Cluster) 20

5 Sample Computer Output of Increased Water Vapor Density (5 Clusters). 21

6 Sample Computer Output of Increased Hours of Water Vapor Density Exceeding a Fixed Value (1 g/m^3). 23

7 Sample Computer Output for Predicted Increase in Hours of Saturation (Fog). 25

8 Relationship Between Relative Humidity Increase and Temperature for an Increase in Water Vapor Density of 1 g/m^3 26

9 The HNEC Cluster Locations in the BATMAN Grid System. 29

10 The Diurnal Cycles of Temperature, Relative Humidity and Wind Speed for January at Hanford 40

11 The Diurnal Cycles of Temperature, Relative Humidity and Wind Speed for July at Hanford. 41

12 The Diurnal and Annual Variation of Average Saturation Deficit (g/m^3) at Hanford. 43

13 Cumulative Frequency Distributions for Saturation Deficits at Hanford 44

14 Percent Probability of Exceeding a Given Number of Hours of Fog at Hanford. 47

15 Cumulative Frequency Distributions for Visibility During Fog at Hanford 48

16 Wind Roses by Atmospheric Stability for Hanford . . . 50

FIGURES (cont'd)

17 Surface Wind Roses for Various Locations on and Surrounding the Hanford Site. (The points of the rose represent the directions from which the winds come) 53

18 Wind Roses for the FFTF and WNP-2 Sites. 54

19 Relationship Between Increased Hours of Fog for an HNEC Using Hybrid Wet/Dry Cooling Systems and the Percent Wet Cooling. 60

20 Hours of Water Vapor Density Increase Exceeding 1 g/m^3 During Summer Months for a Single Cluster at Hanford 67

21 Hours of Water Vapor Density Increase Exceeding 1 g/m^3 During Summer Months for a 20 Reactor Energy Center at Hanford. 68

22 Hours of Water Vapor Density Increase Exceeding 1 g/m^3 During Summer Months for a 40 Reactor Energy Center at Hanford. 69

A1 Input Statements and Formats for BATMAN. A-2

A2 A Sample Input Data Deck for Computation of Increases in Water Vapor Density A-6

A3 A Sample Input Data Deck for Computation of Increases in Fog A-7

A4 BATMAN Computer Code A-11

IMPACT OF A HANFORD NUCLEAR ENERGY CENTER ON GROUND LEVEL FOG AND HUMIDITY

INTRODUCTION

Battelle, Pacific Northwest Laboratory is currently involved in the evaluation of the nuclear energy center concept as it might be applied to development of the Energy Research and Development Administration's Hanford Reservation. In that study a number of subjects have been examined in detail and the results presented in technical reports[1-4]; the over-all results have been summarized in an interim report[5]. During the past year the examination of various heat sink management options has continued in greater depth. The results of this work are contained in Selection of Heat Disposal Methods for a Hanford Nuclear Energy Center[6]. This document presents the details of a study of the atmospheric impacts of an Hanford Nuclear Energy Center (HNEC) that might result from the use of evaporative cooling alternatives. Specific cooling systems considered include once-through river cooling, cooling ponds, cooling towers, helper cooling ponds and towers and hybrid wet/dry cooling towers. The specific impacts evaluated are increases in fog and relative humidity.

The energy center concept generally involves the grouping of 10 to 40 power plants on a common site. The center may contain supporting fuel cycle facilities, however the major heat releases and atmospheric effects are expected to be associated directly with power generation. A summary of the postulated atmospheric effects of heat rejection from nuclear energy centers is presented in Reference 7. These effects have been postulated on the basis of theory, models, analogy and speculation. Unfortunately some of the more spectacular

effects are primarily the result of the last two processes. While a complete listing is not particularly important here, typical effects include: increases in humidity, cloudiness and fog, enhancement of precipitation and modification of precipitation patterns, triggering of severe weather such as thunderstorms, and the concentration of vorticity resulting in the formation of large dust devils.

The specific atmospheric effects which might be associated with a particular energy center are generally related to the form of heat rejection, the flux density and area of heat rejection, and the climate of the energy center site. For example fog and humidity increases are associated with low level wet cooling systems, while more spectacular effects such as concentration of vorticity are postulated for closely spaced cooling systems with a high energy flux.

The conceptual center being evaluated for Hanford (HNEC), which is located in South-central Washington State is shown in Figure 1, consists of 20 to 40 power plants with associated switching and transmission facilities, a fuel fabrication plant, two fuel reprocessing plants and a waste storage facility[5]. Each of the reactors is assumed to be rated at 1250 MW_e, so that total heat rejection from a 40 reactor energy center is approximately 10^5 MW. Specific locations for the individual power plants have not been established, however it has been assumed that they will be grouped in clusters of 4 with each cluster covering approximately 1 sq. mi. Preliminary site evaluation indicates that the total area covered by the energy center will be between 100 and 300 sq. mi. with the larger value representing the full 40 reactor case. These values are in contrast to the 75 sq. mi. assumed for 40 reactor nuclear energy centers in the NECSS study.

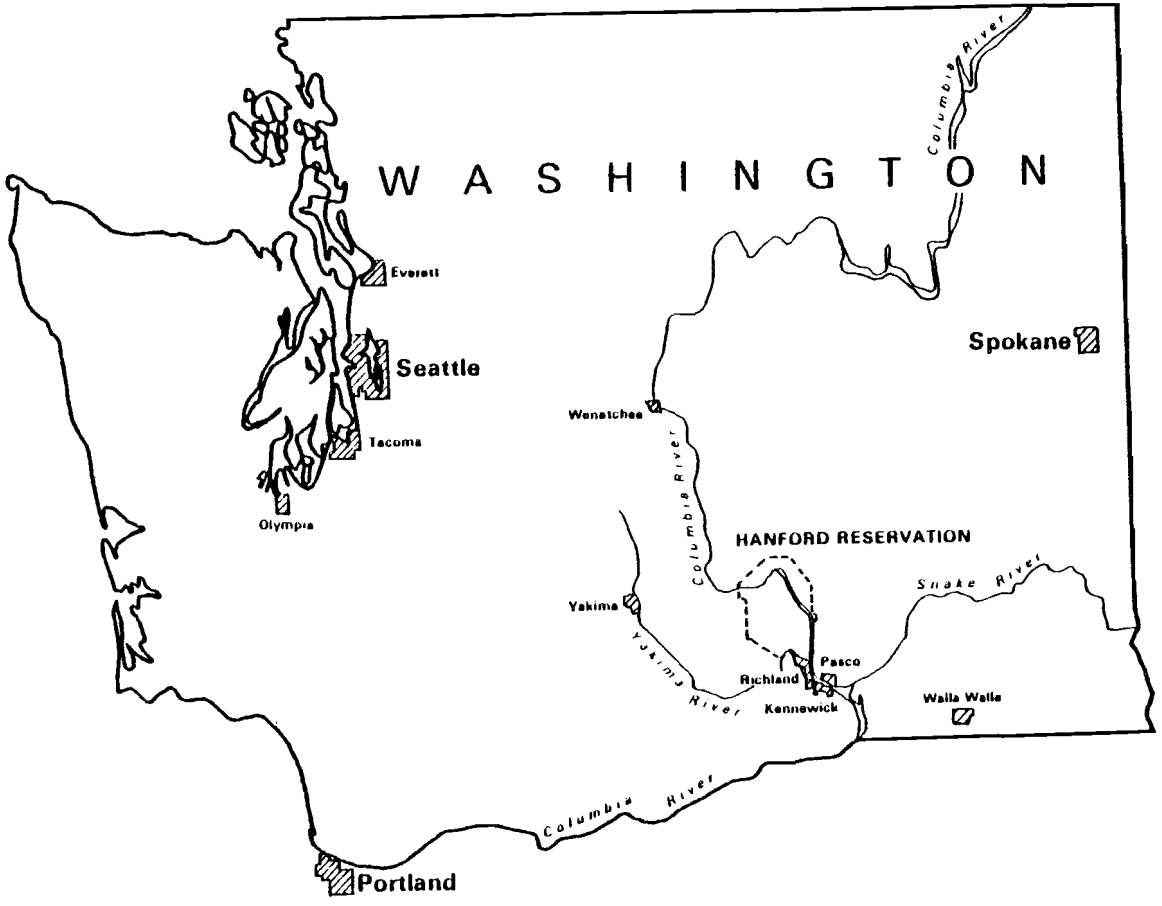

FIGURE 1. The Hanford Reservation Location

A preliminary study of heat sink management for the HNEC[4] has indicated that, from an engineering standpoint, a variety of cooling systems are potentially suitable for handling the heat dissipation. These systems range from once through cooling to dry cooling towers and include several hybrid systems. The selection of the cooling system mix to be assumed in evaluation of the HNEC concept has been a matter of some concern along with selection of specific locations for the clusters. An attempt has been made to resolve both issues through the development of a comprehensive heat sink management plan that would result in the most favorable balance between resource utilization, economics and environmental impact. In this effort it has been necessary to evaluate the effects of heat dissipation so that their significance could be rationally assessed.

Rational evaluation of the significance of any effect of heat rejection requires that the extent and timing of the effect be estimated quantitatively, and that significance be defined in meaningful terms. Each of the effects postulated in the NECSS report[7] has been considered in a cursory manner to screen out improbable impacts and those which can not be adequately evaluated at this time.

Concentration of vorticity has been related to high density of the rejected heat and relatively large areas. This was a major concern for the energy centers considered in the NECSS where the flux density was about .5 KW/M^2. The flux density for the HNEC would be between .1 and .3 KW/M^2. There are no simple methods for quantifying the frequency, magnitude or effect of vortices which might be generated. As a result, detailed consideration of vorticity concentration has been postponed until better tools are developed.

The status with respect to modification of precipitation patterns and the triggering of storms is somewhat better. Theory and numerical models exist which can provide insight into these postulated effects. Several investigators are currently pursuing this avenue of research. When suitable results are achieved they will be applied to HNEC, although recently publicized problems in the National Hail Research Experiment[8] raise questions about the reliability of quantitative estimates in this area.

The only atmospheric effects that are most amenable to treatment at this time are those associated with the addition of moisture to atmosphere. Even in this case the treatment is semi-quantitative at best. The effects of cooling systems on fog and humidity are the atmospheric impacts of heat rejection that have been used in selection of a overall HNEC heat sink management plan.

At the outset of the evaluation it was assumed that the addition of heat and moisture were not, in themselves, significant. Similarly it was assumed that a postulated small change in any naturally occurring atmospheric phenomenon would not be significant. Rather, significance must be achieved by meeting some specific criteria. Four possible areas for criteria have been identified. These include: a statistically significant change in a meteorological variable, substantial adverse economic impact of a postulated change, initiation of an ecological change, and adverse public reaction. The criteria other than that of statistical significance are still not satisfactorily defined, but the general areas provide guidance on the detail required in specification of a postulated impact.

ATMOSPHERIC MODEL

The introductory remarks above contain the seeds of the atmospheric modeling requirements for input to selection of an optimum heat sink management scheme. The number of combinations of reactor locations and cooling systems, plus the need to evaluate each combination under a variety of meteorological conditions indicate that a flexible, inexpensive model be used in the evaluation. Further the need to differentiate between the atmospheric impacts of various cooling system mixes indicates that the model should be as realistic and as sensitive to differences between cooling systems as possible.

With these requirements as a background, BATMAN a Battelle Atmospheric Management computer code was developed. Specifically the code was designed to assist in the selection of viable heat sink management options for the HNEC by providing estimates of the impact of evaporative cooling systems. To accomplish this objective, the code is capable of computing the diffusion of moisture released in the cooling of 1 to 20 arbitrarily placed reactor clusters. The number of reactors in each cluster is limited only in the sense that all reactors in the cluster must utilize the same type cooling system. A mixture of cooling systems within a cluster can be simulated by superpositioning 2 or more clusters with different systems. In reality, BATMAN is a computer code that provides "back of the envelope", computations for up to 20 simultaneous energy releases and 144 receptor locations.

The economy and flexibility needed to examine the many possible HNEC scenarios are incorporated in BATMAN through the use of climatological data input and a modified sector-averaged Gaussian plume diffusion model. Reactor cluster locations and cooling system emission characteristics are input at the time of program execution. The cluster locations

are identified with respect to a receptor grid; it is not necessary that they be on the grid. The receptor grid is a 12x12 matrix of surface points for which increases in water vapor density are computed. This increase may be computed at several levels above the surface for each grid point, if desired. The spacing between grid points may be adjusted with the north-south spacing independent of the east-west spacing.

Currently BATMAN can be run in two modes. In the first mode a specific scenario is examined (i.e., a fixed set of reactor clusters, a specified wind direction and speed, and a single atmospheric stability). BATMAN then provides estimates of increased density of atmospheric water vapor. An estimate of the frequency of occurrence of the scenario can be made if sufficient climatological information is available. The second mode uses climatological input in the form of a joint frequency distribution of occurrence of wind speed, wind direction and atmospheric stability. The number of hours per year that increases in vapor density can be expected to fall within selected ranges is estimated. If additional climatological data on the frequency of occurrence of saturation deficits (in terms of vapor density) are available, BATMAN can produce direct estimates of the increase in hours of fog at each receptor location.

Economy of operation of BATMAN is enhanced by computing diffusion estimates only if a receptor is in the plume from a given cluster. After all receptor locations are considered for one cluster the process is repeated for successive clusters until all have been treated. The change in water vapor density at each receptor location is the sum of the contributions from all clusters.

In the following sections the details and features of BATMAN are described. The computer code and a short users guide are presented in Appendix A at the end of this document.

Main Program BATMAN

BATMAN performs the typical function of a main program. It controls the flow of information by handling input and output, and by calling subroutines which perform most of the actual computations. In addition to these functions BATMAN computes the source term for each reactor cluster, determines the appropriate virtual source as a function of wind direction, and combines the results of the individual cluster impacts to estimate the impact of the energy center.

The moisture source term is determined from input data on number of reactors in a cluster, rates electrical power output and cooling system type. Additional inputs required in the source term evaluation are overall thermal efficiency of the power plant and the fraction of the waste heat which is rejected in the latent form. The remaining waste heat is assumed to be sensible (increased temperature). Radiative heat transfer is neglected. The total latent heat release is then used to compute a rate of evaporation. The thermal efficiencies and latent heat fraction are functions of cooling system type and atmospheric conditions. The relationships between efficiency and atmospheric conditions are summarily treated by use of seasonal or annual values. More detailed treatment of these relationships is not warranted because of the nature of the basic model.

The fundamental climatological data input to BATMAN consists of information on wind direction, wind speed, atmospheric stability, temperature, plume width and mixing depths. With these data and a moisture source term the model can compute

increases in water vapor density and the frequency of occurrence of increases within specified ranges. If the model is to convert the water vapor increase to frequency of occurrence of fog, additional climatological input is required. This information includes the number of hours being considered and the distribution of water vapor saturation deficits.

Wind direction must be specified in terms of sectors starting with sector 1 as the first sector east of north and increasing in a clockwise direction. The number of sectors is limited only by dimensions of the program. Currently the program is set for 16 sectors. Calm and variable winds should be distributed among the sectors. The distribution of these winds in proportion to the frequency of occurrence of directions during the remainder of the time should be conservative.

As with wind direction, the number of wind speed categories is limited by the program dimensions. The limitation is on the product of wind speed and direction classes and is currently set at 96. Thus, with 16 wind direction sectors, the number of wind speed classes is limited to 6.

The limitation on the product can easily be increased to accommodate more wind direction and/or speed classes. However, an increase in the number of classes rapidly increases computer storage requirements. For instance, increasing the number of direction classes to 36 and speed classes to 10 would increase storage requirements by almost 3200 words.

BATMAN will accept atmospheric stability data in the 4 category Hanford stability classification scheme or in either the 6 or 7 category Pasquill-Gifford scheme[9]. The stability classification scheme is specified by indicating the number of categories, with categories numbered in order of increasing stability.

A temperature input is required for plume rise computations if cooling towers are specified in the source description. The model is not particularly sensitive to the temperature input, therefore, a seasonal or annual average is adequate.

The diffusion model is used in a sector-averaged model, thus it is necessary to define the width of the sector occupied by the plume. There are no mathematical restrictions on the width of this sector, however, common sense would indicate that it should be at least as wide as the wind direction sectors.

The final climatological input required in all modes of operation for BATMAN is the sepcification of a mixing depth. The mixing depth is the upper limit to the vertical spread of the moisture plumes. As moisture reaches this level, it is reflected. If the mixing level is specified as zero, vertical diffusion of the plumes is unbounded.

Additional climatological data on the water vapor saturation deficit must be provided if the frequency of occurrence of fog is to be computed. This information is the expected number of hours of saturation deficit within ranges which may be specified. The model is currently limited to 10 ranges, but again that limit can be increased if necessary.

Finally, it is necessary to specify several physical parameters in addition to the source term, and climatology. These parameters include the grid spacing; the number of levels of interest and their heights; the type cooling systems, their dimensions and release heights, and a critical wind speed if cooling towers are specified. The critical wind speed is used in conjunction with ambient wind speed to determine when plume rise should be limited by downwash and when building wake effects should be considered.

The number of levels which can be considered is limited to a maximum of 10, but is also limited by the number of saturation deficit classes. The product of saturation deficit classes and levels must be less than 20. The grid spacing is restricted only by the cooling system dimensions. The model is not meant for a fine scale examination of effects near the sources. Thus the grid spacing should be larger than the characteristic horizontal dimensions of the cooling system. North-south and east-west grid spacings need not be the same.

Subroutine PRISE

Subroutine PRISE computes the plume rise for cooling tower releases. Prior to calling PRISE, BATMAN checks the wind speed. If the wind speed is equal to or greater than the critical speed, the plume rise is assumed to be zero and the effective release height is set equal to the actual release height. Otherwise, PRISE is called and the plume rise is computed. Following the plume rise computation the effective release height is determined. If it is above the mixing layer and the actual release height is below the lid, plume rise is reduced to make the effective release height equal to the top of the mixing layer.

Computation of plume rise is based on Briggs' formulae for final plume rise[10]. In these formulae, plume rise is a function of the sensible heat flux, the wind speed, atmospheric stability, atmospheric temperature and actual release height. The formulae do not account for latent heat flux, which in cooling towers may be several times the sensible heat flux. As a cooling tower plume condenses this latent heat contributes to additional plume rise. Therefore, provision has been made for inclusion of a latent heat correction factor.

In these formulae it is not appropriate to allow the wind speed to approach zero too closely. Thus, for wind speeds less than 1 m/s, the following assumptions were made: for stable atmospheric conditions the calm formulation was used, and for neutral and unstable conditions the wind speed was assumed to be 0.5 m/s.

The use of final plume rise formulae reduced the number of required plume use computations and is generally justifiable because of coarse grid spacing. Had plume rise been treated as a function of distance from the source the number of plume rise computations would have been several times as large.

Subroutine RCPTOR

The function of subroutine RCPTOR is to determine whether a receptor is within the plume from a cluster or not, and if it is to determine the distance from the virtual point source to the receptor.

The problem solved by RCPTOR is shown schematically in Figure 2. Position A is the location of the cooling system which is specified in the cooling system description along with a typical horizontal dimension for the system. Position B is the virtual point source. It is computed from the cooling system width, the angular width of the plume and the wind direction. The distance between A and B is constant once the source and plume widths are specified. Position C is a known point in the grid. Thus the positions of three vertices of a triangle are known.

From this information the remaining sides of the triangle, the distances between the actual and virtual sources and the receptor, can be computed. If the distance between the virtual source and the receptor is less than either of the other sides of the triangle, the receptor is not in the plume

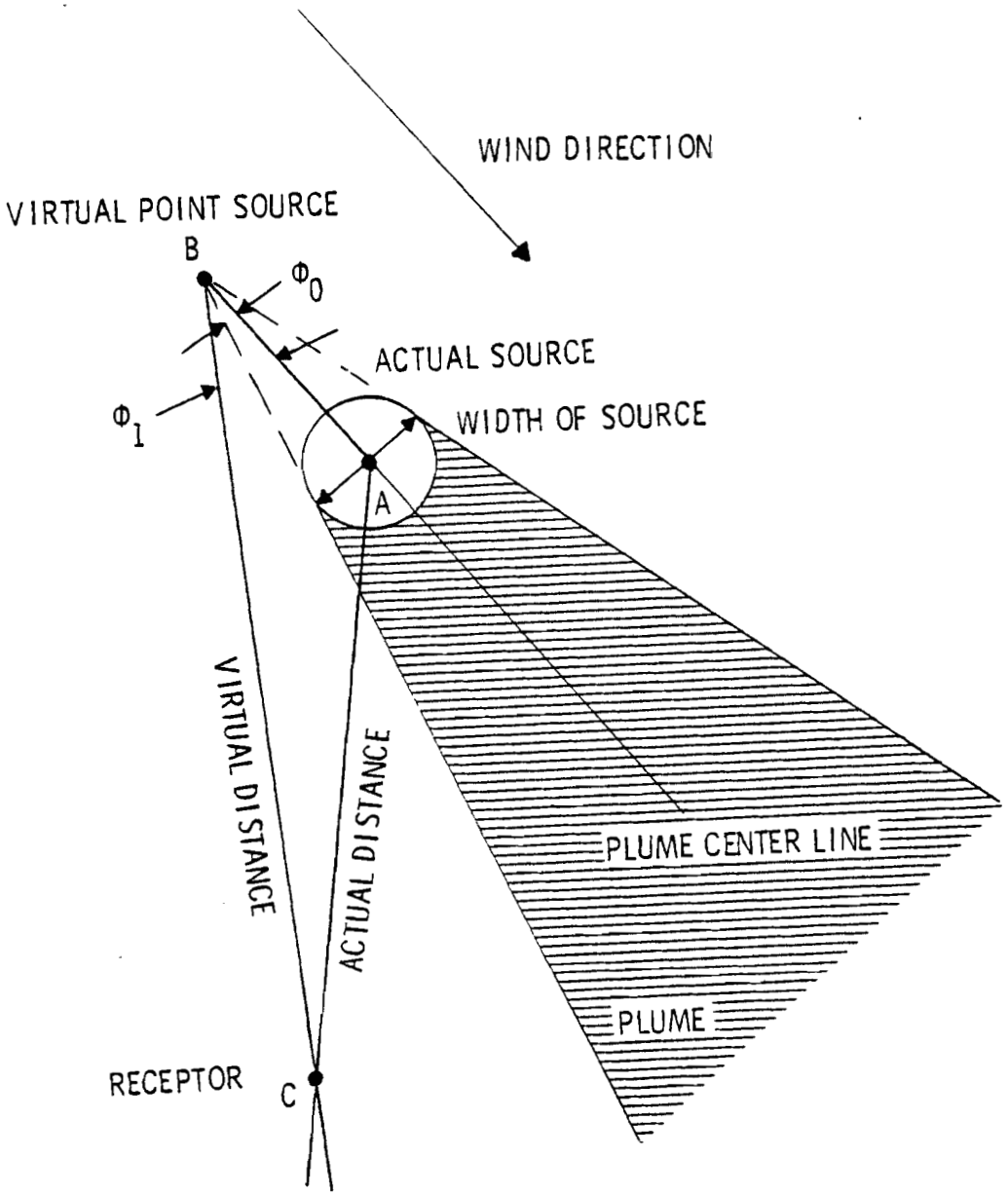

FIGURE 2. Plume Source and Receptor Geometry

and RCPTOR returns to the main program to start consideration of the next receptor. If this virtual distance is the longest side of the triangle, the angle at B, labeled ϕ_1 is compared with 1/2 the plume angular width, ϕ_o. When ϕ_1 is less than or equal to ϕ_o, RCPTOR initiates the diffusion computation. Otherwise the return from RCPTOR initiates consideration of the next receptor.

Subroutine SIGMAZ

The first step in the diffusion computation is the computation of the vertical dispersion parameter σ_z. Under normal conditions σ_z is a function of atmospheric stability and distance from the source. In BATMAN the distance between the receptor and virtual point source is used. When wind speeds are above the critical wind speed and low-level mechanical draft cooling towers are used, the value of σ_z is corrected for wake effects.

The basic formulations used for the relationships between stability, distance and σ_z are those suggested by Briggs[11]. A seventh relationship has been added to treat the Pasquill-Gifford G stability class. The relationships are given in Table 1 and shown in Figure 3. Table 1 also serves to show the relationship between the Pasquill-Gifford and Hanford stability classes. The existence of the G stability class is in doubt and is currently an issue receiving attention.

Plumes from low-level, mechanical draft cooling towers are assumed to downwash and enter the wake behind the tower when the wind speed exceeds the critical speed. In these cases, the plume undergoes a rapid initial vertical dispersion due to the cooling tower wake. This effect is accounted for in subroutine SIGMAZ.

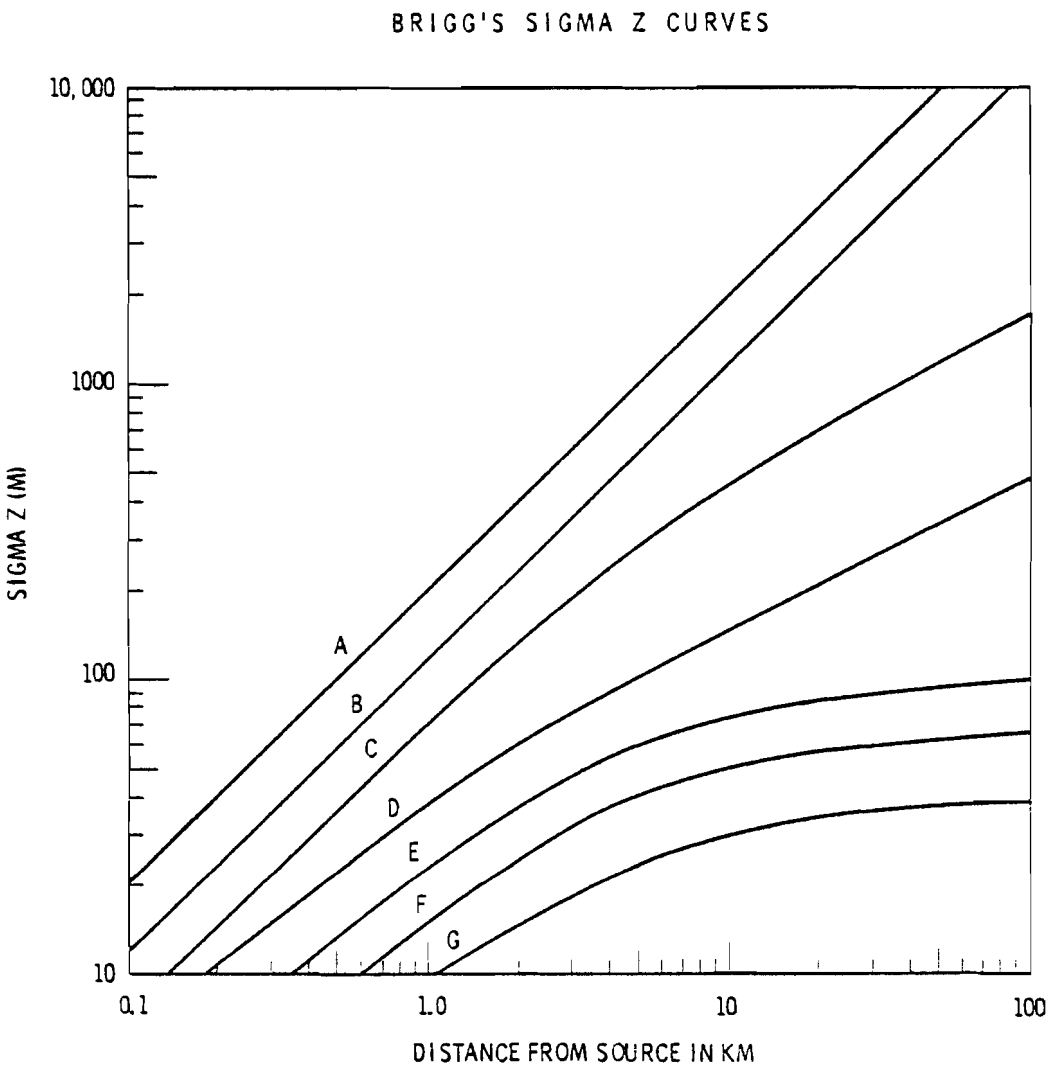

FIGURE 3. Sigma Z Curves

TABLE 1. Relationships Between σ_z, Atmospheric Stability and Distance Between the Receptor and Virtual Point Source

Stability Class		σ_z
Pasquill-Gifford	Hanford	
A		.20x
B	Unstable	.12x
C		$.08x/(1+.0002x)^{\frac{1}{2}}$
D	Neutral	$.06x/(1+.0015x)^{\frac{1}{2}}$
E	Slightly stable	.03x/(1+.0003x)
F	Moderately stable	.02x/(1+.0003x)
G		.012x/(1+.0003x)

A corrected estimate of σ_z is computed using the relationship

$$\sigma_{zc}^2 = \sigma_{zi}^2 + H^2/2\pi \qquad (1)$$

where σ_{zc} is the corrected value, σ_{zi} is the initial uncorrected value and H is the height of the cooling tower. In cases where the source is a cluster of cooling towers with a large width, the net effect of this correction is generally small.

Subroutine DIFFUSE

The last subroutine used by BATMAN is DIFFUSE. It calls SIGMAZ and then uses the result to compute the water vapor density increase at the receptor. DIFFUSE is by far the longest and most complex subroutine.

The diffusion computations in DIFFUSE use a sector-averaged Gaussian plume model with complete reflection at the ground and an optional reflecting lid. The basic sector-

averaged model is described in Section 3.3 of Meteorology and Atomic Energy - 1968[9] while the treatment of the reflecting lid is based upon Section 6.6 of Csanady's Turbulent Diffusion in the Environment[12].

The model that was derived from these sources is:

$$(\Delta\rho_v)_{ki} = \frac{Q_i \hat{n}}{(2\pi)^{3/2}\sigma_z \bar{u}x} \sum_{j=-\infty}^{\infty} \left\{ \exp\left[\frac{(z-h_i+2jH)^2}{-2\sigma_z^2}\right] + \exp\left[\frac{(z+h_i+2jH)^2}{-2\sigma_z^2}\right]\right\} \qquad (2)$$

where: $(\Delta\rho_v)_{ki}$ is the increase in water vapor density at receptor k due to source i,

Q_i is the water vapor release rate of source i,

$\hat{n}$ is related to the assumed plume width, ϕ_o, by $\hat{n} = \pi/\phi_o$ when ϕ_o is in radius,

ϕ_z is the vertical dispersion parameter,

$\bar{u}$ is the wind speed,

x is the distance between the receptor and virtual point source,

z is the height above the ground,

h_i is the effective release height for source i, and

H is the height of the reflecting lid.

Equation 2 can be simplified if any or all of z, h_i and H are zero. The greatest simplification occurs if H is zero. In that case the infinite sum is eliminated. If either h_i is zero the two exponential terms can be combined. If z=o the infinite sum is twice the sum from o to ∞. Finally, if all three are zero, the infinite sum and the exponential terms are eliminated.

DIFFUSE computes the relative water vapor increase $(\Delta\rho_v)_{ki}/Q_i$ by first calculating

$$\frac{\hat{n}}{(2\pi)^{3/2}\sigma_z\bar{u}x}$$

and the denominator in the exponential terms. It then determines what simplifications can be made in the infinite sum. If there is no lid, the infinite sum reduces to the sum of the two exponential terms with j=0 and a check is made to see if the exponential terms may be combined or eliminated. In all cases where H=0 the computations are straight foreward.

If the model cannot be simplified because H=0, DIFFUSE checks the ratio of H/σ_z. In the limit of σ_z becomes large, the vertical profile of the water vapor increase becomes a uniform distribution, and (2) reduces to

$$\frac{(\Delta\rho_v)_{ki}}{Q_i} = \frac{\hat{n}}{2\pi H\bar{u}x} \quad . \tag{3}$$

A uniform distribution can be assumed with an error of less than 0.25% if the ratio H/σ_z is less than 1.5.

When a uniform concentration cannot be assumed with this accuracy, the summation is carried out between j=-2 and j=+2. In this process, all reflection terms that are less than 0.25% of the value of the term when j=0 are neglected. The terms to be neglected can be identified by examination of ratios between z, h_i, H and σ_z.

Finally DIFFUSE computes $(\Delta\rho_v)_{ki}$ according to

$$(\Delta\rho_v)_{ki} = Q_i \left[\frac{(\Delta\rho_v)_{ki}}{Q_i} \right] \quad . \tag{4}$$

The combination of the increases in water vapor density from all of the sources to estimate the total increase is accomplished in BATMAN. The next section describes this process and the treatment of the computational results.

Model Output

BATMAN has the flexibility to examine increases in water vapor content for both special cases and on a climatological basis. This section describes the output for both operational modes and discusses the interpretation of the output.

In both modes BATMAN computes the total increase in water vapor density at each grid point assuming that the contributions of the individual plumes are additive. Thus, the total increase is given by

$$(\Delta\rho_v)_k = \sum_{i=1}^{N} (\Delta\rho_v)_{ki} \tag{5}$$

where N is the number of sources (clusters).

If the effects of a single set of atmospheric conditions (wind speed, direction, stability and mixing depth) are being examined, this information can be obtained. Figure 4 shows a sample of the output of $\Delta\rho_v$ for the case of WNW winds at 6.93 m/s during moderately stable atmospheric conditions for a single 4 reactor cluster with mechanical draft cooling towers located at grid position 6.1, 7.5. These atmospheric conditions occur approximately 3.45% of the time. Figure 5 shows the impact of 20 reactors divided among 5 clusters under the

INCREASE IN MOISTURE (G/M**3) AT Z = 0. METERS

0.00	0.00	0.00	0.00	0.00	0.00	0.00	0.00	0.00	0.00	0.00	0.00
0.00	0.00	0.00	0.00	0.00	0.00	0.00	0.00	0.00	0.00	0.00	0.00
0.00	0.00	0.00	0.00	0.00	0.00	0.00	0.00	0.00	0.00	0.00	0.00
0.00	0.00	0.00	0.00	0.00	0.00	0.00	0.00	0.00	0.00	0.00	0.00
0.00	0.00	0.00	0.00	0.00	0.00	0.00	0.00	0.00	0.00	0.00	0.00
0.00	0.00	0.00	0.00	0.00	0.00	0.00	0.00	0.00	0.00	0.00	0.00
0.00	0.00	0.00	0.00	0.00	0.00	0.00	0.00	.59	.40	.30	.24
0.00	0.00	0.00	0.00	0.00	0.00	0.00	0.00	0.00	0.00	.27	.23
0.00	0.00	0.00	0.00	0.00	0.00	0.00	0.00	0.00	0.00	0.00	.21
0.00	0.00	0.00	0.00	0.00	0.00	0.00	0.00	0.00	0.00	0.00	0.00
0.00	0.00	0.00	0.00	0.00	0.00	0.00	0.00	0.00	0.00	0.00	0.00
0.00	0.00	0.00	0.00	0.00	0.00	0.00	0.00	0.00	0.00	0.00	0.00

THIS CONDITION OCCURS AN AVERAGE OF 302. HOURS PER YEAR

FIGURE 4. Sample Computer Output of Increased Water Vapor Density (1 Cluster)

INCREASE IN MOISTURE (G/M**3) AT Z = 0. METERS

0.00	0.00	0.00	0.00	0.00	0.00	0.00	0.00	0.00	0.00	0.00	0.00
0.00	0.00	0.00	0.00	0.00	0.00	0.00	0.00	0.00	0.00	0.00	0.00
0.00	0.00	0.00	0.00	0.00	0.00	0.00	0.00	0.00	0.00	0.00	0.00
0.00	0.00	0.00	0.00	0.00	2.11	.63	0.00	0.00	0.00	0.00	0.00
0.00	0.00	0.00	0.00	0.00	0.00	2.17	1.44	.54	.44	.37	.17
0.00	0.00	0.00	0.00	0.00	0.00	0.00	.99	1.45	1.10	.60	.51
0.00	0.00	0.00	0.00	0.00	0.00	0.00	0.00	.59	1.20	1.13	.34
0.00	0.00	0.00	0.00	0.00	0.00	0.00	0.00	0.00	0.00	.52	.38
0.00	0.00	0.00	0.00	0.00	0.00	0.00	0.00	0.00	0.00	0.00	.21
0.00	0.00	0.00	0.00	0.00	0.00	0.00	0.00	0.00	0.00	0.00	0.00
0.00	0.00	0.00	0.00	0.00	0.00	0.00	0.00	0.00	0.00	0.00	0.00
0.00	0.00	0.00	0.00	0.00	0.00	0.00	0.00	0.00	0.00	0.00	0.00

THIS CONDITION OCCURS AN AVERAGE OF 302. HOURS PER YEAR

FIGURE 5. Sample Computer Output of Increased Water Vapor Density (5 Clusters)

the same climatic conditions. The grid locations for the 4 additional clusters in Figure 5 were at 5.5, 7.2; 4.7, 6.7; 3.7, 5.4 and 3.7, 4.9. Mechanical draft cooling systems were assumed for all clusters.

If a climatological output is desired, BATMAN can compute the number of hours of water vapor density increase within each specified range. In this case the number of hours of increase is computed as

$$H_o(\Delta\rho_v \geq a)_k = \sum_n \sum_u \sum_s \left[8766 \; P(n,u,s \mid \Delta\rho_v \geq a)_k \right] \qquad (6)$$

where $H_o(\Delta\rho_v \geq a)_k$ is the number of hours that the water vapor density increase is greater than a at receptor k; the summations are over wind direction, speed and atmospheric stability; 8766 is the average number of hours per year; and $P(n,u,s \mid \Delta\rho_v \geq a)_k$ is the joint frequency of occurrence of wind direction, speed and atmospheric stability that result in a water vapor density increase greater than a at receptor k. As many as 10 values for a can be used in any single simulation. A sample of the output is given in Figure 6 using the same 5 clusters used for Figure 5. This output is of value in determining the effects of moisture releases on relative humidity and wet-bulb temperature, but further computations are required to estimate the effect on fog.

If the impact of moisture releases on fog is to be estimated additional climatological information is required. That information describes the probability distribution of atmospheric water vapor saturation deficits, (i.e., the difference between the density of water vapor when air would be saturated and the actual vapor density). The increased number of hours of atmospheric saturation is given by

NUMBER OF HOURS THAT THE INCREASE IN MOISTURE AT Z = 0. METERS EQUALED OR EXCEEDED 1.00 G/M**3

140.3	92.9	92.9	118.3	75.4	96.4	44.7	8.8	41.2	33.3	40.3	40.3
88.4	125.4	94.7	98.2	110.5	98.2	85.0	105.2	12.3	20.2	46.5	46.5
68.4	70.1	127.1	127.1	250.7	323.5	221.8	93.8	63.1	4.4	43.8	75.4
115.7	115.7	130.6	94.7	1297.4	1830.3	434.8	305.1	63.1	296.3	62.2	51.7
50.0	108.9	7.9	28.1	64.9	159.5	2126.6	1050.2	221.8	270.9	241.9	210.4
180.8	50.0	13.1	15.8	34.2	120.1	600.5	1782.1	923.1	823.1	84.2	84.8
180.8	92.9	50.8	.9	46.5	35.9	110.5	848.8	909.0	965.1	641.7	335.7
180.8	100.8	.9	.9	14.9	17.5	43.8	171.8	760.0	638.2	424.3	335.7
180.8	145.5	102.6	107.8	.9	150.8	149.9	170.1	220.9	638.2	394.5	394.5
57.9	102.6	102.6	102.6	123.6	65.7	149.9	150.8	149.0	181.5	394.5	394.5
102.6	102.6	102.6	108.7	109.7	109.6	126.2	143.8	149.0	142.9	394.5	323.5
57.9	102.6	45.6	108.7	108.7	109.6	64.9	64.9	149.0	149.0	78.9	102.6

FIGURE 6. Sample Computer Output of Increased Hours of Water Vapor Density Exceeding a Fixed Value (1 g/m^3)

$$(H_f)_k = \sum_{m=1}^{M} \left\{ H_o (\Delta\rho_v \geq a_m)_k \; P(a_{m-1} \leq d < a_m) \right\} \tag{7}$$

where $(H_f)_k$ is the increase in hours of saturation at k, M is the number of density increase categories and $P(a_{m-1} < d < a_m)$ is the probability that the saturation deficit is between $a_m - 1$ and a_m. Figure 7 shows a sample of the computer output of this information for the same 5 clusters used for previous figures. In this case the increased number of hours of saturation have been interpreted as an increased number of hours of fog.

Output Interpretation

Prior to closing the discussion of the atmospheric model and the model output, some discussion of interpretation of the model output is appropriate. The first two forms of model output describe the increase in moisture content in terms of grams of water vapor per cubic meter of air. This can be related to other measures of humidity such as relative humidity and wet bulb temperature.

The relationship between increase in water vapor density and increase in relative humidity is a function of the temperature of the air. This relationship is shown in Figure 8, where the increase in relative humidity for a 1 g/m^3 increase in water vapor density is given as a function of temperature. Two striking features are evident in the Figure. The first is that at low temperatures a small increase in vapor density will cause a large increase in relative humidity, and the second is that at high temperatures small increases in water vapor have little effect on relative humidity. These features indicate that the greatest direct impacts of moisture releases should occur in the winter and in cool or cold climates.

INCREASE IN NUMBER OF HOURS OF FOG AT 0. METERS

85.4	30.5	29.1	34.6	21.1	26.2	15.6	20.6	19.1	20.4	31.9	22.7
19.3	34.3	34.8	81.1	39.0	32.9	29.9	36.7	26.7	25.7	32.0	34.0
24.7	25.9	30.3	30.5	58.8	84.3	56.4	55.4	52.2	35.0	45.9	53.3
27.0	27.2	23.2	19.0	355.2	454.8	155.1	78.8	61.8	72.9	54.3	46.8
20.5	27.1	14.6	21.0	24.9	88.1	609.1	262.5	128.0	103.4	92.7	67.3
21.6	22.5	13.8	14.7	28.2	33.8	171.2	504.2	214.5	179.6	96.9	88.9
27.6	23.9	11.7	12.3	23.7	33.9	62.6	209.7	258.6	227.7	137.1	111.0
29.3	33.7	11.5	15.2	17.9	22.6	28.7	53.4	191.6	150.0	165.5	117.1
25.3	34.1	35.2	27.9	15.7	39.1	45.6	53.7	85.5	150.4	117.9	120.6
21.8	26.1	30.0	30.7	31.9	28.9	35.1	53.0	62.3	90.5	119.8	111.2
20.9	20.9	26.6	31.4	26.6	31.1	35.5	49.7	44.1	49.8	118.3	93.4
14.8	17.8	21.5	23.9	26.0	34.2	31.5	31.5	42.0	36.7	44.9	76.1

FIGURE 7. Sample Computer Output for Predicted Increase in Hours of Saturation (Fog)

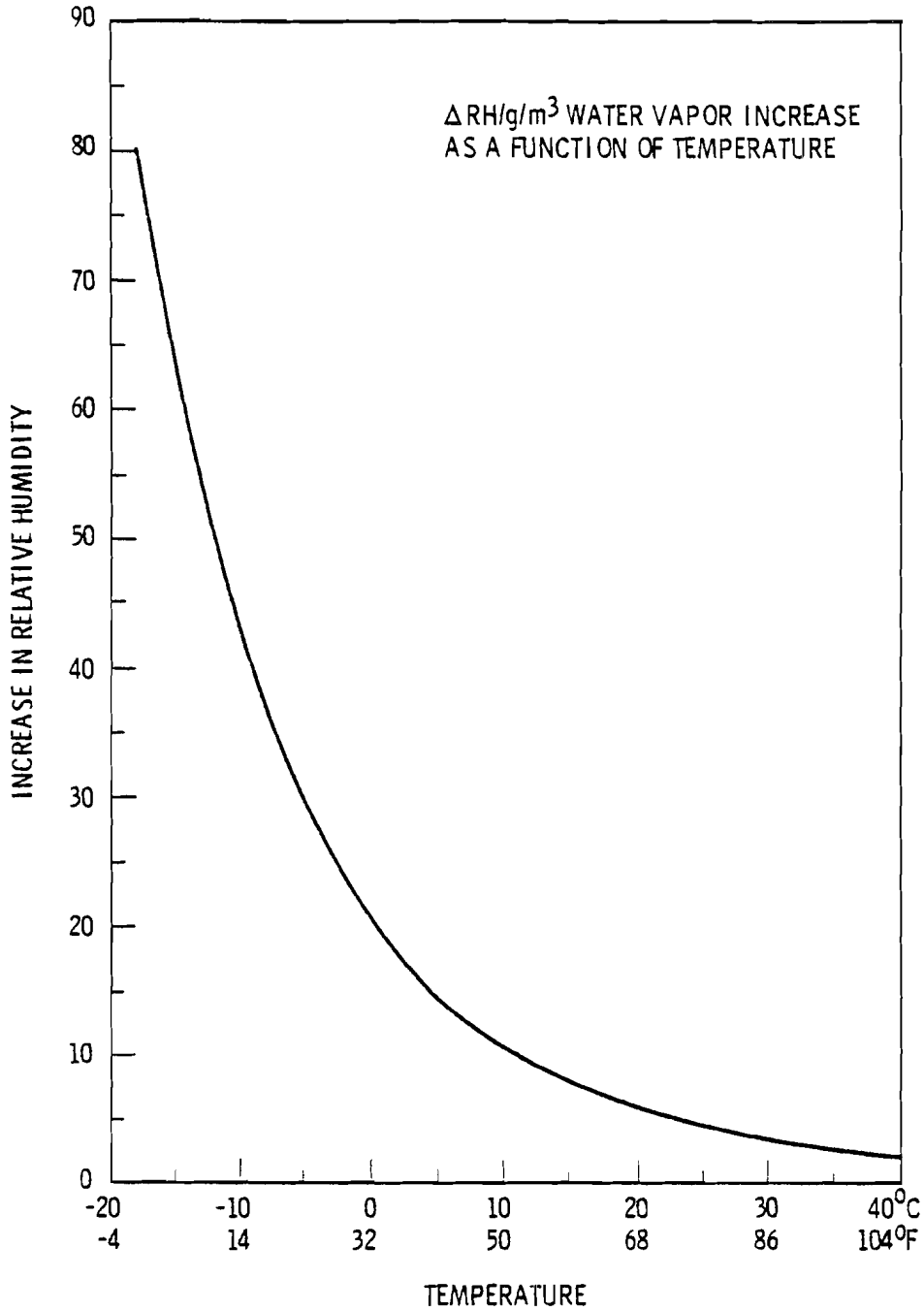

FIGURE 8. Relationship Between Relative Humidity Increase and Temperature for an Increase in Water Vapor Density of 1 g/m^3

Wet-bulb temperature is of interest in the evaluation of the performance of evaporative cooling systems. The performance of these systems decreased as the wet-bulb temperature increases. Addition of moisture raises the atmospheric wet-bulb temperature. The rate of increase in a slowly varying function of temperature, however, in the normal range of atmospheric temperatures it is approximately 1 C° for each gram per cubic meter of moisture increase.

The interpretation of increased hours of saturation was briefly discussed earlier. This interpretation requires some clarification. If the probability in (7) is the probability of saturation deficit during periods without fog then the result is properly interpreted as an increase in the number of hours of fog. But, if the probability covers all hours including those with fog, the output should be interpreted as total hours of fog.

It should also be noted that this interpretation assumes that saturation of the atmosphere is synonymous with fog, when in fact it is not. Fog is defined as a restriction to visibility which is associated with high humidities and water droplets. Fog frequently forms and persists at humidities slightly below saturation and the atmosphere may be very near or at saturation without the formation of fog. Thus, the modeling definition of fog as saturation of the atmosphere is only approximately correct.

THE HNEC MODEL

The evaluation of impacts of moisture releases for an HNEC required that release characteristics be assumed for a variety of potential HNEC configurations. An initial configuration was suggested in Reference 5. However other configurations were considered to estimate effects of changes in the configuration

on the total impact of the moisture release. This section describes the spatial and cooling system configurations evaluated.

In all cases, the HNEC was assumed to consist of discrete clusters with 4 reactors rated at 1250 MW_e in each cluster. In addition, all reactors within a cluster were assumed to use the same type cooling system.

Cluster Locations

During the course of the modeling program, reactor clusters were located at 14 different sites within the Hanford Reservation. Figure 9 depicts the Hanford Reservation (enclosed by dashed lines) and cluster locations within the BATMAN grid system. Exact locations of the clusters are given in Table 2. The Figure also shows the major roads and population centers in the area. The climatological data used for the model simulations were obtained at the Hanford Meteorology Station. The grid system, itself, is oriented North-South with 8 km (5 mi) spacing.

Major topographic features not shown in Figure 9 include Rattlesnake Mountain, the Saddle Mountains and the Horse Heaven Hills. Rattlesnake Mountain runs along the southwest boundary of the Hanford Reservation and effectively blocks the movement of air from Hanford toward the area of Sunnyside, Grandview and Prosser. The Horse Heaven Hills lie to the south of Highway 12 and tend to force air to the southeast to follow the Columbia River. Finally, to the north of the Reservation the Saddle Mountains tend to force airflow from the south through the Columbia River gap near Beverly or deflect it toward the east. These airflow perturbations are not fully reflected in the climatology and cannot be treated by BATMAN.

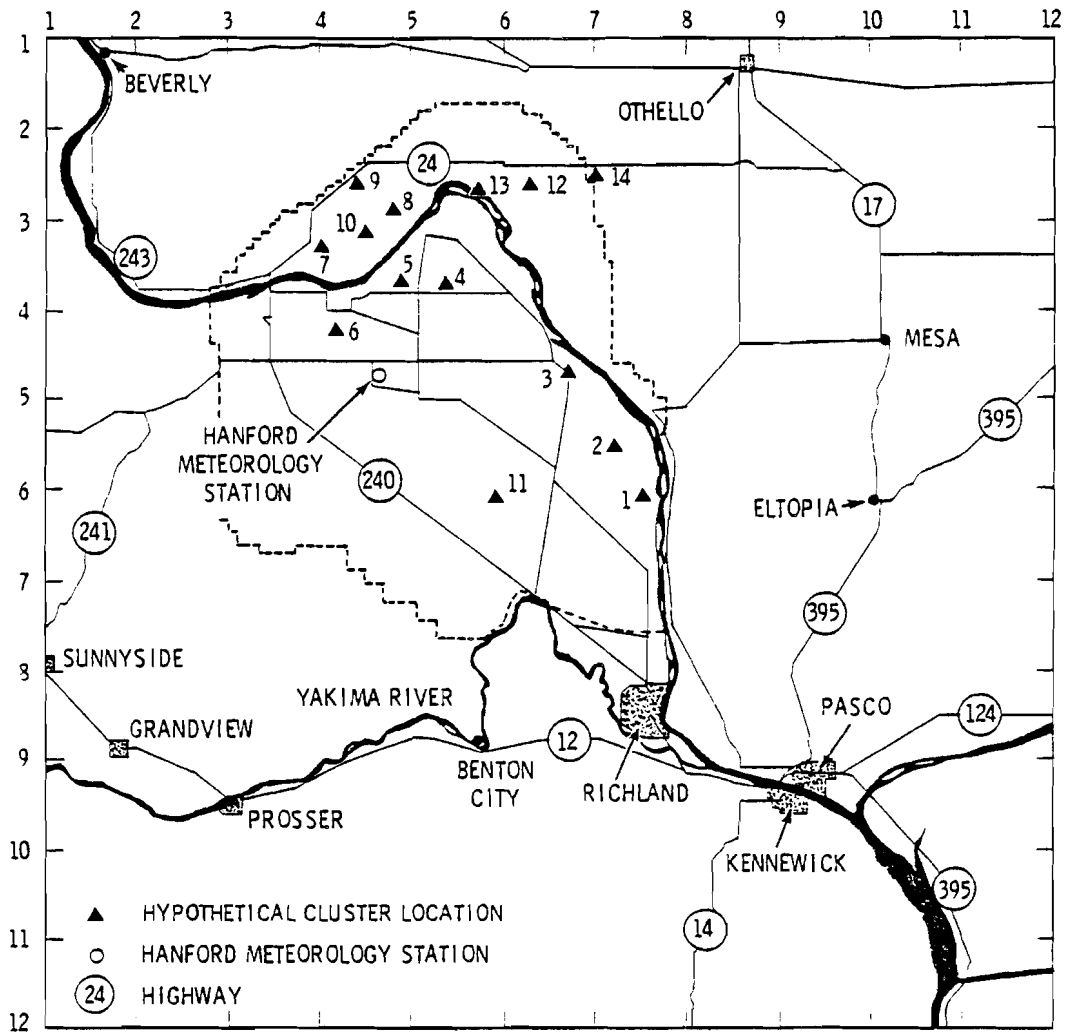

FIGURE 9. The HNEC Cluster Locations in the BATMAN Grid System

Table 2. Positions of the 4 Reactor Clusters for the HNEC Simulations

Cluster	North-South Coordinate	East-West Coordinate
1	6.10	7.50
2	5.50	7.20
3	4.70	6.70
4	3.70	5.40
5	3.70	4.90
6	4.20	4.20
7	3.30	4.00
8	2.90	4.80
9	2.60	4.40
10	3.10	4.50
11	6.10	5.90
12	2.60	6.30
13	2.70	5.80
14	2.50	7.00

Cooling System Models

The original problem which led to this modeling effort was one of heat sink management. Evaluation of cooling system types and locations are included within that problem. As a result a set of rudimentary cooling system models has been included in BATMAN. The cooling system models are not detailed and do not consider many of the physical processes that take place within cooling systems. Rather, the cooling system models provide a means to vary moisture release rates, release heights and horizontal scales. Seven different cooling systems have been simulated, however, there are only three different models. The basic models and their variation are described in this section.

The primary cooling system model in BATMAN is the low-level, mechanical draft cooling tower. This model assumes that the overall efficiency of the energy conversion is 33% and that 80% of the energy rejected will be released as latent heat of vaporization. With these assumptions a moisture source term is computed. The release height of mechanical draft cooling towers is assumed to be 25 m, further a characteristic horizontal dimension for the combined cooling systems in a cluster is assumed to be 1609 m (1 mi). In essence, the plumes from the individual cooling systems within a cluster are assumed to merge immediately.

The mechanical draft cooling tower model is altered to simulate a helper cooling tower on a once through cooling system by reducing the latent heat fraction from .80 to .60. Similarly, to simulate a hybrid, wet/dry cooling tower, the final moisture source term is multiplied by the wet cooling fraction. A tall natural draft cooling tower cluster is simulated by increasing the release height and decreasing the horizontal scale length to 154 and 400 m, respectively. Natural draft cooling towers may not be viable at Hanford, but mechanically assisted cooling towers of the same size may be.

The basic cooling model is simply a ground level, area source model. The pond for a 4 reactor cluster is assumed to be circular with a diameter of 9260 m. The total system efficiency is assumed to be 32%. Unlike the cooling tower model, in which the latent heat fraction was constant, the latent heat fraction in the cooling pond model is highly seasonal. It varies from a low of 56% in the winter to a high of over 200% in the summer. The latent heat release considers evaporation increases caused by construction of a pond on previously dry land. This is the cause of the high summer release rates. The modification of the basic cooling pond model to simulate helper ponds is accomplished by reducing the latent

heat release fraction. Background information on which the latent heat release fraction were based was supplied by the PNL Land Water Resources Department.

Although spray cooling ponds were not simulated, the basic cooling pond model with reduction of the horizontal scale length is the approach that would be taken.

The final cooling system simulated, and in many ways the least satisfactory, was once through cooling using the Columbia River. The approach taken was to assume that the river could be simulated by 5 circular areas that increased in size with distance from the source. The temperature increase in each area was computed assuming that the reactor effluent was thoroughly mixed with the river. The evaporation rate was then computed using the evaporation relationship in the COLHEAT river model[13], the average river temperature, the Clausius-Clapeyron equation, and wind speed. In short, the whole process is both cumbersome and tedious. The results using this approach were not encouraging although they were intuitively reasonable.

The basic parameters of the cooling system models (cooling tower and pond) are given in Tables 3 and 4. Table 3 summarizes the horizontal scales and release heights for these systems, while Table 4 summarizes the overall efficiency and latent heat fractions. The annual average water consumption per reactor for each cooling system is also given in Table 4. It is interesting to note that a lower consumptive use of water is achieved with cooling towers than with cooling ponds.

Heat Sink Management Simulations

The various cooling system models and cluster locations were combined to give 27 cases for evaluation. Initial evaluations indicated that approximately the same results were

Table 3. Characteristic Cooling System Dimensions

Cooling System	Horizontal Scale (m)	Release Height (m)
Mechanical Draft Cooling Towers (also helper)	1609	25
Tall Cooling Towers (assisted Natural Draft)	400	154
Cooling Ponds (also helper ponds)	9260	0

Table 4. Cooling System Thermal Characteristics

Cooling System	Efficiency	Latent Heat Fraction					Annual average water consumption (kg/sec)
		Annual	Winter	Spring	Summer	Fall	
Cooling towers (short or tall)	.333	.800	.800	.800	.800	.800	801
Cooling Ponds	.320	1.260	.560	1.232	2.098	1.133	1340
Helper Cooling Towers	.333	.600	.600	.600	.600	.600	601
Helper Cooling Ponds	.320	.963	.559	.989	1.383	.910	1020

achieved when annual climatological data were used as when the results of simulations using seasonal data were combined. As a result most simulations were made using annual data. In two cases summer climatological data were used to examine the increases in humidity more closely.

The test cases that were used to evaluate the impact of the potential HNEC moisture releases are described in Table 5. The cooling systems and locations simulated in each case are denoted by the small letters in the Table. In Case 1 a single cluster of 4 reactors using mechanical draft cooling towers was examined. This is generally considered to represent the future conditions at Hanford because Site 1 is located near the area in which the Washington Public Power Supply System is constructing 3 reactors. However this was not an attempt to model the WPPSS cooling systems or evaluate their effects. Each of the remaining cases includes a cluster with mechanical draft towers at Site 1.

Cases 2 through 6 were used to examine the effect of cluster location on the population centers and roads in the area. These cases include grouping the clusters near both the north and south sides of the Hanford Reservation, aligning the clusters both perpendicular and parallel to the prevailing wind direction, and spreading them as widely as possible. These cases were selected without regard to other probable siting considerations.

Cases 7 through 11 examine the effects of a 5 cluster HNEC with clusters sited using criteria such as water availability, potential pond sites and distance from population centers. They also provide information on the relative effects of the various cooling systems. The simulations in cases 12 through 14 extended this evaluation to the full 10 cluster (40 reactor) HNEC.

Table 5. Site and Cooling System Combinations Simulated

Case	Site 1	2	3	4	5	6	7	8	9	10	11	12	13	14	Climatology
1	a														annual
2	a	a	a	a	a										annual
3	a			a		a							a	a	annual
4	a					a			a		a			a	annual
5	a			a		a	a		a						annual
6	a	a	a	a							a				annual
7	a			b		b	b		b						annual
8	a			e		e	e		e						annual
9	a			d		d	d		d						annual
10	a	c	c	c	c										annual
11	a	c	c				e		e						annual
12	a	a	a	a	a	a	a		a	a	a				annual
13	a	c	c	c	c	c	c		c	c	c				annual
14	a	c	c	e	c	e	e		e	e	c				annual
15	a	a*	a*	a*	a*										annual
16	a	a+	a+	a+	a+										annual
17	a	a°	a°	a°	a°										annual
18	a	a*	a*	a*	a*	a*	a*		a*	a*	a*				annual
19	a	a+	a+	a+	a+	a+	a+		a+	a+	a+				annual
20	a	a°	a°	a°	a°	a°	a°		a°	a°	a°				annual
21	a	a	a	a	a										annual
22	a	a	a	a	a	a	a		a	a	a				annual
23	a	c	c				d		d						annual
24	a	c	c	d	c	d	d		d	d	c				annual
25	a	c	c	c				f							annual
26	a	c	c					f					f		annual
27	a	c	c	c	c	c		f	c		c		f		annual

Cooling system types

low tower	a
cooling pond	b
tall tower	c
helper tower	d
helper pond	e
river	f

*75% wet, +50% wet, °25° wet

The remaining simulations, except for cases 21 and 22, were done to identify those heat sink management options which minimize the potential impact of the HNEC moisture releases. Test cases 15 through 20 were directed toward the evaluation of hybrid wet/dry cooling systems, while those from 23 through 27 examined combinations of more conventional cooling systems.

The detailed results of the HNEC simulations will be discussed following a description of the Hanford climate.

THE HANFORD CLIMATE

Any evaluation of the impact of heat sink management alternatives on the environment must consider the climate of the region under consideration. Thus it is appropriate to describe the climate of the Hanford area in some detail. The basic reference on Hanford Climate is the Climatography of the Hanford Area prepared in 1972 by Stone, Jenne and Thorp[14]. The temperature and precipitation data in this work indicate that the Hanford area borders between a Steppe (BS) and desert (BW) climate using the Koppen classification scheme[15]. This classification is confirmed by the vegetation types that occupy most of the Hanford Reservation.

General Climatology

Meteorological observations have been made at numerous locations in the Hanford vicinity, but the only extensive records for a single location are those for the Hanford Meteorological Station (HMS). The HMS is located on a plateau at about 750 ft MSL and is about 300 ft above the Columbia River which flows through the reservation to the north and east. There are several significant topographic features within 20 miles of the HMS that affect some aspects of the Hanford climatology including wind.

Prior to the establishment of the HMS in December 1944, meteorological measurements were made by U. S. Weather Bureau cooperative observers between 1912 and 1943 and by the U. S. Weather Bureau in Richland for a short period at the end of 1943 and beginning of 1944.

The climatological data from these sources are summarized in Table 6. This summary gives both monthly and annual statistics for a large number of climatological variables and includes extreme values as well as means. Since 1975, the last year for which data are included in the table, several new records have been set, but there has been little variation in the climatological averages.

In addition to the month to month variation of climatological statistics presented in Table 6, there are distinct daily cycles which are superimposed on the seasonal variation. These daily cycles are most evident in temperature, humidity, and wind speed. The daily temperature cycle is familiar to all. The amplitude of this cycle at Hanford ranges from about 13 F° in December to about 30 F° in July and August. The daily cycle of relative humidity should also be familiar. It is related to the temperature cycle but out of phase, that is when the temperature decreases the humidity increases and conversely when the temperature increases the relative humidity decreases. The magnitude of the daily relative humidity variation at Hanford is about 25% throughout most of the year. However it decreases to about 10% in December and January. The daily wind speed cycle has a minimum during the morning hours and increases during the afternoon hours until it reached a maximum near sunset. It is most pronounced during the summer and almost imperceptible during the months of December and January. Figures 10 and 11 show these daily cycles for the months of January and July respectively.

TABLE 6. AVERAGES AND EXTREMES OF CLIMATIC ELEMENTS AT HANFORD

(BASED ON ALL AVAILABLE RECORDS TO AND INCLUDING THE YEAR 1975)

PAGE 1 OF 2

TEMPERATURE (°F) — 1912-1975 AVERAGES

	DAILY MAXIMUM	DAILY MINIMUM	MONTHLY	HIGHEST MONTHLY	YEAR	LOWEST MONTHLY	YEAR
Jan.	37.0	22.2	29.6	42.5	1953	12.1	1950
Feb.	45.4	27.6	36.4	44.5	1958	21.4	1929
Mar.	56.5	33.2	45.1	49.9	1976	39.4	1955
Apr.	66.1	39.9	53.1	59.6	1934	47.5	1955
May	75.6	48.0	61.9	68.9	1947	56.6	1933
June	83.2	55.4	69.4	75.4	1922	63.0	1953
July	91.9	61.1	76.5	81.8	1960	72.4	1963
Aug.	89.4	59.3	74.3	81.5	1967	69.9	1964
Sept.	79.6	50.7	65.2	71.7	1967	58.8	1926
Oct.	65.3	40.7	53.0	59.0	1952	48.8	1930
Nov.	48.6	31.5	40.0	46.0	1954	31.3	1955
Dec.	39.3	26.0	32.7	42.0	1933	18.5	1919
					July		Jan.
Year	64.6	41.3	53.1	61.8	1960	12.1	1950

TEMPERATURE (°F) — 1912-1975 EXTREMES

	DAILY MAXIMUM RECORD HIGHEST	YEAR	RECORD LOWEST	YEAR	DAILY MINIMUM RECORD HIGHEST	YEAR	RECORD LOWEST	YEAR
Jan.	72	1971	-2	1950	53	1971	-23	1934
Feb.	71	1974	-3	1950	55	1932	-21	1950
Mar.	83	1960	26	1960	54	1942	6	1955
Apr.	95	1934	41	1945	60	1956	12	1935
May	103	1936	49	1918	70	1956	28	1954
June	110	1912	55	1966	81	1924	33	1933
July	115	1939	59	1966	82	1925	41	1935
Aug.	113	1961	63	1970	81	1961	40	1918
Sept.	102	1950	52	1934	72	1955	25	1926
Oct.	90	1933	31	1935	60	1945	6	1935
Nov.	75	1935	14	1955	52	1959	-1	1955
Dec.	68	1933	-3	1919	56	1975	-27	1919
		July		Feb.		July		Dec.
Year	115	1939	-3	1950	82	1925	27	1919

DEGREE DAYS (BASE 65°F) — HEATING 1945-1975 TOTALS

	MEAN MONTHLY	MAXIMUM MONTHLY	YEAR	MINIMUM MONTHLY	YEAR
Jan.	1085	1640	1950	694	1951
Feb.	778	1147	1956	576	1958
Mar.	641	794	1955	476	1943
Apr.	386	522	1955	264	1947
May	154	255	1962	36	1947
June	34	90	1953	3	1958
July	3	22	1955	0	1975
Aug.	5	32	1968	0	1974
Sept.	71	179	1972	13	1967
Oct.	377	479	1946	210	1952
Nov.	747	1008	1955	567	1954
Dec.	990	1224	1964	822	1957
Year	5211	1640	1950	0	1975

DEGREE DAYS (BASE 65°F) — COOLING 1960-1975 TOTALS

	MEAN MONTHLY	MAXIMUM MONTHLY	YEAR	MINIMUM MONTHLY	YEAR
Jan.	0	0	----	0	----
Feb.	0	0	----	0	----
Mar.	0	0	----	0	----
Apr.	1	5	1968	0	1975
May	49	93	1971	3	1967
June	192	310	1969	59	1971
July	404	518	1960	212	1963
Aug.	338	508	1967	171	1964
Sept.	107	216	1967	27	1970
Oct.	2	10	1971	0	1975
Nov.	0	0	----	0	----
Dec.	0	0	----	0	----
Year	1093	518	1960	0	1975

PRECIPITATION (INCHES) — 1912-1975 TOTALS

	MEAN MONTHLY	MAXIMUM MONTHLY	YEAR	MINIMUM MONTHLY	YEAR	MAX. IN 24 HOURS	YEAR
Jan.	0.92	2.47	1970	0.13	1962	1.08	1948
Feb.	0.60	3.68	1940	T	1967	1.24	1916
Mar.	0.37	1.86	1957	0	1942	0.59	1949
Apr.	0.38	1.22	1969	0	1933	0.53	1951
May	0.47	2.03	1972	0	1931	1.19	1972
June	0.56	2.92	1950	0	1919	1.50	1934
July	0.15	0.81	1966	0	1939	0.73	1914
Aug.	0.30	1.16	1970	0	1955	0.69	1975
Sept.	0.30	1.34	1947	T	1961	0.82	1947
Oct.	0.58	2.72	1957	0	1917	1.91	1957
Nov.	0.86	3.05	1926	T	1939	0.78	1966
Dec.	0.89	2.53	1931	0.11	1946	1.00	1958
					Oct.		June
Year	6.28	3.08	1940	0	1957	1.91	1934

PRECIPITATION (INCHES) — 1912-1975 TOTALS — SNOW, ICE PELLETS (SLEET)

	MEAN MONTHLY	MAXIMUM MONTHLY	YEAR	MAX. IN 24 HOURS	YEAR	MAXIMUM DEPTH	YEAR
Jan.	5.1	23.4	1950	7.1	1954	12.0	1969
Feb.	2.4	26.0	1916	5.6	1975	10.0	1969
Mar.	0.3	4.2	1951	2.2	1957	2.3	1957
Apr.	T	T	1975	1	1975	0	----
May	1	1	1960	1	1960	0	----
June	0	0	----	0	----	0	----
July	0	0	----	0	----	0	----
Aug.	0	0	----	0	----	0	----
Sept.	0	0	----	0	----	0	----
Oct.	4	1.5	1973	1.5	1973	1.5	1973
Nov.	1.3	12.7	1955	4.8	1955	5.1	1946
Dec.	3.9	19.1	1964	5.4	1965	12.1	1964
			Feb.		Jan.		Dec.
Year	13.0	26.0	1916	7.1	1954	12.1	1964

WIND (mph) — 1945-1975 AVERAGES

	PREVAILING DIRECTION	MEAN MONTHLY SPEED	HIGHEST MONTHLY	YEAR	LOWEST MONTHLY	YEAR
Jan.	NW	6.6	10.3	1972	3.1	1955
Feb.	NW	7.1	9.4	1961	4.6	1963
Mar.	WNW	8.4	10.7	1964	5.9	1958
Apr.	WNW	9.1	11.1	1972	7.4	1958
May	WNW	9.9	10.5	1965	5.8	1957
June	WNW	9.2	10.7	1949	7.7	1950
July	WNW	8.6	9.6	1963	6.8	1955
Aug.	WNW	8.0	9.1	1946	6.0	1956
Sept.	WNW	7.5	9.2	1961	5.4	1957
Oct.	WNW	6.7	9.1	1946	4.4	1952
Nov.	NW	6.1	7.9	1945	2.9	1954
Dec.	NW	6.1	8.3	1968	3.9	1963
			Apr.			Nov.
Year	WNW	7.7	11.1	1972	2.9	1956

WIND (mph) — PEAK GUSTS

	SPEED	DIRECTION	YEAR
Jan.	80	SW	1972
Feb.	65	SW	1971
Mar.	70	SW	1956
Apr.	73	SSW	1972
May	71	SSW	1948
June	72	SW	1957
July	55	WSW	1968
Aug.	66	SW	1961
Sept.	65	SSW	1953
Oct.	63	SSW	1950
Nov.	64	SSW	1949
Dec.	71	SW	1955
			Jan.
Year	80	SW	1972

RELATIVE HUMIDITY (%) — 1946-1975 AVERAGES

	MEAN	HIGHEST MONTHLY	YEAR	LOWEST MONTHLY	YEAR
Jan.	75.2	88.8	1960	60.0	1963
Feb.	70.0	86.9	1963	54.0	1967
Mar.	55.8	65.9	1950	44.0	1965
Apr.	46.5	64.5	1963	36.9	1966
May	42.3	61.9	1948	31.2	1966
June	39.5	53.5	1950	30.0	1949
July	31.8	40.5	1955	21.9	1959
Aug.	34.8	43.8	1968	24.5	1967
Sept.	40.6	55.1	1959	33.2	1974
Oct.	57.0	74.2	1962	42.5	1952
Nov.	73.5	88.1	1972	64.2	1963
Dec.	80.1	90.5	1950	69.0	1968
			Dec.		July
Year	53.9	90.5	1950	21.9	1959

RELATIVE HUMIDITY (%) — 1946-1975 EXTREMES

	HIGHEST	YEAR	LOWEST	YEAR
Jan.	100	1975	13	1963
Feb.	100	1975	14	1962
Mar.	100	1974	12	1965
Apr.	100	1973	9	1954
May	100	1975	7	1953
June	100	1972	10	1964
July	99	1972	6	1951
Aug.	100	1972	7	1951
Sept.	100	1962	10	1962
Oct.	100	1975	10	1952
Nov.	100	1975	16	1959
Dec.	100	1975	26	1972
		Dec.		July
Year	100	1975	6	1951

SKY COVER (SCALE 0-10) — 1946-1975 AVERAGES (SUNRISE TO SUNSET)

	MONTHLY	HIGHEST MONTHLY	YEAR	LOWEST MONTHLY	YEAR
Jan.	7.8	9.0	1969	4.3	1949
Feb.	7.4	8.9	1961	5.9	1964
Mar.	6.9	7.9	1950	4.9	1965
Apr.	6.4	8.1	1963	3.7	1951
May	5.8	7.7	1950	4.5	1949
June	5.3	7.0	1950	2.8	1961
July	2.8	4.5	1974	0.9	1953
Aug.	3.2	5.9	1968	0.6	1955
Sept.	4.0	6.1	1959	1.4	1975
Oct.	5.9	8.0	1975	3.9	1952
Nov.	7.6	9.1	1972	6.2	1957
Dec.	8.1	9.2	1962	6.8	1954
			Dec.		Aug.
Year	5.9	9.2	1962	0.6	1955

SOLAR RADIATION (LANGLEYS)* — 1953-1975 AVG. DAILY TOTALS

	MONTHLY	HIGHEST MONTHLY	YEAR	LOWEST MONTHLY	YEAR
Jan.	120	136	1973	88	1955
Feb.	202	238	1960	164	1954
Mar.	340	388	1965	305	1961
Apr.	475	535	1973	374	1963
May	576	634	1970	511	1962
June	628	695	1960	543	1953
July	659	714	1971	558	1955
Aug.	558	613	1955	475	1968
Sept.	423	463	1975	354	1959
Oct.	262	299	1958	216	1975
Nov.	132	150	1957	97	1964
Dec.	92	116	1970	57	1969
			July		Dec.
Year	372	714	1973	57	1969

SOLAR RADIATION (LANGLEYS)* — 1953-1975 EXTREME DAILY TOTALS

	HIGHEST MONTHLY	YEAR	LOWEST MONTHLY	YEAR
Jan.	277	1969	16	1971
Feb.	422	1958	37	1970
Mar.	542	1968	47	1972
Apr.	704	1972	75	1974
May	782	1959	67	1962
June	821	1971	112	1965
July	844	1974	118	1972
Aug.	721	1957	107	1959
Sept.	591	1970	61	1957
Oct.	434	1975	33	1974
Nov.	295	1971	14	1969
Dec.	196	1972	9	1973
		June		Dec.
Year	821	1971	9	1973

EXTREME AVERAGES OR TOTALS AND YEAR OR SEASON OF OCCURRENCE

1912-1975 TEMPERATURE AVERAGES (°F)

HIGHEST ANNUAL	56.2	1958+
LOWEST ANNUAL	50.2	1929
HIGHEST WINTER (D-J-F)	41.1	1933-34
LOWEST WINTER	24.2	1948-49
HIGHEST SPRING (M-A-M)	58.2	1947
LOWEST SPRING	48.0	1955
HIGHEST SUMMER (J-J-A)	78.2	1958
LOWEST SUMMER	70.3	1954
HIGHEST FALL (S-O-N)	56.6	1963
LOWEST FALL	49.6	1946

1912-1975 PRECIPITATION TOTALS (IN.)

GREATEST ANNUAL	11.45	1950
LEAST ANNUAL	3.26	1967
SNOW, ICE PELLETS (SLEET)		
GREATEST SEASONAL	43.6	1915-16
LEAST SEASONAL	0.3	1957-58

1945-1975 WIND SPEED AVERAGE (mph)

HIGHEST ANNUAL	8.3	1968+
LOWEST ANNUAL	6.3	1957

1946-1975 RELATIVE HUMIDITY AVERAGE (%)

HIGHEST ANNUAL	57.9	1950+
LOWEST ANNUAL	49.4	1967

1946-1975 SKY COVER AVERAGES (SUNRISE TO SUNSET, SCALE 0-10)

HIGHEST ANNUAL	6.4	1966
LOWEST ANNUAL	5.1	1949

1953-1975 SOLAR RADIATION AVERAGE DAILY TOTAL (LANGLEYS)

HIGHEST ANNUAL	390	1973
LOWEST ANNUAL	357	1967

TABLE 6. (cont) **AVERAGES AND EXTREMES OF CLIMATIC ELEMENTS AT HANFORD CON,T.**

(BASED ON ALL AVAILABLE RECORDS TO AND INCLUDING THE YEAR 1975)

NUMBER OF DAYS (1945-1975) * *

	CLEAR					PTLY CLDY	CLOUDY					THUNDERSTORMS					HEAVY FOG (VIS. 1/4 MI. OR LESS)					PRECIP. 0.10 INCH OR MORE					SNOW 1.0 INCH OR MORE				
	MEAN MONTHLY	GREATEST MONTHLY	YEAR	LEAST MONTHLY	YEAR	MEAN	MEAN MONTHLY	GREATEST MONTHLY	YEAR	LEAST MONTHLY	YEAR	MEAN MONTHLY	GREATEST MONTHLY	YEAR	LEAST MONTHLY	YEAR	MEAN MONTHLY	GREATEST MONTHLY	YEAR	LEAST MONTHLY	YEAR	MEAN	GREATEST MONTHLY	YEAR	LEAST MONTHLY	YEAR	MEAN MONTHLY	GREATEST MONTHLY	YEAR	LEAST MONTHLY	YEAR
Jan.	4	7	1963	0	1955+	7	20	27	1969	17	1963	0	0	----	0	----	5	14	1965	0	1949	3	8	1970	0	1972+	2	10	1950	0	1967+
Feb.	5	9	1968+	1	1972+	7	17	26	1958	12	1964	#	1	1972+	0	1975+	3	11	1963	0	1971+	2	5	1961+	0	1972+	2	4	1975+	0	1974+
Mar.	6	12	1965+	2	1961	9	15	22	1968	9	1965	#	1	1969+	0	1975+	1	5	1951	0	1975+	2	8	1957	0	1973+	#	2	1957+	0	1975+
Apr.	7	12	1962	1	1963	11	13	21	1963	6	1956	1	3	1948	0	1975+	#	1	1975+	0	1974+	3	5	1948	0	1973+	0	0	----	0	----
May	9	14	1973	2	1960	11	11	19	1960	6	1958	2	7	1956	0	1974+	#	1	1958	0	1975+	2	4	1967+	0	1968+	0	0	----	0	----
June	10	21	1961	5	1972+	10	10	15	1973+	5	1960+	3	8	1972+	0	1963+	#	1	1971	0	1975+	2	8	1950	0	1973+	0	0	----	0	----
July	20	26	1960	13	1974	7	3	9	1974	1	1961	2	7	1975	0	1973+	0	0	---	0	----	1	3	1974+	0	1973+	0	0	----	0	----
Aug	19	30	1955	11	1968	7	4	13	1968	0	1955	2	8	1953	0	1974+	#	1	1959	0	1975+	1	4	1975	0	1974+	0	0	----	0	----
Sept.	15	27	1975	8	1969	8	7	13	1969	1	1975	1	4	1959	0	1975+	#	1	1957	0	1975+	1	5	1959	0	1975+	0	0	----	0	----
Oct.	10	14	1970	1	1975	8	13	22	1973	9	1970	#	1	1975+	0	1974+	1	6	1962	0	1974+	2	8	1950	0	1972+	#	1	1973	0	1975+
Nov.	4	10	1957	1	1973+	6	19	25	1973+	15	1961	0	0	----	0	----	6	13	1965	0	1960	3	10	1973	0	1967	#	6	1955	0	1974+
Dec.	3	7	1972+	1	1962+	6	22	28	1962	18	1967+	#	1	1971	0	1975+	8	17	1950	2	1968+	3	9	1964	0	1949+	2	6	1964	0	1974+
			Aug		Jan.				Dec.		Aug.			June					Dec.					Dec.		Sept			Jan.		
Year	112	30	1955	0	1955+	97	154	78	1962	0	1969+	11	8	1972+	0	----	24	17	1950	0	----	23	9	1964	0	1975+	6	10	1950	0	----

NUMBER OF DAYS (1945-1975) / NUMBER OF DAYS (1912-1975)

	3" OR MORE SNOW ON GND.					PEAK GUST 40 MPH OR GREATER					MAX. TEMP. 90 OR ABOVE					MAX. TEMP. 100 OR ABOVE					MAX. TEMP. 32 OR BELOW					MIN. TEMP. 32 OR BELOW					MIN. TEMP. 0 OR BELOW				
	MEAN MONTHLY	GREATEST MONTHLY	YEAR	LEAST MONTHLY	YEAR	MEAN MONTHLY	GREATEST MONTHLY	YEAR	LEAST MONTHLY	YEAR	MEAN MONTHLY	GREATEST MONTHLY	YEAR	LEAST MONTHLY	YEAR	MEAN MONTHLY	GREATEST MONTHLY	YEAR	LEAST MONTHLY	YEAR	MEAN MONTHLY	GREATEST MONTHLY	YEAR	LEAST MONTHLY	YEAR	MEAN MONTHLY	GREATEST MONTHLY	YEAR	LEAST MONTHLY	YEAR	MEAN MONTHLY	GREATEST MONTHLY	YEAR	LEAST MONTHLY	YEAR
Jan.	5	23	1969	0	1975+	3	11	1972	0	1973+	0	0	----	0	----	0	0	----	0	----	11	29	1917	0	1967+	29	31	1960+	9	1953	2	14	1950	0	1975+
Feb	3	16	1950	0	1974+	3	6	1961+	0	1973+	0	0	----	0	----	0	0	----	0	----	3	15	1956	0	1924+	22	28	1934+	5	1958	1	9	1929	0	1975+
Mar.	0	0	----	0	----	3	9	1956	1	1973+	0	0	----	0	----	0	0	----	0	----	#	2	1960	0	1975+	16	25	1934+	6	1968+	0	0	----	0	----
Apr.	0	0	----	0	----	3	7	1972	0	1967	#	4	1926	0	1975+	0	0	----	0	----	0	0	----	0	----	5	15	1935	0	1974+	0	0	----	0	----
May	0	0	----	0	----	2	6	1971+	0	1963+	3	11	1924	0	1974+	#	1	1966+	0	1975+	0	0	----	0	----	#	3	1938	0	1975+	0	0	----	0	----
June	0	0	----	0	----	2	6	1973	0	1971+	9	20	1940+	0	1953	1	9	1970	0	1975+	0	0	----	0	----	0	0	----	0	----	0	0	----	0	----
July	0	0	----	0	----	1	4	1962+	0	1975+	21	29	1943	8	1963	7	16	1971+	0	1963+	0	0	----	0	----	0	0	----	0	----	0	0	----	0	----
Aug.	0	0	----	0	----	1	5	1951	0	1974+	18	29	1915	7	1948	4	16	1942	0	1975+	0	0	----	0	----	0	0	----	0	----	0	0	----	0	----
Sept.	0	0	----	0	----	2	4	1946	0	1975+	5	16	1938	0	1970+	#	2	1955+	0	1975+	0	0	----	0	----	#	4	1933+	0	1975+	0	0	----	0	----
Oct.	0	0	----	0	----	2	8	1967	0	1974+	#	1	1933	0	1975+	0	0	----	0	----	#	2	1935	0	1975+	5	12	1916	0	1962+	0	0	----	0	----
Nov.	#	10	1955	0	1975+	2	5	1973+	0	1974+	0	0	----	0	----	0	0	----	0	----	2	15	1955	0	1974+	17	30	1936	4	1949	#	1	1955+	0	1975+
Dec.	2	14	1955	0	1975+	3	8	1957+	0	1969+	0	0	----	0	----	0	0	----	0	----	8	19	1914	0	1974	26	31	1963+	14	1933	1	14	1919	0	1975+
			Jan					Jan.					July					July					Jan					Dec.					Jan.		
Year	10	23	1969	0	----	27	11	1972	0	----	56	29	1943+	0	----	12	16	1971+	0	----	24	29	1937	0	----	119	31	1963+	0	----	4	14	1950+	0	----

NUMBER OF DAYS

CLEAR (0-3 TENTHS SKY COVER, SR TO SS)

GREATEST ANNUAL (1946-75)	141	1951
LEAST ANNUAL (1946-75)	85	1966

CLOUDY (8-10 TENTHS SKY COVER, SR TO SS)

GREATEST ANNUAL (1946-75)	181	1969+
LEAST ANNUAL (1946-75)	84	1949

THUNDERSTORMS

GREATEST ANNUAL (1945-75)	23	1948
LEAST ANNUAL (1945-75)	3	1949

HEAVY FOG (VIS. 1/4 MILE OR LESS)

GREATEST SEASONAL (1945-75)	42	1950-51
LEAST SEASONAL (1945-75)	9	1948-49

PRECIPITATION 0.10 INCH OR MORE

GREATEST ANNUAL (1946-75)	39	1950
LEAST ANNUAL (1946-75)	10	1965

SNOW 1.0 INCH OR MORE

GREATEST SEASONAL (1946-75)	15	1955-56
LEAST SEASONAL (1946-75)	0	1957-58

3 IN. OR MORE SNOW ON GROUND

GREATEST SEASONAL (1946-75)	40	1964-65
LEAST SEASONAL (1946-75)	0	1966-67+

PEAK GUST 40 MPH OR GREATER

GREATEST ANNUAL (1945-75)	41	1961
LEAST ANNUAL (1945-75)	13	1958

MAX. TEMPERATURE 90 OR ABOVE

GREATEST ANNUAL (1912-75)	85	1940+
LEAST ANNUAL (1912-75)	31	1964

MAX. TEMPERATURE 100 OR ABOVE

GREATEST ANNUAL (1912-75)	32	1942
LEAST ANNUAL (1912-75)	1	1954

MAX. TEMPERATURE 32 OR BELOW

GREATEST SEASONAL (1912-75)	53	1955-56
LEAST SEASONAL (1912-75)	1	1937-38

MIN. TEMPERATURE 32 OR BELOW

GREATEST SEASONAL (1912-75)	141	1916-17
LEAST SEASONAL (1912-75)	75	1957-58

MIN. TEMPERATURE 0 OR BELOW

GREATEST SEASONAL (1912-75)	18	1949-50
LEAST SEASONAL (1912-75)	0	1974-75+

REFERENCE NOTES

* CALORIES/cm²

* * SKY COVER AND PRECIPITATION OBSERVATIONS NOT BEGUN UNTIL 1946

\# LESS THAN 1/2

\+ ALSO ON EARLIER YEARS

LOCATION AND HISTORY

PRESENT LOCATION 25 MILES NW OF RICHLAND, WASHINGTON

LATITUDE 46°34' N, LONGITUDE 119°36' W ELEVATION 733 FEET

OBSERVATIONS FROM 1912 TO 1944 WERE BY UNITED STATES WEATHER BUREAU COOPERATIVE OBSERVERS AT A SITE ABOUT 10 MILES ENE OF PRESENT LOCATION. SINCE 1944 OBSERVATIONS HAVE BEEN MAINTAINED ON A 24 HOUR-A-DAY BASIS BY THREE DIFFERENT ERDA CONTRACTORS.

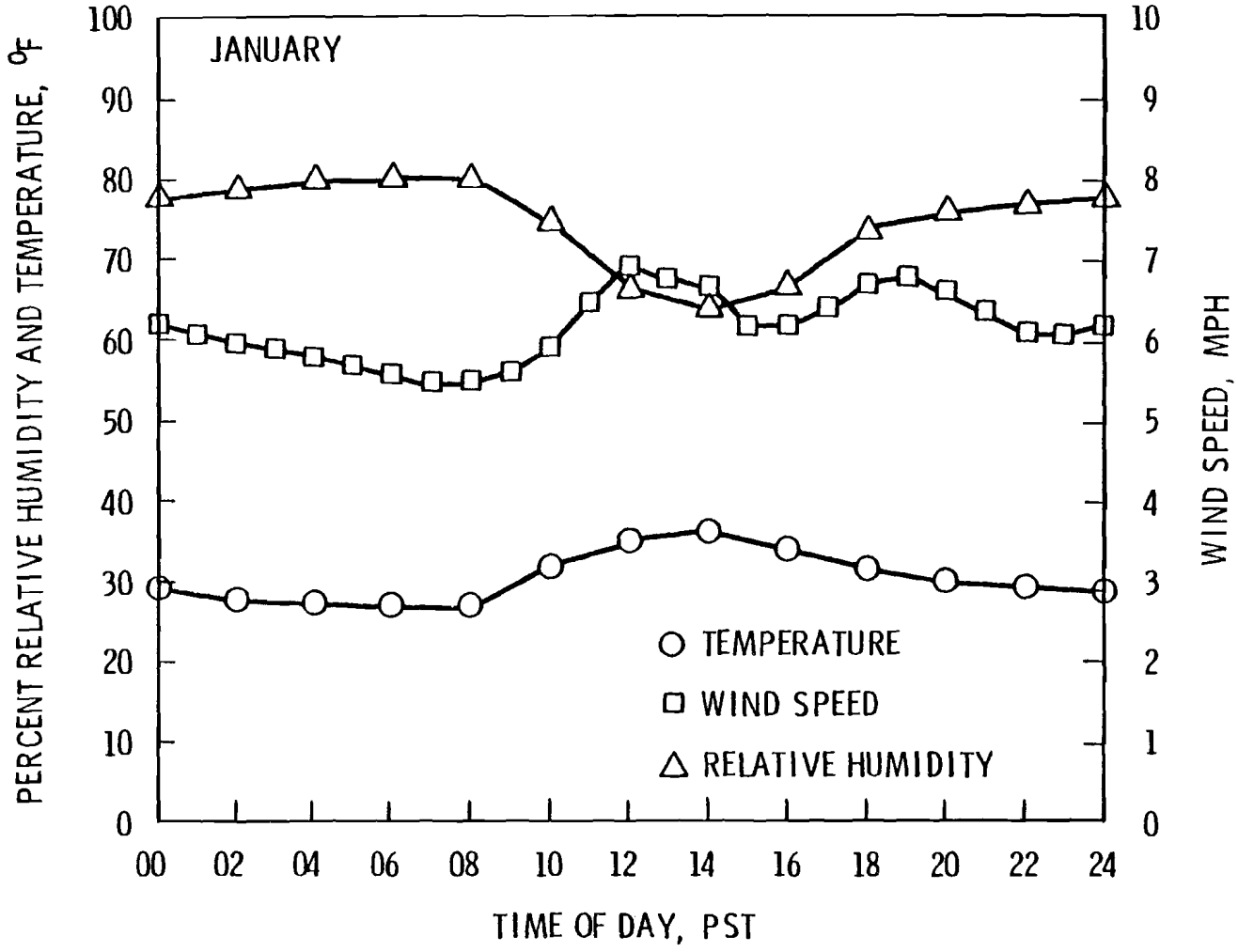

FIGURE 10. The Diurnal Cycles of Temperature, Relative Humidity and Wind Speed for January at Hanford

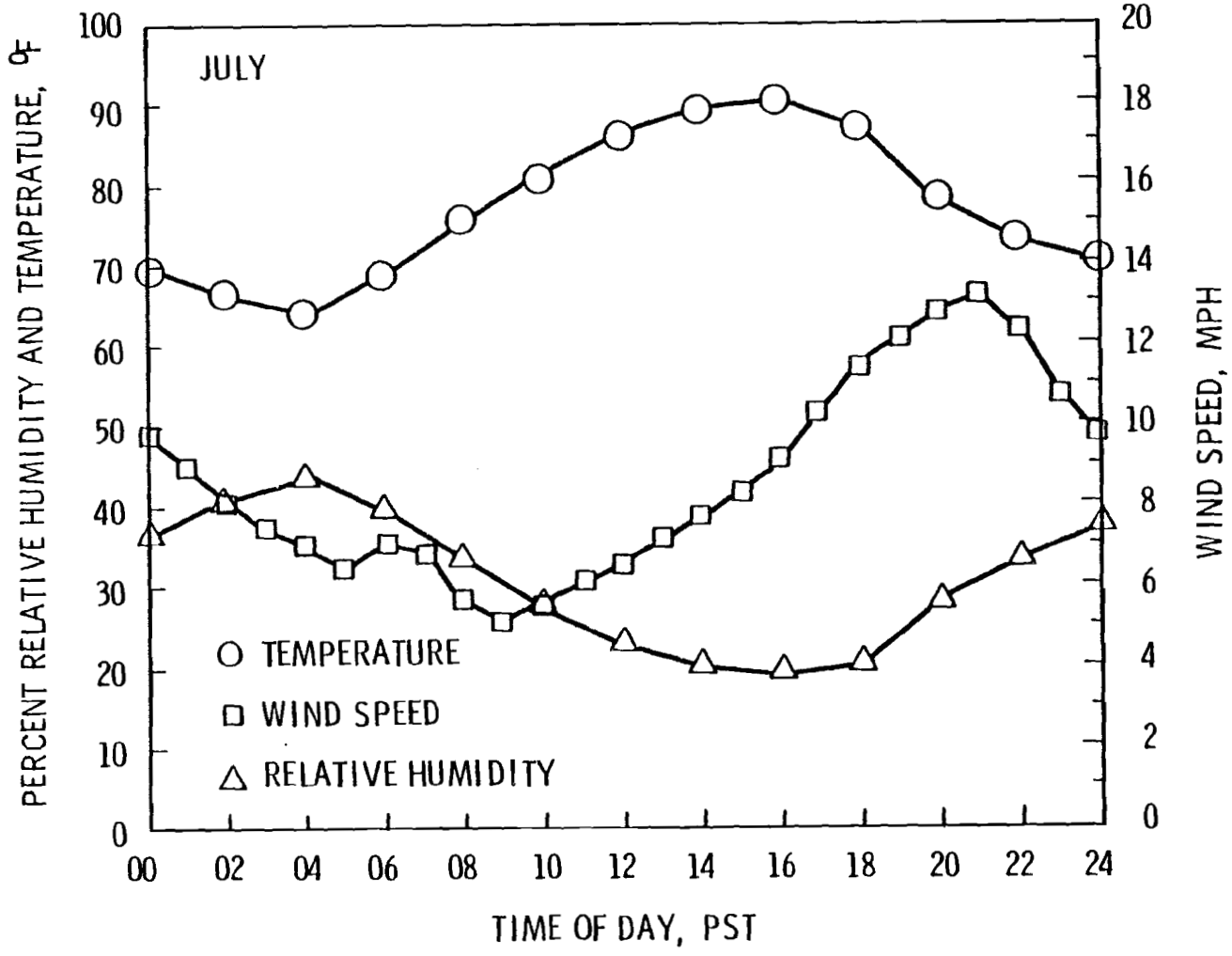

FIGURE 11. The Diurnal Cycles of Temperature, Relative Humidity and Wind Speed for July at Hanford

The observations of temperature and humidity at Hanford during the period from 1960 through 1970 were used to establish the saturation deficit climatology. The seasonal and diurnal variations of both temperature and humidity shown in Table 6 and Figures 10 and 11 would indicate that the average saturation deficit should show pronounced seasonal and daily variation. This is very much the case as is shown in Figure 12. This Figure shows a minimum deficit at about the time of sunrise and a maximum in mid-afternoon. December and January nights have particularly low deficits and are therefore the most probable times for induced saturation from moisture releases. During the summer, the average deficits are relatively large at all times even though they show a very large daily oscillation.

The distribution of the hourly saturation deficit values was determined. The particular portion of the distribution that is of interest is that describing the probability of small deficits. Figure 13 shows the probability that the saturation deficit will be less than a given value (the cumulative distribution function). Distributions are shown for both total hours and hours without fog. It should be noted that these distributions functions approach a single value for large deficits, and that they differ noticeably for low saturation deficits.

The most frequent restriction to visibility in the Hanford area is fog that occurs on an average of 38 days per year. On 24 of these days the visibility is restricted to less than 1/2 mile. Fog is highly seasonal, although it has occurred in every month. On a monthly basis, relative humidities range from a low of 30.5% in July to a high of 80.8% in December. High humidities (>90%) occur less than 1% of the time in the summer, about 9% of the time in the fall, almost 31% of the time in the winter and slightly more than 3% of the time in

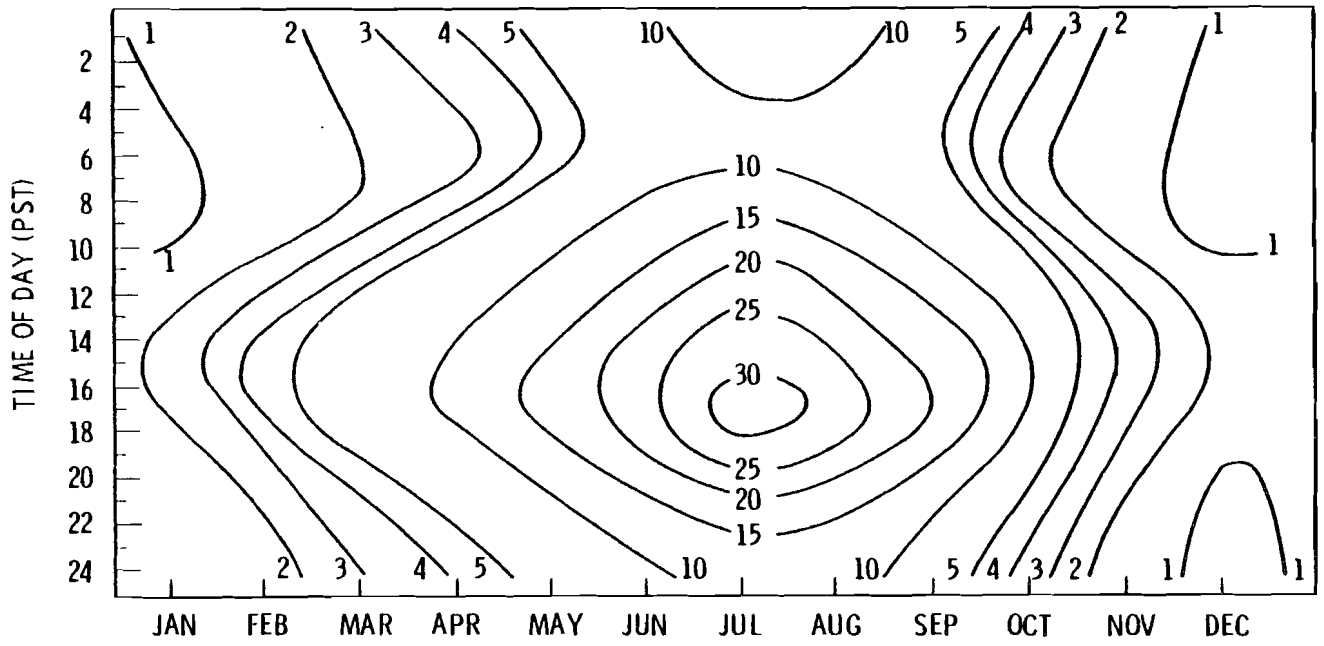

FIGURE 12. The Diurnal and Annual Variation of Average Saturation Deficit (g/m^3) at Hanford

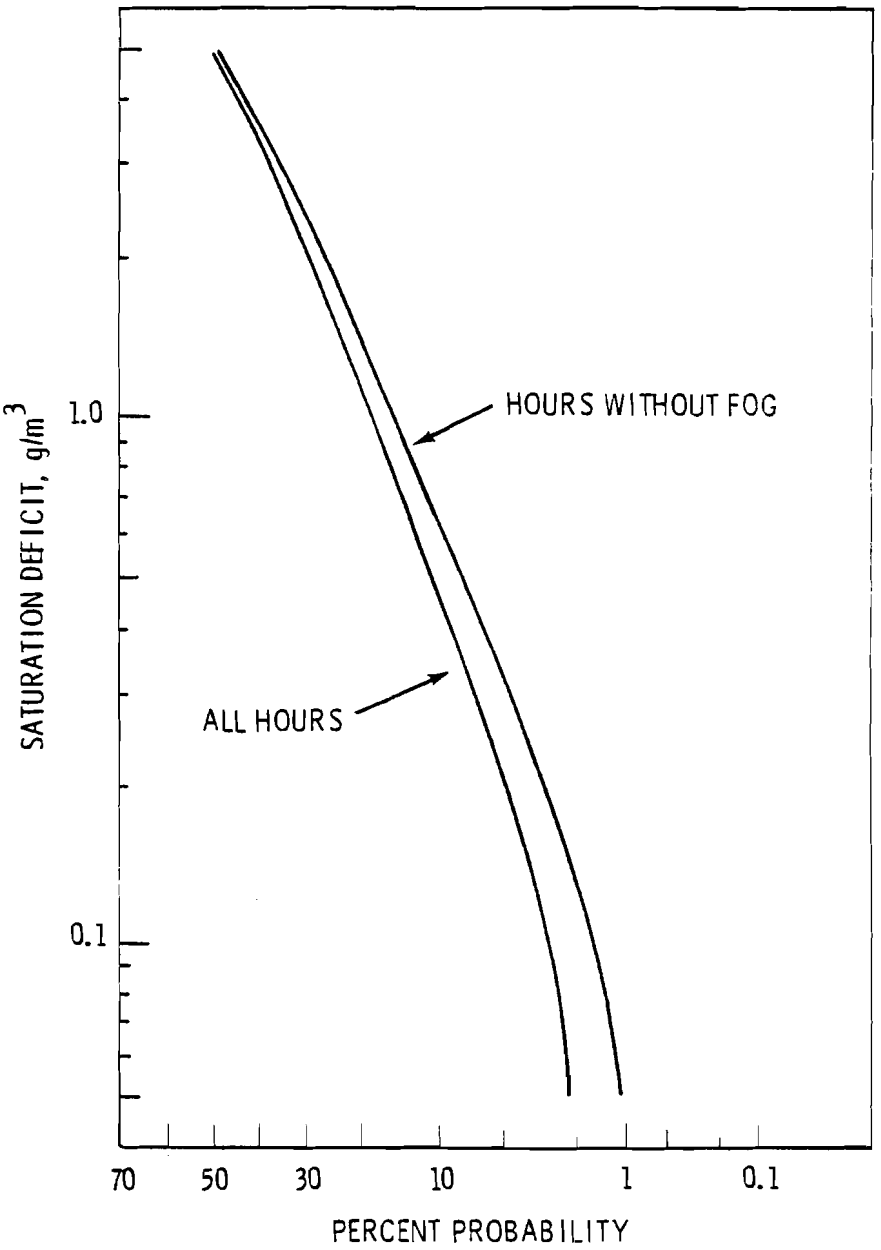

FIGURE 13. Cumulative Frequency Distributions for Saturation Deficits at Hanford

the spring. These statistics are reflected in the occurrence of fog. Of the annual average of 278 hours of fog, 95% occurs from November through February. This percentage increases to 99.7% when the months of October and March are included.

Hanford fogs are generally associated with low wind speed conditions. More than 70% of the hours of fog occur when the wind speed is less than 3.5 mph, and the average wind speed during fog is 2.5 mph. Table 7 gives detailed statistics on the duration and maximum persistence of both total and dense fog by months. January 1976 set a record for most hours of fog in a single month, 257. During that month fog was observed on a total of 20 days, including the last 16 days of the month.

Fog statistics indicate large natural variations in the occurrence of fog. The annual number of hours of fog at Hanford approximately follows a log-normal distribution as shown in Figure 14. Using observed values, a standard geometric deviation has been estimated for both hours of fog (0.285) and hours of visibility less than 1/2 mi. (0.362). Examination of more recent records does not indicate a change following deactivation of the reactors at Hanford.

Hours of fog is a rather nebulus figure for use in evaluation of impacts of large moisture releases. A better measure is related to visibility during fog. Cumulative frequency distributions of visibility during fog at Hanford (1960-1970) are shown in Figure 15 as cumulative distribution functions (cdf). The curve on the right in the figure represents the cdf for all cases of fog. The curve on the left represents those cases when the atmosphere was at or near saturation, (i.e., the saturation deficit in terms of water vapor density $\leq .05\ g/m^3$). It is obvious, that an increase in atmospheric moisture increases the density fog (reduce visibility) as well as increase the frequency.

Table 7. Total Duration and Maximum Persistence of Fog Tabulated in Hours for Hanford for the Period 1945-1970

ALL FOG (VIZ 0-6 MILES)	AVG TOTAL DURATION	MAX TOTAL DURATION	YEAR	MIN TOTAL DURATION	YEAR	AVG DURATION PER DAY OF OCCURRENCE	MAX. PERSISTENCE(3)	YEAR
JAN	68.3	193.4	1965	0	1949	7.2	58.1	1955
FEB	36.4	206.2	1963	0	1967	6.2	58.0	1963
MAR	4.4	20.6	1951	0	1968+	3.1	12.2	1949
APR	0.3	2.8	1950	0	1970+	1.4	2.8	1950
MAY	0.3	2.7	1958	0	1970+	1.2	2.7	1958
JUNE	#	0.5	1948	0	1970+	0.5	0.5	1948
JULY	#	0.7	1966	0	1970+	0.7	0.7	1966
AUG	#	1.0	1959	0	1970+	1.0	0.7	1959
SEPT	0.3	5.5	1957	0	1970+	2.0	2.6	1957
OCT	7.6	63.6	1962	0	1970+	3.9	39.0	1962
NOV	55.4	148.0	1952	1.0	1960	6.8	65.4	1963
DEC	105.4	193.8	1947	6.5	1968	8.7	72.3	1947
Y	278.4	462.5(1)	1964-65	147.7(2)	1948-49	7.0	72.3	1947-48
DENSE FOG (VIZ 1/4 MI OR LESS)								
JAN	20.4	52.4	1955	0	1949	3.4	15.0	1953
FEB	12.7	86.7	1963	0	1967+	3.8	16.7	1963
MAR	1.8	7.8	1949	0	1968+	2.2	5.0	1961
APR	0.1	1.8	1955	0	1970+	1.8	0	----
MAY	0.1	1.6	1958	0	1970+	1.6	1.6	1958
JUNE	0	0	----	0	----	0	0	----
JULY	0	0	----	0	----	0	0	----
AUG	#	1.0	1959	0	1970+	1.0	0.7	1959
SEPT	0.1	3.2	1957	0	1970+	3.2	1.4	1957
OCT	3.1	35.2	1962	0	1970+	3.1	15.8	1962
NOV	21.1	71.4	1952	0	1960	4.1	20.6	1963
DEC	42.0	119.8	1947	1.3	1968	5.4	47.0	1957
Y	101.4	201.5(1)	1962-63	47.3(2)	1948-49	4.2	47.0	1957-58

* TOTAL DURATION DENOTES TOTAL NUMBER OF HOURS AND TENTHS OF HOURS IN WHICH FOG IS OBSERVED.

\# DENOTES LESS THAN 0.05 HOUR

(1) DENOTES THE GREATEST NUMBER OF HOURS IN A SEASON

(2) DENOTES THE LEAST NUMBER OF HOURS IN A SEASON

(3) MAXIMUM PERSISTENCE OF DENSE FOG IS BASED ON THE PERIOD 1953-70

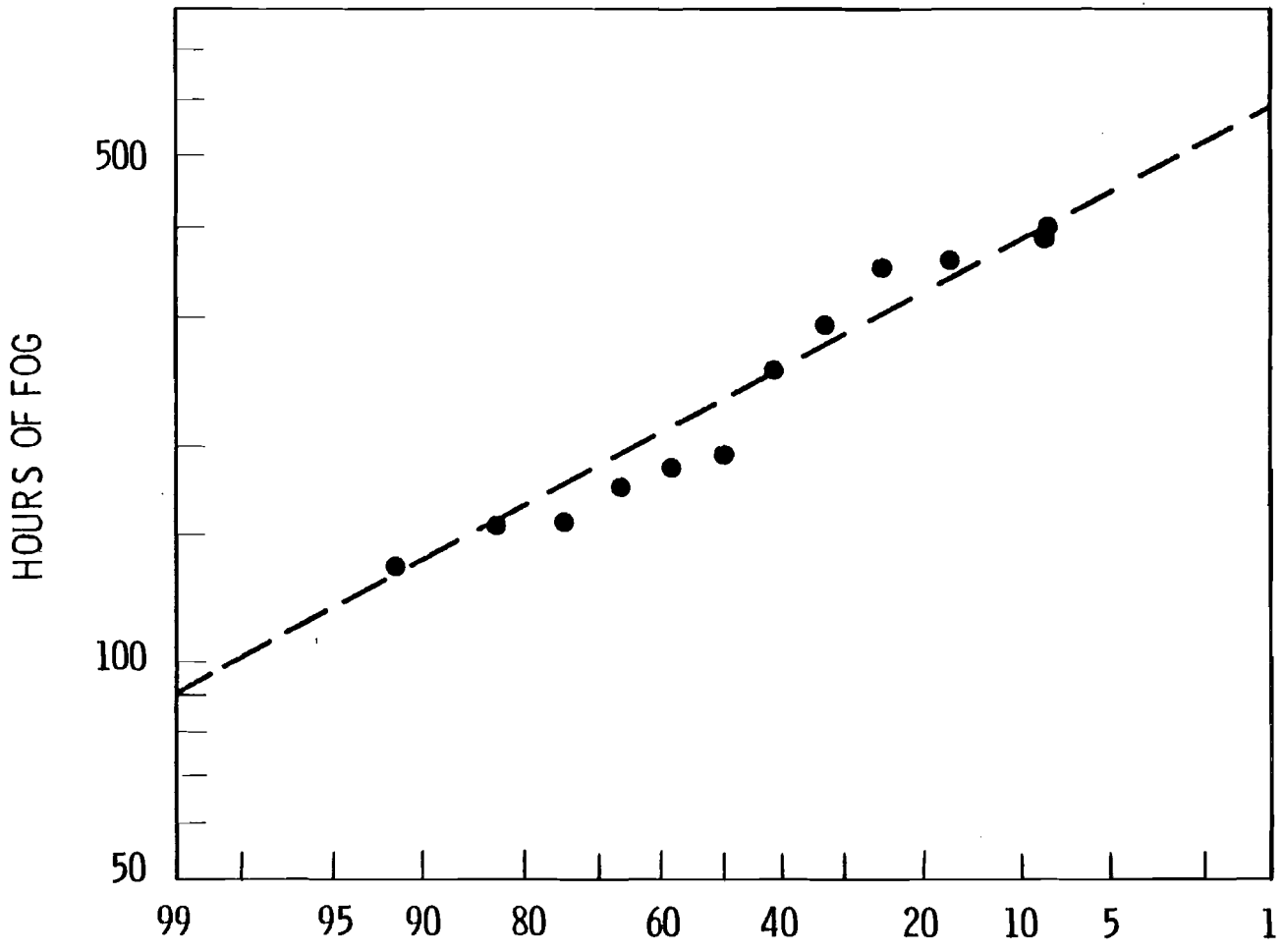

FIGURE 14. Percent Probability of Exceeding a Given Number of Hours of Fog at Hanford

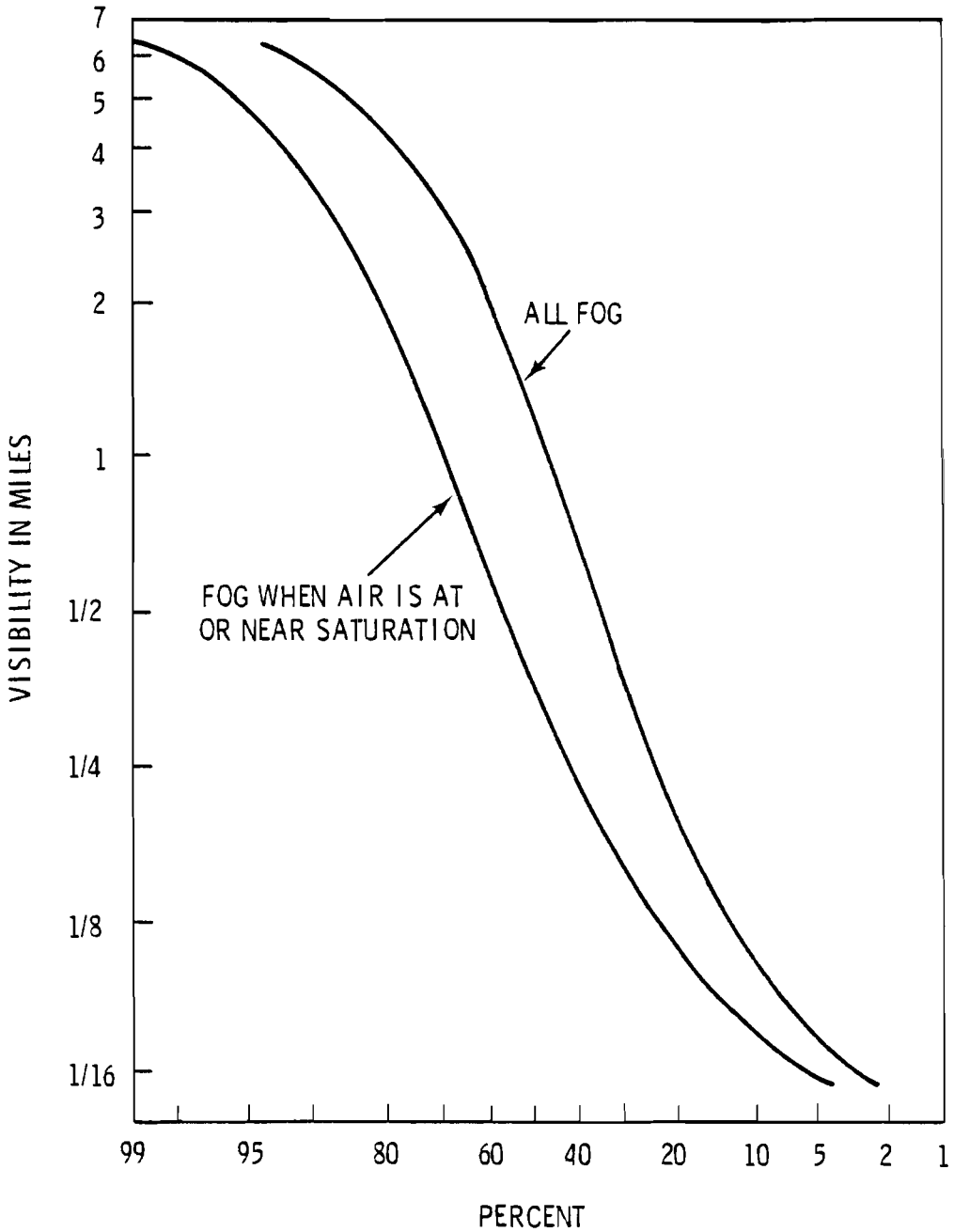

FIGURE 15. Cumulative Frequency Distributions for Visibility During Fog at Hanford

The climatological data for the HMS are generally assumed to be representative of the entire region, although local variations in the climate are known to exist. Variations of importance are those associated with the Columbia River and the major topographic features which form the sides of the basin. There are differences between the northern and southern portions of the Hanford reservation. These are primarily small differences in temperature, humidity and wind.

Diffusion Climatology

The major impact of a Hanford Nuclear Energy Center on the atmosphere will result from the release of waste heat. The extent of the impact will be further related to the ability of the atmosphere to disperse the heat. The primary factors which govern dispersion or diffusion are atmospheric stability and the wind. The stronger the wind or less stable the atmosphere the more rapid the dispersion.

Results of numerous atmospheric diffusion experiments at Hanford indicate that 4 categories adequately describe atmospheric stability variations for the purposes of diffusion modeling. Figure 16 shows wind roses for Hanford for each of these stability categories and for all categories combined. The data are presented in tabular form in Table 8. The wind roses clearly show the prevailing wind direction at Hanford is from the west northwest and northwest.

If this area were void of significant topographic features, the major impact of an HNEC would be expected to occur to the east-southeast and southeast. However, the influence of the existing topographic features makes this a very tenuous assumption. Air flow measurements made over the reservation in the past few years indicate there are frequent local circulation patterns in which the HMS wind direction does not adequately

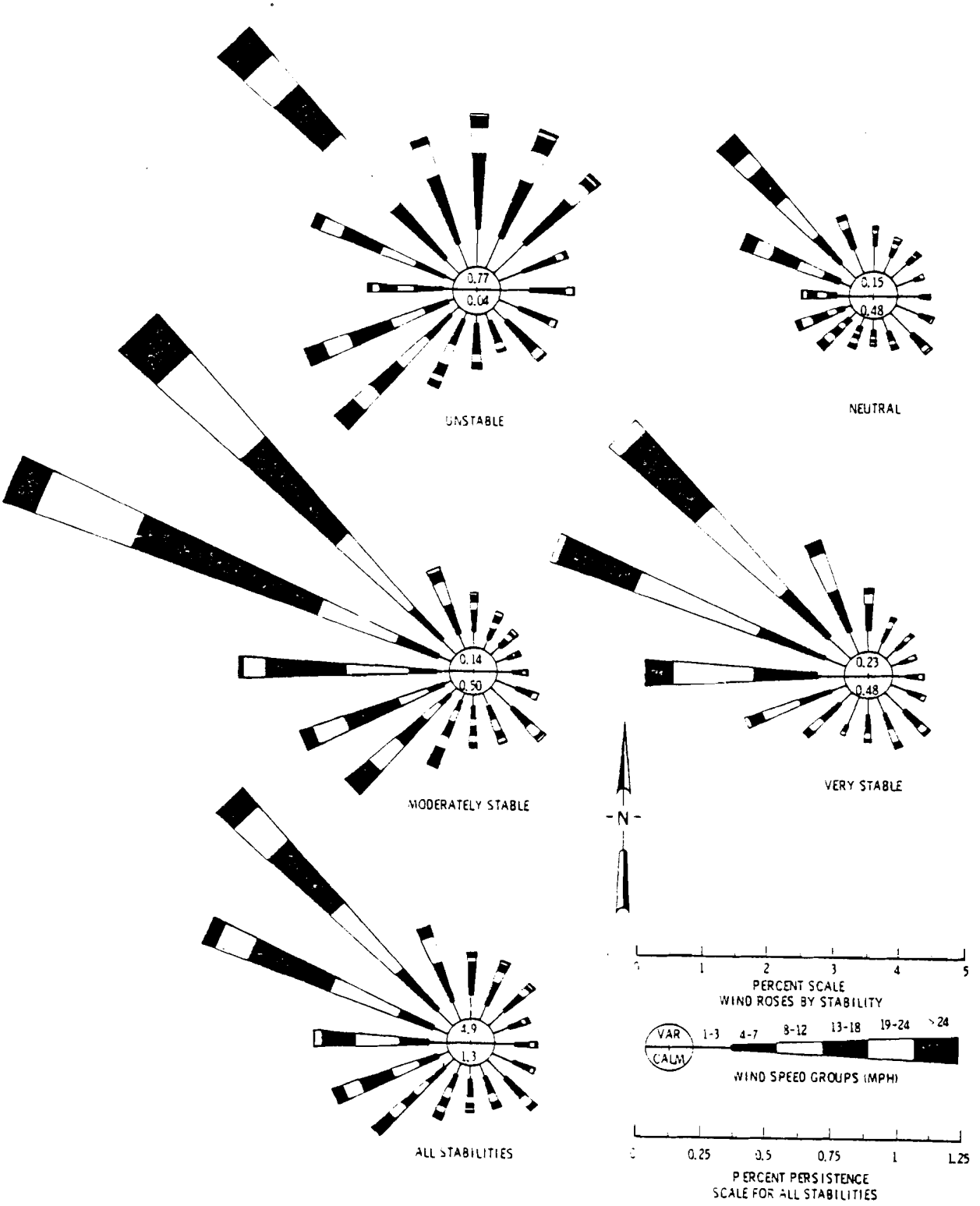

FIGURE 16. Wind Roses by Atmospheric Stability for Hanford

Table 8. Joint Probability of Wind Direction, Wind Speed and Atmospheric Stability at 200' for Hanford

		NNE	NE	ENE	E	ESE	SE	SSE	S	SSW	SW	WSW	W	WNW	NW	NNW	N	VAR.	CALM	TOTAL
0 - 3	VS	0.06	0.06	0.04	0.06	0.06	0.12	0.07	0.07	0.06	0.05	0.06	0.10	0.08	0.10	0.11	0.09	0.08	0.09	1.37
	MS	0.29	0.30	0.24	0.29	0.40	0.55	0.32	0.29	0.23	0.26	0.25	0.44	0.41	0.56	0.48	0.49	0.25	0.66	6.71
	N	0.44	0.57	0.42	0.49	0.56	0.56	0.26	0.26	0.18	0.20	0.16	0.28	0.31	0.50	0.61	0.63	0.31	0.69	7.43
	U	0.37	0.44	0.25	0.30	0.25	0.26	0.13	0.11	0.08	0.10	0.08	0.10	0.09	0.19	0.22	0.38	0.30	0.06	3.71
4 - 7	VS	0.04	0.04	0.03	0.03	0.04	0.09	0.09	0.09	0.07	0.10	0.15	0.24	0.23	0.22	0.17	0.09	0.01	0.	1.75
	MS	0.28	0.21	0.18	0.21	0.30	0.50	0.34	0.32	0.29	0.39	0.52	1.02	1.21	1.35	0.94	0.54	0.03	0.	8.62
	N	0.35	0.38	0.27	0.32	0.36	0.47	0.27	0.26	0.22	0.31	0.29	0.39	0.56	1.04	0.72	0.56	0.08	0.	6.86
	U	0.77	0.71	0.44	0.46	0.44	0.52	0.29	0.33	0.33	0.36	0.26	0.28	0.33	0.75	0.78	0.86	0.23	0.	8.13
8 -12	VS	0.01	0.00	0.00	0.00	0.00	0.03	0.06	0.03	0.02	0.05	0.12	0.26	0.34	0.59	0.20	0.02	0.	0.	1.74
	MS	0.17	0.15	0.09	0.10	0.13	0.27	0.29	0.17	0.20	0.40	0.86	1.71	2.85	2.52	0.73	0.27	0.00	0.	10.94
	N	0.21	0.12	0.07	0.07	0.09	0.13	0.13	0.13	0.23	0.40	0.44	0.48	0.86	1.36	0.33	0.21	0.	0.	5.24
	U	0.40	0.29	0.11	0.08	0.07	0.14	0.10	0.11	0.25	0.41	0.38	0.22	0.43	1.01	0.39	0.36	0.00	0.	4.75
13-18	VS	0.00	0.00	0.	0.00	0.	0.01	0.02	0.01	0.01	0.01	0.04	0.10	0.28	0.81	0.07	0.00	0.	0.	1.38
	MS	0.10	0.06	0.03	0.04	0.02	0.10	0.18	0.12	0.17	0.42	0.86	1.25	3.45	2.66	0.24	0.11	0.	0.	9.80
	N	0.15	0.06	0.02	0.01	0.01	0.04	0.07	0.11	0.23	0.49	0.63	0.55	1.13	1.06	0.11	0.10	0.	0.	4.78
	U	0.21	0.11	0.03	0.01	0.00	0.02	0.03	0.04	0.13	0.40	0.49	0.19	0.51	0.79	0.07	0.12	0.	0.	3.16
19-24	VS	0.	0.	0.	0.	0.	0.00	0.01	0.00	0.00	0.00	0.00	0.01	0.04	0.12	0.00	0.	0.	0.	0.20
	MS	0.02	0.02	0.01	0.01	0.00	0.02	0.05	0.08	0.13	0.32	0.35	0.20	1.02	1.08	0.02	0.01	0.	0.	3.33
	N	0.05	0.04	0.01	0.00	0.00	0.02	0.03	0.07	0.20	0.46	0.45	0.22	0.84	0.81	0.02	0.04	0.	0.	3.26
	U	0.05	0.04	0.01	0.00	0.	0.00	0.01	0.02	0.08	0.26	0.31	0.09	0.29	0.59	0.01	0.02	0.	0.	1.79
OVER 24	VS	0.	0.	0.	0.	0.	0.00	0.	0.00	0.00	0.00	0.00	0.00	0.00	0.00	0.	0.	0.	0.	0.01
	MS	0.00	0.00	0.	0.	0.	0.00	0.02	0.05	0.15	0.21	0.12	0.03	0.22	0.31	0.00	0.00	0.	0.	1.13
	N	0.02	0.01	0.00	0.00	0.	0.00	0.01	0.06	0.25	0.50	0.26	0.07	0.54	0.75	0.01	0.01	0.	0.	2.49
	U	0.01	0.02	0.01	0.	0.	0.	0.00	0.01	0.08	0.34	0.25	0.07	0.17	0.46	0.00	0.00	0.	0.	1.42
TOTALS	VS	0.11	0.11	0.07	0.10	0.11	0.25	0.24	0.20	0.16	0.22	0.39	0.71	0.96	1.85	0.56	0.20	0.09	0.09	6.44
	MS	0.87	0.75	0.55	0.65	0.85	1.44	1.20	1.02	1.17	2.01	2.96	4.65	9.16	8.49	2.41	1.42	0.28	0.66	40.53
	N	1.22	1.19	0.78	0.89	1.02	1.22	0.78	0.89	1.31	2.35	2.23	2.00	4.24	5.52	1.79	1.56	0.39	0.69	30.07
	U	1.82	1.62	0.84	0.86	0.76	0.95	0.56	0.63	0.95	1.87	1.77	0.93	1.82	3.77	1.48	1.74	0.53	0.06	22.96

represent air flow over the entire reservation. Evidence of these local circulations is seen in Figure 17, which shows wind roses for several locations on and surrounding the Hanford Reservation. In some cases these circulations will act to increase the rate at which the waste heat is dispersed, and in other cases they will have the opposite affect. Figure 18 further demonstrates differences in wind that can be observed at two places in relatively close proximity. The physical separation between the FFTF and the WNP-2 sites is about 2 miles, with FFTF to the west of WNP-2. The large frequency of winds from south-southwest through west at FFTF can be attributed to local circulations related to Rattlesnake Mountain that do not affect WNP-2.

A detailed evaluation of the transport and diffusion of thermal effluents from an HNEC would be a complex and relatively expensive process as a result of the local circulations. Therefore, a relatively simple dispersion model that uses HMS wind and stability data and assumes straight line transport has been used to examine the impact of various HNEC heat sink management alternatives on fog and humidity. The results of this evaluation are discussed in the next Section.

HNEC SIMULATION RESULTS

More than 50 different numerical simulations using BATMAN have been made to examine the potential impacts of moisture releases from a Hanford Nuclear Energy Center on fog and ground level humidity. Presentation of a complete set of the numerical results is beyond the scope of the present work. Rather, a summary of the pertinent results is presented. In the following sections, the predicted impact on the total number of hours of fog, the effect of site location and cooling system choice on the fog impact, and the effect of the HNEC

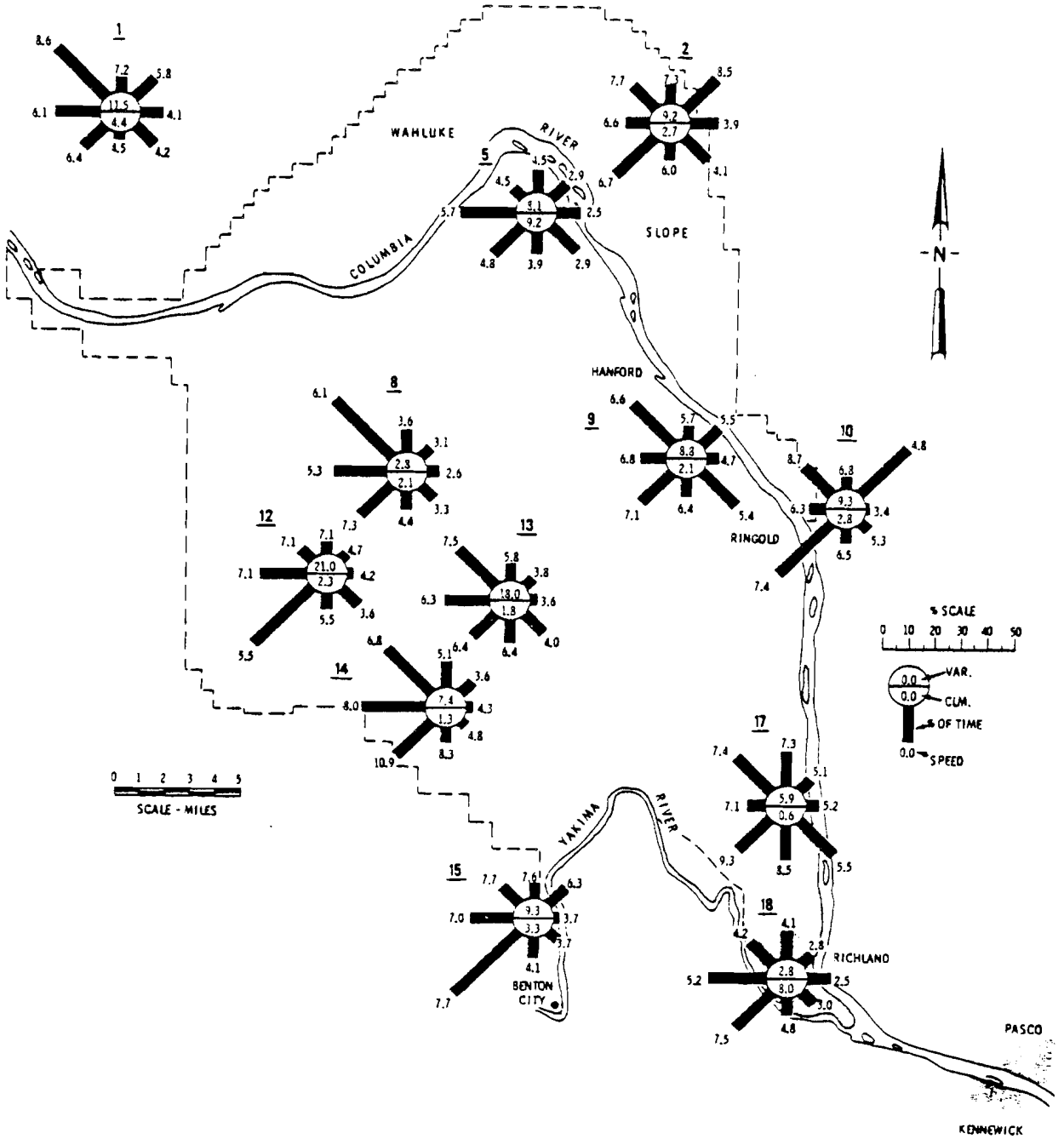

FIGURE 17. Surface Wind Roses for Various Locations on and Surrounding the Hanford Site. (The points of the rose represent the directions from which the winds come)

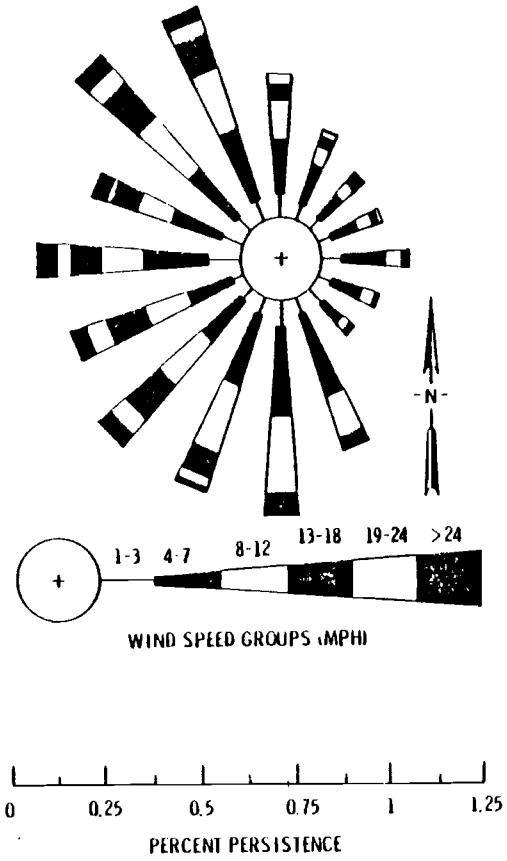

FFTF

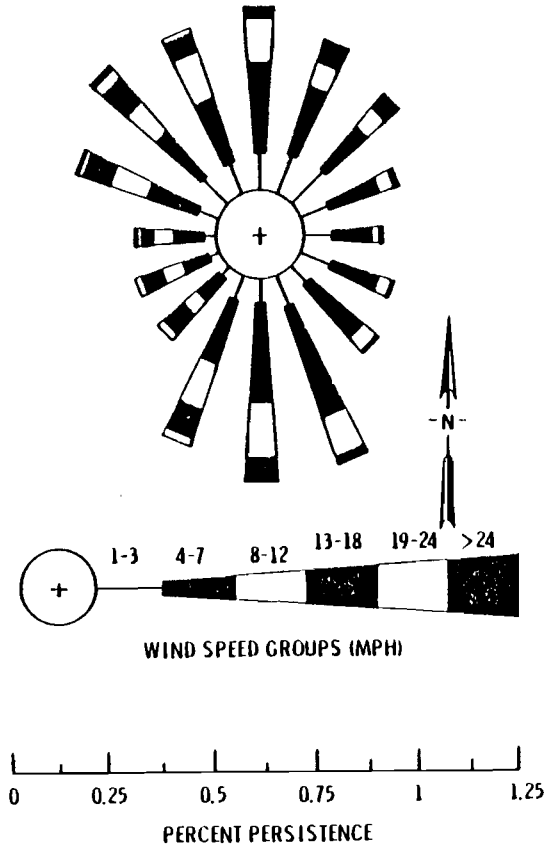

WNP-2

FIGURE 18. Wind Roses for the FFTF and WNP-2 Sites

on visibility are discussed. In addition, the statistical significance of the predicted increases in fog is evaluated. Finally, the effects of an HNEC on summer humidity are examined.

The Predicted Increase in Hours of Fog

For each case BATMAN computed the predicted increase in fog at all grid points. Rather than summarize the predictions at specific locations, a number of general areas have been selected. These areas are: the Tri-Cities (Richland, Kennewick and Pasco), Eltopia, Othello, Beverly, the Hanford Meteorological Station, and Benton City. Table 9 gives the predicted increase in hours of fog at each of these locations for the 27 cases under consideration.

The numbers given in the Table are representative of the general region; they should not be taken as absolute. It is more realistic to compare the predictions for various cases at a site and to make evaluations on that basis than it is to assume each number is accurate.

The Tri-Cities is the most populous area near Hanford. Thus increases in fog in that area would have the maximum impact on individuals. Predicted increases in fog range from 15 hours for a single, 4 reactor cluster to 288 hours for a 40 reactor energy center. The larger predicted increases in fog could have a significant socio-economic effect.

Eltopia was selected to represent the agricultural region east of the Columbia River and north of Pasco. It also represents the conditions on Highway 395 north of Pasco. Increases in fog in this area might have some impact on agriculture, but the probable timing of fog would tend to mitigate this impact. A potentially more significant impact is the reduction of visibility along the highway. There are already frequent accidents above this section of road. In general the predicted

Table 9. Predicted Increases in Hours of Fog in Selected Areas

Case	Tri-Cities Average	Eltopia	Othello	Beverly	Hanford Met Station	Benton City
1	15	6	1	6	2	2
2	98	97	19	30	30	39
3	88	84	36	21	112	28
4	106	57	30	33	116	33
5	102	74	32	31	129	35
6	100	81	16	29	29	21
7	250	208	118	187	578	152
8	207	154	94	161	480	135
9	78	52	26	25	84	25
10	55	41	11	26	14	14
11	122	83	41	118	197	74
12	210	197	75	53	168	88
13	112	84	28	44	50	50
14	288	211	118	191	524	175
15	74	68	18	23	19	26
16	57	37	11	18	15	21
17	37	32	8	11	4	10
18	164	147	51	46	110	69
19	117	97	34	34	71	48
20	63	37	13	22	24	24
23	60	36	12	30	30	20
24	144	127	50	47	103	49
25	44	34	9	21	10	12
26	34	29	6	18	8	7
27	90	54	25	40	37	30

increases in fog for Eltopia are smaller than for the Tri-Cities, but they are larger than for other areas off the Hanford Reservation.

The impact of an HNEC on the area north of the Hanford Reservation is represented by the predictions for Othello and Beverly. The population in the area is small, however Highways 24 and 243 are reasonably well traveled. In general the predicted increases here are relatively small. This is a reflection of atmospheric conditions favorable to diffusion and a low frequency of occurrence of southerly winds.

Advantages of Hanford as a potential site for a nuclear energy center are the large area available and the distance to populated locations. These factors tend to diminish the effect of any impact that moisture releases might have on fog. The predictions for Hanford Meteorological Station were selected to represent the conditions in the vicinity of and within the NEC. As such it is to be expected that the largest increases in fog should occur there. Under some conditions the impact there is twice that for the Tri-Cities. However, there are other cases where the reverse is true.

Finally Benton City was selected to represent the region to the west of Richland and south of Rattlesnake Mountain. Increases in fog in this area could significantly affect traffic along Highway 12. They could also affect agriculture by preventing or reducing the severity of late spring freezes that damage fruit crops in the area. In most cases the predicted fog increases for Benton City are relatively small.

The Influence of Site Location on Fog Increases

If the predicted increases in fog in Table 9 for cases 2 through 6 are examined, the influence of general siting strategies on the impact of fog increases can be evaluated. In cases 2 and 3 the clusters are located on lines approximately

perpendicular and parallel, respectively, to the prevailing wind direction. In case 4 they are spread over the entire reservation, and in cases 5 and 6 they are clustered on the north and south sides of the reservation, respectively. In each case all clusters were assumed to use low-level, mechanical draft cooling towers.

The effect of varying cluster locations on the predicted increase of fog in the Tri-Cities is rather small. The single largest factor in the changes in the predictions is the use of sites 6 and 7 or site 11. In general the variations in the other areas of interest off the Hanford Reservation are also small, and can be tied to the use of particular sites rather than a particular siting strategy.

The Hanford Meteorology Station represents the area where the predicted fogging impact is most affected by the choice of cluster locations. Because of the prevailing Northwest winds, the HMS is very susceptible to increases in fog when clusters are located at sites 6 and 7.

On the basis of foregoing evaluation, it was concluded that, except for local effects, the formation of fog was a secondary factor in determining the location of the clusters. As a corollary, it was concluded that the fogging impact of an HNEC would be only secondarily related to the ultimate location of reactor clusters.

The Influence of Cooling System Type on Fog Increases

The influence of cooling system type on the increase in fog was examined for a 20 reactor HNEC using the results of cases 2, 7 through 10, and 15 through 17. In these cases the clusters were positioned to take advantage of river water for helper cooling systems, natural basins for ponds, and proximity of the Tri-Cities for cooling towers.

The results given in Table 9 indicate that for conventional cooling systems the greatest fogging impact is caused by ponds. Tall cooling towers (natural draft or mechanically-assisted, natural draft) have the least impact. The Columbia River is too small to accommodate a 20 reactor HNEC on once through cooling, however substitution of the river for a portion of load should reduce the total impact off the Reservation. This is confirmed by the results of cases 25 and 26.

The impacts predicted for the use of either cooling ponds or helper cooling ponds were enough larger than those for cooling towers and helper towers to eliminate consideration of these two systems as the primary systems in a 40 reactor center. Case 14 did consider the combination of tall cooling towers and helper ponds, and it will be noted that this combination has the greatest impact on the Tri-Cities. It is improbable that adequate sites exist for cooling more than 2 or 3 clusters with ponds at Hanford.

The use of hybrid wet/dry cooling towers can significantly reduce the predicted increases in hours of fog. The results of cases 1, 2, 15, 16 and 17 have been combined to indicate the potential reduction as shown in Figure 19. By the use of a sufficiently large dry cooling fraction, hybrid wet/dry systems can reduce the fogging impact to essentially zero. The 15 hours of fog shown for 0% wet cooling result from 4 low-level, wet towers assumed for site 1 in all simulations.

Examination of the results of the mixed cooling system simulations shows that the use of once-through cooling for 1 or 2 clusters has essentially the same effect as using a relatively large fraction (∿50%) of dry cooling.

On this basis, it is concluded that the use of tall cooling towers supplemented with once-through cooling is the optimum combination of conventional cooling systems. Almost

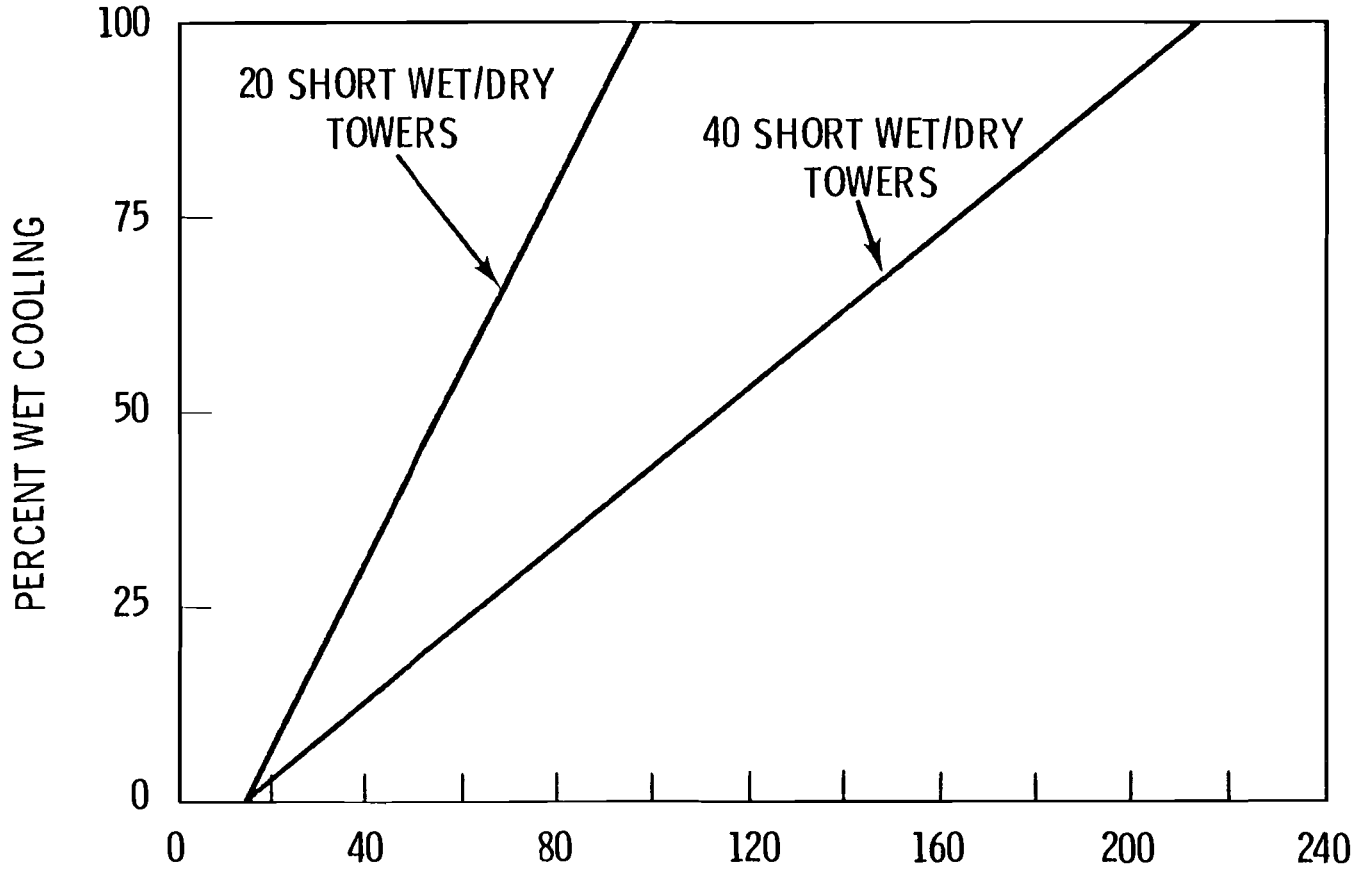

FIGURE 19. Relationship Between Increased Hours of Fog for an HNEC Using Hybrid Wet/Dry Cooling Systems and the Percent Wet Cooling

as acceptable is the sole use of tall towers. If a lesser impact on fog is required the only alternative, short of not constructing an HNEC, is the use of hybrid wet/dry towers with a very high percentage of dry cooling. It is also concluded that ponds are not acceptable for HNEC cooling for other than as emergency systems.

The Reduction of Visibility in the Tri-Cities

As indicated earlier, hours of fog is a somewhat nebulus impact. Fog may be relatively light and have little impact, or it may be dense and have a very significant economic impact. Thus, to establish the socio-economic impact of an HNEC through increased fog, it is necessary to describe the increase in frequency of fog in terms of visibility. This is also important as an aid in reducing the subjectiveness of the definition of fog when dealing with the public.

In order to convert hours of fog to visibility, it was necessary to develop a relationship between the two. The moisture releases from an NEC can contribute to fog by causing fog to form or by making naturally occurring fog more dense. Both contributions must be considered when making the conversion from hours of fog to visibility.

The relationship between increases in fog and increases in the occurrence reduced visibility assumed in this study is:

$$\Delta Hv_k = [\Delta Hf_k + (Hf - Hv)P_k(\Theta)]P(V<V_r|d\leq.05\ g/m^3) \qquad (8)$$

where ΔHv_k is the increase in hours of $V<V_r$ at receptor k; ΔHf_k is the increase in the total hours of fog (Table 9); Hf is the average number of hours of natural fog; Hv is the average number of hours with $V<V_r$ under current conditions; $P_k(\Theta)$ is the probability the wind direction will carry moisture from the

HNEC to the receptor, $P(V<V_r|d\leq.05\ g/m^3)$ is the probability that the visibility will be less than V_r given the occurrence of fog and a saturation deficit of .05 g/m^3 or less (Figure 15); and V and V_r are the visibility and reference visibility respectively. For an HNEC and a receptor in the Tri-Cities, $P_k(\Theta)$ is .2205. Further, assuming that HMS fog statistics are representative for the Tri-Cities, Hf is 278 hours. For visibilities of 3, 1, 1/2, 1/8 and 1/16 miles the values of Hv are 195, 132, 97, 39 and 8 hours, respectively.

The increased visibility reductions that are predicted for the Tri-Cities are given in Table 10. It will be noted that for the single cluster case, and for other cases where the predicted increase in total hours of fog is small, the increase in the number of hours with visibility restriction to less than 3 miles exceeds the increased hours of fog. It will also be noted that the maximum increase in hours of visibility less than 1/16 mile is less than a factor of 5 larger than the increase predicted for a single 4 reactor cluster.

The increases given in Table 10 are combined with climatological information on visibility in Table 11 to show the predicted conditions in the Tri-Cities for various HNEC configurations. The various visibility categories were chosen with transportation in mind. When visibility drops below 3 mi, flight rules change from visual to instrument and many private pilots are effectively grounded. At 1 mile all flight operations at the Richland Airport stop, and at 1/2 mile the Pasco Airport closes. When the visibility falls to 1/8 mile or less, ground transportation is affected.

The Statistical Significance of the Predicted Increases

The mention of the impact of visibility reduction on transportation indicates a potential measure of significance

Table 10. Predicted Increases in Hours of Reduced Visibility in the Tri-Cities

	All Fog	Hours of Visibility <3	<1	<1/2	<1/8	<1/16
4 Reactor Cluster						
1	15	29	33	31	16	4
20 Reactor Center						
2	98	103	91	79	36	9
7	250	237	198	165	73	17
8	207	199	167	141	62	15
9	78	85	77	67	31	8
10	55	65	61	54	26	6
11	122	124	108	92	42	10
15	74	82	74	65	30	7
16	57	65	62	55	26	6
17	37	49	48	44	22	5
23	60	69	65	57	27	7
25	44	55	53	48	23	6
26	34	46	46	42	21	5
40 Reactor Center						
12	210	202	170	142	63	15
13	112	115	101	87	40	9
14	288	271	224	187	82	19
18	164	161	137	116	52	12
19	117	120	104	89	41	10
20	63	72	67	59	28	7
24	144	144	123	105	47	11
27	90	96	86	74	34	8

Table 11. Predicted Fog Conditions in the Tri-Cities with an HNEC (current conditions and predicted increases)

	Total Hours of Fog	Hours with Visibility				
		<3	<1	<1/2	<1/8	<1/16
Current Conditions	278	195	132	97	39	8
4 Reactor Cluster						
1	293	224	165	128	55	12
20 Reactor Center						
2	376	298	223	176	75	17
7	528	432	330	262	112	25
8	485	394	299	238	101	23
9	356	280	209	164	70	16
10	333	260	193	151	65	14
11	400	319	240	189	81	18
15	352	277	206	162	69	15
16	335	260	194	152	65	14
17	315	244	180	141	61	13
23	338	264	197	154	66	15
25	322	250	185	145	62	14
26	312	241	178	139	60	13
40 Reactor Center						
12	488	397	302	239	102	23
13	390	310	233	184	79	17
14	566	466	356	284	121	27
18	442	356	269	213	91	20
19	395	315	236	186	80	18
20	341	267	199	156	67	15
24	422	339	255	202	86	19
27	368	291	218	171	73	16

of the predicted increases. Other socio-economic tests of significance can be envisioned; they are difficult to evaluate. It is possible, however, to evaluate the statistical significance of the predicted increases by using the Hanford fog data and making several assumptions.

If natural climatic change is neglected, pre and post operational climatological data are assumed to exist, and the HNEC is completed at a single time, the hypothesis that an increase in fog has occurred can be tested. The t-statistic for examining the change of geometric mean in a log-normal distribution is

$$t_{\alpha,f} = \frac{\ell n\left(\frac{H_f + \Delta H}{H_f}\right)}{\sigma_{\ell n H_f}\left[\frac{1}{n_o} + \frac{1}{n_1}\right]^{\frac{1}{2}}} \qquad (9)$$

where α is the level of significance, f is the number of degrees of freedom $(n_o + n_1 - 2)$, H_f is geometric mean number of hours of fog, and ΔH is the increase, $\sigma_{\ell nH}$ is the standard geometric deviation of the distribution of H, and n_o and n_1 are the number of years of fog of climatology before and after the HNEC started operation. For 26 years of Hanford data H_f is 278 hours and $\sigma_{\ell nH}$ is .285.

Rather than compute a t-statistic, it is more informative to use tabled values of t and use (9) to compute the minimum statistically significant increases at a 5% level assuming values for n_1. This has been done and the results are given in Table 12 for both total increase in hours of fog and increase in hours of fog with visibility less than 1/2 mile (H_r = 101 and $\sigma_{\ell nH}$ = .362).

Table 12. Minimum Statistically Significant Increases in Fog in the Tri-Cities

Years of HNEC Operation	Increased Hours of Fog	Increased Hours with Visibility <1/2 mi
2	102	58
4	83	40
6	68	33
16	46	22
36	36	17
∞	27	13

The minimum statistically significant increases in Table 12 should be compared with the appropriate predictions in Tables 9 and 10. It is immediately obvious that many of the predicted increases are statistically significant. It is also evident that the predicted increases in dense fog (visibility less than 1/2 mile) may be significant when the increase in total hours of fog is not.

The Impact on Summer Humidity

Summer simulations were run to determine the impact of an HNEC on humidity to provide information for use in estimating the potential moisture release on human comfort. Figures 20, 21 and 22 show the number of hours that water vapor increases resulting from low-level, mechanical draft cooling towers would exceed 1 g/m^3 for a single cluster, a 20 reactor center and a 40 reactor center at Hanford, respectively. An increase of 1 g/m^3 in water vapor is equivalent to an increase in relative humidity of about 2% at 95 °F (see Figure 8). At a lower temperature more typical of morning and evening hours the increase in relative humidity would be between 5 and 10%.

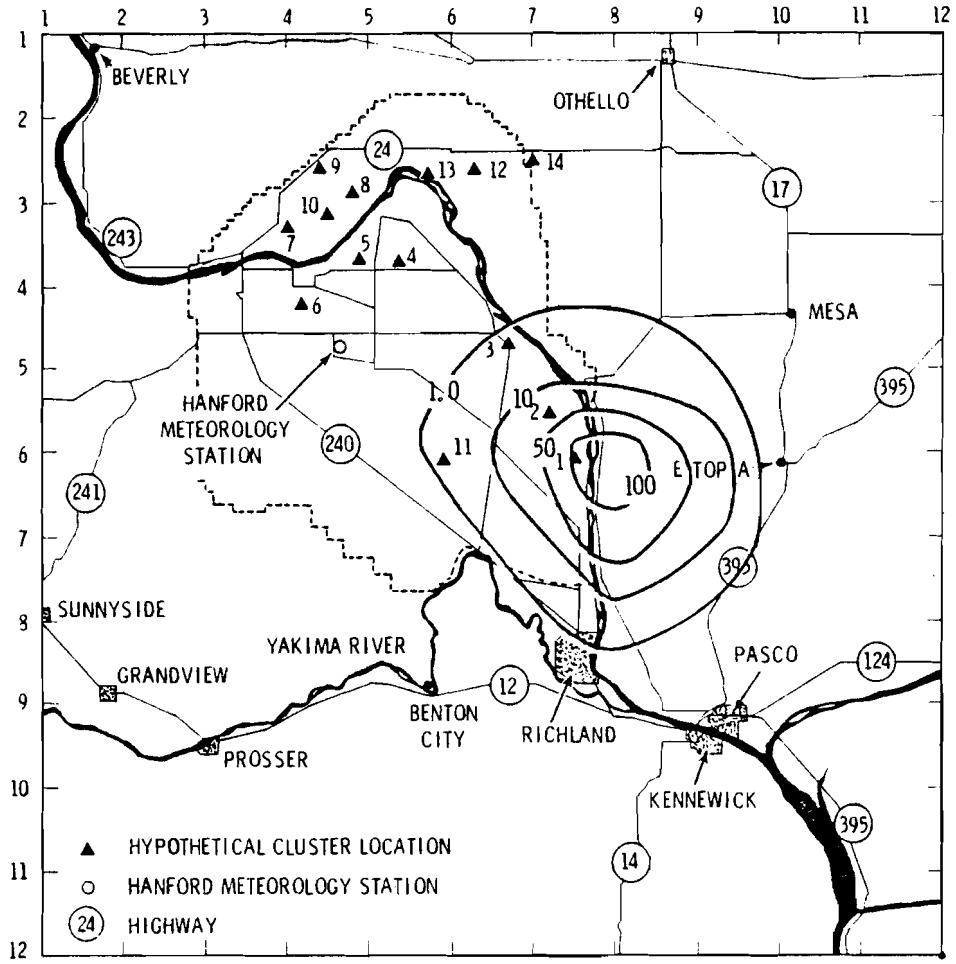

FIGURE 20. Hours of Water Vapor Density Increase Exceeding 1 g/m^3 During Summer Months for a Single Cluster at Hanford

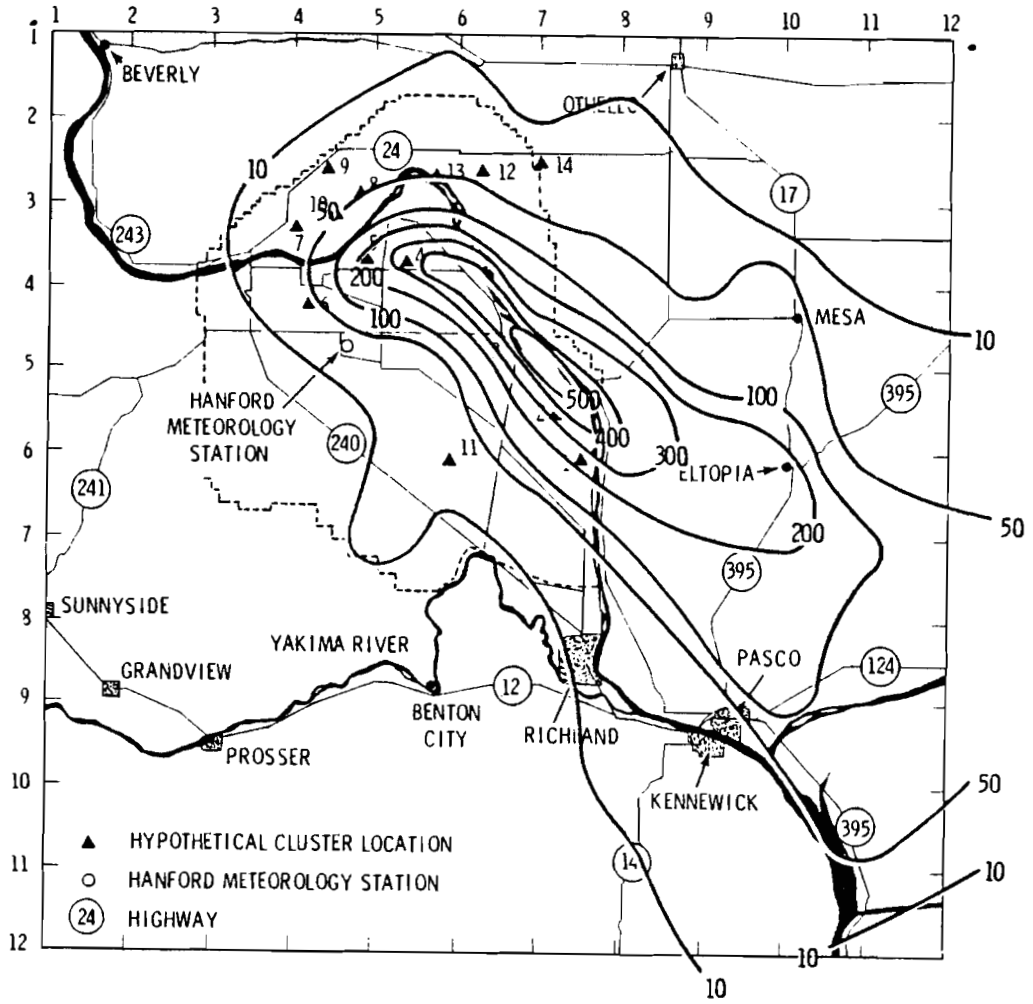

FIGURE 21. Hours of Water Vapor Density Increase Exceeding 1 g/m^3 During Summer Months for a 20 Reactor Energy Center at Hanford

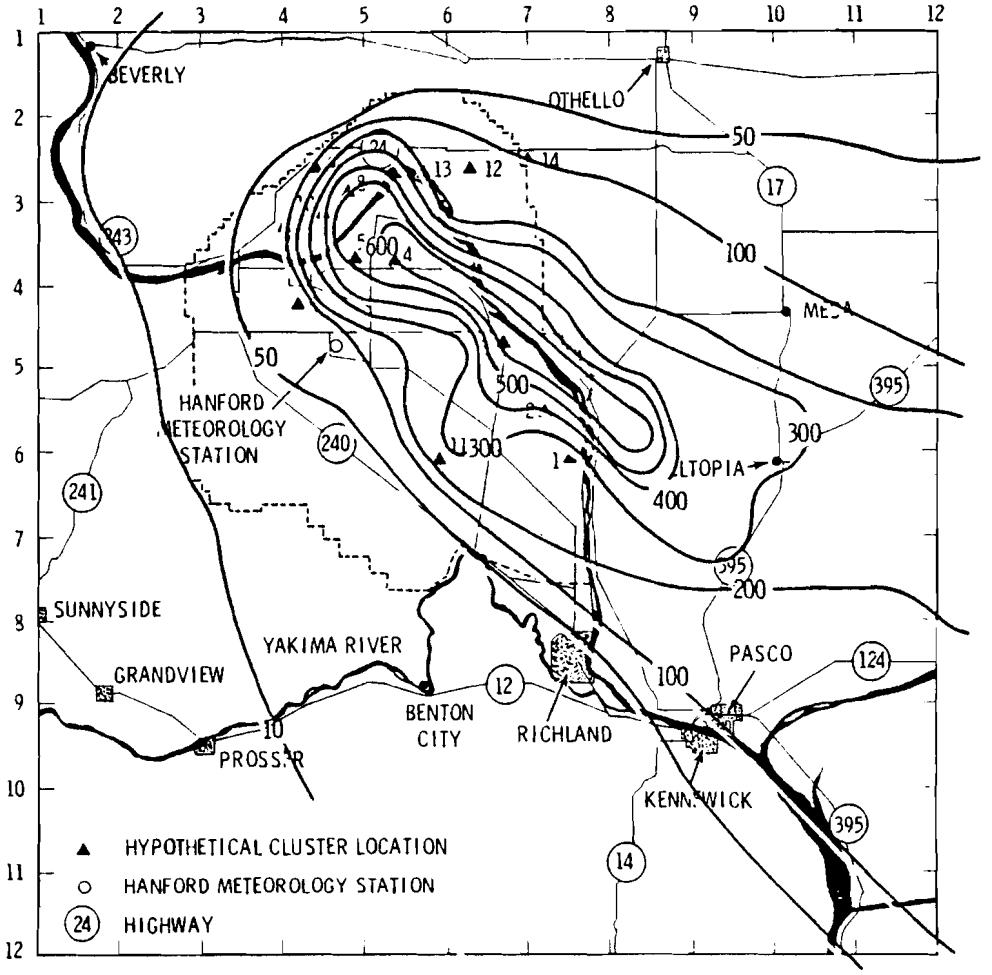

FIGURE 22. Hours of Water Vapor Density Increase Exceeding 1 g/m^3 During Summer Months for a 40 Reactor Energy Center at Hanford

In examining these figures it is interesting to note the increase in both the frequency and areal extent of the HNEC impact as the number of reactors grows. Figure 20 shows the impact of a single cluster to be negligible and almost totally confined to the Hanford Reservation. As the number of clusters increases to 5, the effect becomes more prevalent to the east of the Reservation, but still affects relative humidity in the Tri-Cities less than 100 hours. The full 40 reactor HNEC increases the atmospheric humidity by 1 g/m^3 in the Tri-Cities about 150 hours each summer.

While the predicted humidity increases are small at the normal summer time temperatures they may cause some discomfort. No attempt has been made to evaluate changes in a temperature humidity or comfort index due to the increased humidity.

CONCLUSIONS

The major conclusions of this study are:

1) The cooling systems used in an HNEC will be a primary factor in determining the fogging impact. For a given HNEC size the impact can be minimized by using a combination of tall (natural or mechanically assisted natural draft) cooling towers and once-through cooling. Hybrid wet/dry cooling towers can achieve a relatively low impact if a large fraction of the cooling (≥50%) is accomplished by dry heat exchange. The maximum fogging impact would be associated with cooling ponds.

2) The positions of the 4 reactor clusters of the HNEC within the Reservation would only have a secondary effect on the fogging impact. Increase in fog should not be an important factor in selection of cluster locations.

3) The number of hours of fog in the Tri-Cities could be increased by almost 300 for a 40 reactor HNEC and 250 for a 20 reactor center if conventional, low-level evaporative cooling systems are used. Other areas surrounding the Hanford Reservation would be affected less frequently. On the Reservation the number of hours of fog at the Hanford Meteorology Station could increase by almost 600.

4) The moisture releases from an HNEC would increase the density of naturally occurring fog. The changes in number of hours with low visibility are percentagewise greater than those in the total number of hours of fog.

5) Both the predicted increases in number of hours of fog and numbers of hours of low visibility are greater than the minimum statistically significant increases. Thus, they would be apparent in climatological data.

6) The statistical significance of the predicted increases does not indicate the extent of their socio-economic impact. It is necessary to evaluate these increases in socio-economic terms to identify the extent of the problems which might occur from increased fogging.

7) BATMAN is a relatively simple model which glosses over many physically important considerations in estimating the increased frequency of fog. If the predicted increases in fog are determined to present a serious problem, a detailed study should be made using more realistic models.

REFERENCES

1. J. K. Soldat, Radiological Impact of a Nuclear Energy Center on the Environment, BNWL-B-333, Battelle, Pacific Northwest Laboratories, Richland, WA, January 1974.

2. Electric Power Transmission for a Hanford Nuclear Energy Center, BNWL-B-426, Battelle, Pacific Northwest Laboratories, Richland, WA, September 1975.

3. E. T. Merrill and R. M. Fleishman, Status Report - Conceptual Fuel Cycle Studies for the Hanford Nuclear Energy Center, BNWL-B-437, Battelle, Pacific Northwest Laboratories, Richland, WA, November 1975.

4. W. W. Laity, Heat Sink Management for a Hanford Nuclear Energy Center, BNWL-B-448, Battelle, Pacific Northwest Laboratories, Richland, WA, November 1975.

5. The Hanford Nuclear Energy Center, An Interim Conceptual Study, BNWL-B-458, Battelle, Pacific Northwest Laboratories, Richland, WA, October 1975.

6. J. R. Young, L. D. Kannberg, J. V. Ramsdell, W. H. Rickard and D. G. Watson, Selection of Heat Disposal Methods for a Hanford Nuclear Energy Center, BNWL-2003, Battelle, Pacific Northwest Laboratories, Richland, WA, June 1976.

7. Nuclear Energy Center Site Survey-1975, Part III. Technical Considerations, NUREG-0001, U. S. Nuclear Regulatory Commission, January 1976.

8. "Hail Suppression Up in the Air," Science, 191:932, 1976.

9. F. A. Gifford, Jr., "An Outline of Theories of Diffusion in the Lower Layers of the Atmosphere," in Meteorology and Atomic Energy-1968, D. Slade, ed., TID-24190, U. S. Atomic Energy Commission, July 1968.

10. G. A. Briggs, Plume Rise, TID-25075, U. S. Atomic Energy Commission, November 1969.

11. G. A. Briggs, "Diffusion Estimation for Small Emissions," Atmospheric Turbulence and Diffusion Laboratory 1973 Annual Report, ATDL-106, pp. 83-145, December 1974.

12. G. T. Csanady, Turbulent Diffusion in the Environment, D. Reidel, Boston, MA, 248 pp., 1973.

13. The Colheat River Simulation Model, HEDL-TME-72-103, Hanford Engineering Development Laboratory, Richland, WA, August 1972.

14. W. A. Stone, D. E. Jenne and J. M. Thorp, Climatography of the Hanford Area, BNWL-1605, Battelle, Pacific Northwest Laboratories, Richland, WA, 1972.

15. S. Petterson, Introduction to Meteorology, McGraw-Hill, New York, 327 pp., 1958.

APPENDIX A

BATMAN USER'S GUIDE AND COMPUTER CODE

BATMAN USER'S GUIDE AND COMPUTER CODE

Although no attempt has been made to optimize the programming in BATMAN, it is a relatively compact code. The maximum core required in compilation on a CDC 6600 is less than 20,000 words, and the maximum in program execution is less than 12,000 words. Program run time is about 20 sec for a 5 complex NEC with 320 possible combinations of wind direction, wind speed and atmospheric stability. Computations for a 10 complex reactor require about 35 sec. This appendix describes the input deck required to run BATMAN, gives 2 examples of input decks, and gives a listing of the program.

The input deck for BATMAN consists of 16 different types of cards. The read and associated format statements for these cards are shown in Figure A1. Not all of these cards are required for a given simulation.

The first card, NCASES, indicates the number of different simulations to be run in a single submission. It is followed by a cards, IOPT, which controls input and output options. If IOPT(1)=0 the code computes the increases in water vapor density for a single set of atmospheric conditions and prints them (see Figures 4 and 5). If IOPT(1)=1, increases in vapor density are computed for several sets of atmospheric conditions and the results are converted to hours of increase within selected ranges (see Figure 6). IOPT(2) controls the number of climatic data cards. If IOPT(2)=1, the program reads in the number of climate cards, otherwise it computes the number of cards from the number of wind direction and speed categories. Setting IOPT(3)=1 causes BATMAN to convert the hours of increased water vapor density into increased hours of saturation (fog) (see Figure 7).

```
      READ(5,10020) NCASES
      READ(5,10020) IOPT
      READ(5,10023) NXLIM,(XLIM(I),I=1,10)
      READ(5,10001) EFF(1),FQ(1),EFF(2),FQ(2),EFF(3),FQ(3),EFF(4),FQ(4),
     +    EFF(5),FQ(5)
      READ(5,10011) NS,NU,KSTAR,T
      IF(IOPT(2).EQ.1) READ(5,10023) NDC
      READ(5,10023)IDIR(I),UBAR(I),(FREQ(I,J),J=1,KSTAR)
      READ(5,10023) NHOURS
      IF(IOPT(3).EQ.1) READ(5,10012) (AHOURS(IH),IH=1,NXLIM)
      READ(5,10026) NZ,(Z(I),I=1,10)
      READ(5,10012)ANG,ZLID,UBC
      READ(5,10012) XSPACE,YSPACE
      READ(5,10012) CF
      READ(5,10000) HEAD
      READ(5,10002) NSITES
      READ(5,10004)NUNITS(I),KTYPE(I),POS(I,1),POS(I,2),QE(I),HO(I),W(I)
```

```
10000 FORMAT(10A8)
10001 FORMAT(10X,14F5.3)
10002 FORMAT(10X,14I5)
10004 FORMAT(10X,2I5,6F10.2)
10011 FORMAT(10X,3I5,5F10.0)
10012 FORMAT(10X,10F7.2)
10020 FORMAT(10X,10I1)
10023 FORMAT(10X,I5,13F5.2)
10026 FORMAT(10X,I5,13F5.0)
```

FIGURE A1. Input Statements and Formats for BATMAN

The third card in the deck defines ranges for summarization of the frequency of vapor density increases. It is an optional card required only if IOPT(1)=1. The first entry on the card is the number of categories; it is followed by the lower limit for each category (g/m^3), in increasing order. The upper limit of all categories is assumed to be infinite. The fourth control card contains information on the overall efficiencies and latent heat release fractions associated with the various cooling system types.

The climatological data input starts with the fifth card. NS, NU, and KSTAB are the number of wind direction sectors, wind speed and atmospheric stability categories, respectively. The final entry on this card is an average temperature (°K) for use in plume rise computations. This parameter is not necessary unless cooling towers are simulated.

If a limited set of atmospheric conditions is being examined and IOPT(2)=1, a card is required which specifies the number of climatological data cards to follow. If IOPT(2)=0, BATMAN computes NDC = NS x NU.

Next, the climatological data cards are read in. Each card consists of a wind direction sector, wind speed (m/s), and the frequency of occurrence (%) for each stability category with the given direction and speed. These cards are followed by a card containing the number of hours in the period being considered (8766 if annual averages are desired).

The final climatological card contains information on the climatology of saturation deficits and is needed only if IOPT(3)=1. The data on this card are the hours available for the formation of fog in each of the saturation deficit classes defined by the limits on card 3. The lower limit of the first class is assumed to be zero and the divisions between successive

classes are defined by the values of XLIM(I). If this card is used, there must be available hours for a total of NXLIM classes.

The four cards that follow define the computational grid and the individual cluster plume characteristics. The first card of the group determines the number of computational levels in the vertical (NZ) and establishes the height of each level Z(I). It is not necessary to define more than 1 level for computations. The second card sets the angular width of the plume (in degrees), establishes the height of the limit on vertical dispersion, ZLID(m), and sets a critical wind speed UBC, (m/s) which limits the rise of cooling tower plumes. If ZLID is zero, the plume is permitted to rise to the full height estimated in Subroutine PRISE and vertical dispersion is unlimited. If the wind speed exceeds UBC in any case, the plume rise for that case is set to zero and downwash and wake corrections are made. The following card establishes the grid spacing. XSPACE is the north-south spacing and YSPACE is the east-west spacing. It is not necessary that XSPACE and YSPACE be the same, however the computer output has approximately equal spacing in the two directions. The values of XSPACE and YSPACE should be large compared to the characteristic horizontal dimensions of the cooling systems simulated. The final card in this group is a plume rise correction factor to account for additional plume rise resulting from the release of latent heat. A value of 3 has been used for this factor.

The last group of 3 card types defines the case being simulated. This group must be repeated NCASES times. The first card in the group is a heading card which describes the case being simulated, and the second card gives the number of sources (clusters) in the case. The final card type is the source description. The information on this card includes the number of reactors in the cluster, the type cooling system and

its position in grid coordinates, the rated output of the reactor in MW_e, the moisture release height (m), and a characteristic horizontal dimension for the cluster. One card of this type is required for each cluster in the case. If a cluster uses two cooling system types, each must be described on a separate card. In this case the positions may be superimposed on one another.

Figures A2 and A3 give sample data decks for use with BATMAN. These Figures are followed by a complete listing of the BATMAN Code.

```
NCASES          2
IOPT        1
FFF/FQ  AN .333 .800 .3201.260 .333 .800 .333 .600 .320 .963
CLIMATE P    16    5    4       285.
NDC             1
DATA WNW/7   13 6.93             3.45
NHOURS      3766
LEVELS          7    .  50. 100. 200. 300. 400. 500.
ANG/LID/UC  22.5  500.      3.0
SPACING   8000.  8000.
CF              3.
CASE A     4 REACTORS      SITE 1     LOW TOWERS     WNW/7  MOD STABLE
NSITES          1
SITE 1          4    1       6.1        7.5     1250.        25.      1609.
CASE B     20 REACTORS  SITES 1-5    LOW TOWERS      WNW/7   MOD STABLE
NSITES          5
SITE 1          4    1       6.1        7.5     1250.        25.      1609.
SITE 2          4    1       5.5        7.2     1250.        25.      1609.
SITE 3          4    1       4.7        6.7     1250.        25.      1609.
SITE 4          4    1       3.7        5.4     1250.        25.      1609.
SITE 5          4    1       3.7        4.9     1250.        25.      1609.
```

FIGURE A2. A Sample Input Data Deck for Computation of Increases in Water Vapor Density

```
NCASES          1
IOPT       1 1
XLIM            8  .05  .50 1.00 1.50 2.00 3.00 4.00 5.00
EFF/FQ  AN .333 .800 .3201.260 .333 .800 .333 .600 .320 .963
CLIMATE P     16    5    4      285.
ANNUAL   1     1  .67  .42  .51  .34  .07
ANNUAL   2     1 2.46  .79  .35  .28  .04
ANNUAL   3     1 4.47  .40  .21  .17  .01
ANNUAL   4     1 6.93  .21  .15  .10  .00
ANNUAL   5     1 9.61  .05  .05  .02  .00
ANNUAL   6     2  .67  .49  .66  .35  .07
ANNUAL   7     2 2.46  .73  .39  .21  .04
ANNUAL   8     2 4.47  .29  .12  .15  .00
ANNUAL   9     2 6.93  .11  .06  .06  .00
ANNUAL  10     2 9.61  .04  .04  .02  .00
ANNUAL  11     3  .67  .27  .49  .27  .04
ANNUAL  12     3 2.46  .45  .27  .18  .03
ANNUAL  13     3 4.47  .11  .07  .09  .00
ANNUAL  14     3 6.93  .03  .02  .03  .00
ANNUAL  15     3 9.61  .01  .01  .01  .00
ANNUAL  16     4  .67  .33  .57  .34  .07
ANNUAL  17     4 2.46  .47  .32  .21  .03
ANNUAL  18     4 4.47  .08  .07  .10  .00
ANNUAL  19     4 6.93  .01  .01  .04  .00
ANNUAL  20     4 9.61  .00  .00  .01  .00
ANNUAL  21     5  .67  .27  .65  .46  .07
ANNUAL  22     5 2.46  .45  .36  .30  .04
ANNUAL  23     5 4.47  .07  .09  .13  .00
ANNUAL  24     5 6.93  .00  .01  .02  .00
ANNUAL  25     5 9.61  .00  .00  .00  .00
```

FIGURE A3. A Sample Input Data Deck for Computation of Increases in Fog

Figure A3 (continued)

ANNUAL	26	6	.67	.29	.65	.63	.13
ANNUAL	27	6	2.46	.53	.47	.50	.09
ANNUAL	28	6	4.47	.14	.13	.27	.03
ANNUAL	29	6	6.93	.02	.04	.10	.01
ANNUAL	30	6	9.61	.00	.02	.02	.00
ANNUAL	31	7	.67	.14	.30	.36	.08
ANNUAL	32	7	2.46	.30	.27	.34	.09
ANNUAL	33	7	4.47	.10	.13	.29	.06
ANNUAL	34	7	6.93	.03	.07	.18	.02
ANNUAL	35	7	9.61	.01	.04	.07	.01
ANNUAL	36	8	.67	.12	.30	.34	.08
ANNUAL	37	8	2.46	.34	.26	.33	.09
ANNUAL	38	8	4.47	.11	.13	.17	.03
ANNUAL	39	8	6.93	.04	.11	.12	.01
ANNUAL	40	8	9.61	.03	.13	.13	.00
ANNUAL	41	9	.67	.09	.20	.26	.07
ANNUAL	42	9	2.46	.34	.22	.29	.07
ANNUAL	43	9	4.47	.25	.23	.20	.02
ANNUAL	44	9	6.93	.13	.23	.17	.01
ANNUAL	45	9	9.61	.16	.45	.28	.00
ANNUAL	46	10	.67	.11	.23	.30	.06
ANNUAL	47	10	2.46	.37	.31	.39	.10
ANNUAL	48	10	4.47	.41	.40	.40	.05
ANNUAL	49	10	6.93	.40	.49	.42	.01
ANNUAL	50	10	9.61	.60	.96	.53	.00
ANNUAL	51	11	.67	.09	.18	.28	.07
ANNUAL	52	11	2.46	.27	.29	.52	.15
ANNUAL	53	11	4.47	.38	.44	.86	.12
ANNUAL	54	11	6.93	.49	.63	.86	.04
ANNUAL	55	11	9.61	.56	.71	.47	.00

Figure A3 (continued)

```
ANNUAL  56   12  .67  .11  .33  .51  .12
ANNUAL  57   12 2.46  .29  .40 1.03  .25
ANNUAL  58   12 4.47  .22  .48 1.71  .26
ANNUAL  59   12 6.93  .19  .55 1.25  .10
ANNUAL  60   12 9.61  .16  .29  .23  .01
ANNUAL  61   13  .67  .10  .36  .48  .09
ANNUAL  62   13 2.46  .34  .57 1.22  .23
ANNUAL  63   13 4.47  .43  .86 2.85  .34
ANNUAL  64   13 6.93  .51 1.13 3.45  .28
ANNUAL  65   13 9.61  .46 1.38 1.24  .04
ANNUAL  66   14  .67  .21  .58  .65  .12
ANNUAL  67   14 2.46  .77 1.05 1.36  .22
ANNUAL  68   14 4.47 1.01 1.36 2.52  .59
ANNUAL  69   14 6.93  .79 1.06 2.66  .81
ANNUAL  70   14 9.61 1.05 1.56 1.39  .12
ANNUAL  71   15  .67  .24  .70  .56  .13
ANNUAL  72   15 2.46  .80  .73  .94  .17
ANNUAL  73   15 4.47  .39  .33  .73  .20
ANNUAL  74   15 6.93  .07  .11  .24  .07
ANNUAL  75   15 9.61  .01  .02  .02  .00
ANNUAL  76   16  .67  .43  .72  .57  .10
ANNUAL  77   16 2.46  .89  .57  .54  .09
ANNUAL  78   16 4.47  .36  .21  .27  .02
ANNUAL  79   16 6.93  .12  .10  .11  .00
ANNUAL  80   16 9.61  .02  .04  .01  .00
NHOURS      8766
AHOURS  AN  84.27 630.87 575.15 483.43 419.25 756.5  666.14 563.51
LEVELS        1   0.
ANG/LID/UC  22.5  500.00   3.
SPACING   8000.  8000.
CF            3.
CASE 12   40 REACTORS    SITES 1-7,9-11      ANNUAL CLIMATOLOGY  SHORT TOWERS
```

Figure A3 (continued)

NSITES	10						
SITE 1	4	1	6.1	7.5	1250.	25.	1609.
SITE 2	1	1	5.5	7.2	1250.	25.	1609.
SITE 3	1	1	4.7	6.7	1250.	25.	1609.
SITE 4	1	1	3.7	5.4	1250.	25.	1609.
SITE 5	1	1	3.7	4.9	1250.	25.	1609.
SITE 6	1	1	4.2	4.2	1250.	25.	1609.
SITE 7	1	1	3.3	4.0	1250.	25.	1609.
SITE 9	1	1	2.6	4.4	1250.	25.	1609.
SITE 10	1	1	3.1	4.5	1250.	25.	1609.
SITE 11	1	1	6.1	5.9	1250.	25.	1609.

```
      PROGRAM BATMAN(INPUT,OUTPUT,TAPE5=INPUT,TAPE6=OUTPUT)
      DIMENSION NUNITS(20),KTYPE(20),POS(20,2),QE(20),HO(20),W(20),
     +    QT(20),QR(20),QL(20),QS(20),DV(20,2),VPOS(20,16,2),
     +   IDIR(96),UBAR(96),FREQ(96,7),
     +    Z(10),CHI(10),XLIM(10),IOPT(10),TYPE(7),
     +    HEAD(10),AHOURS(10),
     +    QWR(20),QW(20),EFF(7),FQ(7),
     +    XTOTAL(12,12,20)
      KASE = 0
      READ (5,10023) NCASES
      PRINT 10050,NCASES
10050 FORMAT(1H1,10X,*NCASES CONSIDERED*,I8)
      PRINT 10007
      READ(5,10020) IOPT
10020 FORMAT(10X,10I1)
      GO TO (10,20) IOPT(1)+1
   10 PRINT 10021
10021 FORMAT(1H0,10X,*OUTPUT CONCENTRATION INCREASES*)
      GO TO 30
   20 PRINT 10022
10022 FORMAT(1H0,10X,*OUTPUT HOURS OF CONCENTRATION INCREASE*)
      READ(5,10023) NXLIM,(XLIM(I),I=1,10)
10023 FORMAT(10X,I5,13F5.2)
      PRINT 10024,NXLIM,(XLIM(I),I=1,NXLIM)
10024 FORMAT(1H ,10X,I5,' CONCENTRATION INCREASE LOWER LIMITS (G/M**3)
     +ARF',10F6.2)
   30 CONTINUE
      TYPE(1)=10H LOW  TOWER
      TYPE(2)=10H      POND
      TYPE(3)=10HTALL  TOWER
      TYPE(4)=10H    H TOWER
      TYPE(5)=10H    H POND
      TYPE(6)=10H      RIVER
```

FIGURE A4. BATMAN Computer Code

Figure A4 (continued)

```
      READ(5,10001) EFF(1),FQ(1),EFF(2),FQ(2),EFF(3),FQ(3),EFF(4),FQ(4),
     +    EFF(5),FQ(5),EFF(6),FQ(6),EFF(7),FQ(7)
10001 FORMAT(10X,14F5.3)
      PRINT 10009
10009 FORMAT(1H0,10X,*COOLING TYPE   EFFICIENCY  LATENT FRACTION*)
      DO 115 I=1,7
      PRINT 10010, TYPE(I),EFF(I),FQ(I)
10010 FORMAT(1H ,10X,A10,8X,F5.3,11X,F5.3)
  115 CONTINUE
C     INPUT CLIMATOLOGICAL DATA
      READ(5,10011) NS,NU,KSTAB,T
10011 FORMAT(10X,3I5,5F10.0)
      PRINT 10044,NS,NU,KSTAB,T
10044 FORMAT(1H ,10X,*CLIMATOLOGICAL PARAMETERS *,I5,2I5,F10.0)
      C1=6.2832/NS
      NDC=NS*NU
      IF(IOPT(2).EQ.1) READ (5,10023) NDC
      DO 120 I=1,NDC
      READ(5,10023)IDIR(I),UBAR(I),(FREQ(I,J),J=1,KSTAB)
10012 FORMAT(10X,10F7.2)
      DO 119 J=1,KSTAB
  119 FREQ(I,J)=FREQ(I,J)/100
      PRINT 10045,IDIR(I),UBAR(I),(FREQ(I,J),J=1,KSTAB)
10045 FORMAT(11X,*CLIMATOLOGICAL DATA *,I5,F7.2,7F8.4)
  120 CONTINUE
      READ(5,10023) NHOURS
      PRINT 10025,NHOURS
10025 FORMAT(1H ,10X,*TOTAL NUMBER OF HOURS =*,I6)
      IF(IOPT(3).EQ.1) READ(5,10012) (AHOURS(IH),IH=1,NXLIM)
      READ(5,10026) NZ,(Z(I),I=1,10)
10026 FORMAT(10X,I5,13F5.0)
      PRINT 10027,NZ,(Z(I),I=1,NZ)
```

Figure A4 (continued)

```
10027 FORMAT(1H ,10X,*CONCENTRATION COMPUTED AT*,I5,* LEVELS, (IN METERS
     +)*,10F6.0)
      IF(NXLIM*NZ-19) 50,50,40
   40 PRINT 10028
10028 FORMAT(1H1,10X,*TOO MANY CONCENTRATION GROUPS AND LEVELS*)
      GO TO 20000
   50 CONTINUE
      C2=.017453
C     INPUT LIMITS ON PLUME SPREAD, VERTICAL DISPERSION AND WAKE EFFECTS
      READ(5,10012)ANG,ZLID,UBC
      ANGR=ANG*C2
      CANG=COS(ANGR/2)
      TANG=TAN(ANGR/2)
      SANG=CANG*TANG
      PRINT 10013,ANG,ANGR
10013 FORMAT(1H ,10X,*ANGULAR WIDTH OF PLUMES IS*,F7.2* DEGREES/*,F7.4,
     +    * RADIANS*)
      IF(ZLID.GT.0) PRINT 10014,ZLID
10014 FORMAT(11X,*VERTICAL DISPERSION IS LIMITED BY A LID AT *,F7.0,
     +    * METERS*)
      IF(ZLID.LE.0) PRINT 10015
10015 FORMAT(11X,*VERTICAL DISPERSION IS NOT LIMITED BY A LID*)
      PRINT 10016,UBC
10016 FORMAT(11X,*DOWNWASH AND WAKE EFFECTS ARE ASSUMED FOR WIND SPEEDS
     +ABOVE *,F5.1,* M/S*)
C     INPUT GRID SPACING
      READ(5,10012) XSPACE,YSPACE
      PRINT 10017,XSPACE,YSPACE
10017 FORMAT(1H ,10X,*NORTH-SOUTH GRID SPACING  ,F7.0,  METERS, EAST-WEST
     + GRID SPACING*,F7.0,* METERS*)
C     INPUT PLUME RISE CORRECTION FACTOR
      READ(5,10012) CF
      PRINT 10018,CF
```

Figure A4 (continued)

```
10018 FORMAT(1H ,10X,*PLUME RISE CORRECTION FACTOR FROM CLOUD MODEL IS*,
     +    F10.3)
C     INPUT OF REACTOR COMPLEX DATA
    5 CONTINUE
      KASE=KASE+1
      READ(5,10000) HEAD
10000 FORMAT(10A8)
      PRINT 10019,HEAD
10019 FORMAT(1H1,10X,10A8)
      PRINT 10007
      PRINT 10007
      READ(5,10002) NSITES
10002 FORMAT(10X,14I5)
      IF(NSITES.LE.20) GO TO 100
      PRINT 10003
10003 FORMAT(1H0,10X,*TOO MANY SITES*)
      GO TO 20000
  100 CONTINUE
      DO 105 I=1,NSITES
      READ(5,10004)NUNITS(I),KTYPE(I),POS(I,1),POS(I,2),QE(I),HO(I),W(I)
10004 FORMAT(10X,2I5,6F10.2)
      K=KTYPE(I)
      IF(K.EQ.6) GO TO 101
      QT(I)=QE(I)/EFF(K)
      QR(I)=QT(I)-QE(I)
      QL(I)=QR(I)*FQ(K)
      QS(I)=QR(I)-QL(I)
      QW(I)=NUNITS(I)*QL(I)*400
      GO TO 105
  101 CONTINUE
      QWR(I)=0.
      QL(I)=(NUNITS(I)/4)*QE(I)*W(I)*W(I)*.0007854
      QWR(I)=QL(I)/2.5
```

Figure A4 (continued)

```
      QE(I)=0.
      QS(I)=0.
      QR(I)=0.
  105 CONTINUE
      PRINT 10005,NSITES
10005 FORMAT(1H0,10X,*THIS RUN CONSIDERS *,I5,* REACTOR COMPLEXES*)
      PRINT 10006
10006 FORMAT(1H0,10X,*SITE  UNITS   XPOS   YPOS     TYPE     HEIGHT  WID
     +TH   QT      QE      QR      QL      QS      QW *)
      PRINT 10007
10007 FORMAT(1H )
      DO 110 I=1,NSITES
      K=KTYPE(I)
      QW1=QW(I)/1000
      IF(K.EQ.6) QW1=QWR(I)
      PRINT 10008,I,NUNITS(I),POS(I,1),POS(I,2),TYPE(K),H0(I),W(I),QT(I)
     +    ,QE(I),QR(I),QL(I),QS(I),QW1
10008 FORMAT(11X,I4,I7,2F7.2,2X,A10,F8.1,7F7.0)
  110 CONTINUE
C     COMPUTE DISTANCE TO VIRTUAL SOURCE FOR EACH COMPLEX AND DETERMINE
C     VIRTUAL SOURCE POSITION AS A FUNCTION OF WIND DIRECTION
      DO 130 I=1,NSITES
      DV(I,1)=W(I)/(2*TANG)
      DV(I,2)=DV(I,1)*DV(I,1)
      POS(I,1)=XSPACE*(POS(I,1)-1)
      POS(I,2)=YSPACE*(POS(I,2)-1)
      DO 125 J=1,NS
      D=J*C1
      VPOS(I,J,1)=POS(I,1)-DV(I,1)*COS(D)
      VPOS(I,J,2)=POS(I,2)+DV(I,1)*SIN(D)
10040 FORMAT(1H ,10X,*DISTANCE TO VIRTUAL SOURCE, REAL AND VIRTUAL SOURC
     +E COORDINATES*,5F10.0)
  125 CONTINUE
```

Figure A4 (continued)

```
  130 CONTINUE
C     COMPUTE INCREASE IN CONCENTRATION
      I3=0
      DO 5000 ID=1,NS
      DO 4000 IU=1,NU
      I3=I3+1
      DO 3000 IS=1,KSTAB
      IF(FREQ( I3  ,IS).LE.0) GO TO 3000
      DO 2000 IC=1,NSITES
      PR=0.0
      IF(HO(IC).LE.0.) GO TO 135
      IF(UBAR(IU).LE.UBC)
     +    CALL PRISE(KSTAB,IS,UBAR(IU),T,HO(IC),QS(IC),CF,PR),RETURNS(90
     +00)
      IF(PR.GE.ZLID) PR=ZLID-HO(IC)
  135 CONTINUE
      HE=HO(IC)+PR
10029 FORMAT(1H ,10X,*PLUME RISE AND EFFECTIVE RELEASE HEIGHT ARE (METER
     +S)*,2F10.0)
      IF(ZLID.GT.0.AND.HE.GT.ZLID) GO TO 2000
      DO 1000 IX=1,12
      XR=(IX-1)*XSPACE
      DO 999 IY=1,12
      YR=(IY-1)*YSPACE
      I2=IDIR(I3)
      CALL RCPTOR(POS(IC,1),POS(IC,2),VPOS(IC,I2,1),VPOS(IC,I2,2),XR,YR,
     +    CANG,DV(IC,1),DV(IC,2),DR),RETURNS(999)
10030 FORMAT(1H ,10X,*SITE NUMBER, RECEPTOR POSITION AND VIRTUAL DISTANC
     +E ARE *,3I6,F10.0)
      IF(KSTAB.GE.6) ICT=KTYPE(IC)
      IF(KSTAB.EQ.4) ICT=KTYPE(IC)+7
      ISW= 5.2832/ANGR+.5
      IF(KTYPE(IC).EQ.6) QW(IC)=QWR(IC)*UBAR(IU)
```

Figure A4 (continued)

```
      CALL DIFFUSE(ISW,IS,UBAR(IU),                    UBC,DR,ZLID,HE,QW(IC),
     +     ICT,NZ,Z,CHI)
      DO 200 IZ=1,NZ
      XTOTAL(IX,IY,IZ)=CHI(IZ)+XTOTAL(IX,IY,IZ)
      CHI(IZ)=0
  200 CONTINUE
  999 CONTINUE
 1000 CONTINUE
 2000 CONTINUE
      HOURS=FREQ(  I3  ,IS)*NHOURS
      GO TO (5000,2100),IOPT(1)+1
 2100 CONTINUE
      DO 2230 IX=1,12
      DO 2220 IY=1,12
      DO 2210 IZ=1,NZ
      DO 2200 IL=1,NXLIM
      IIZ=IL*NZ+IZ
      IF(XTOTAL(IX,IY,IZ).GE.XLIM(IL)) XTOTAL(IX,IY,IIZ)=
     +   XTOTAL(IX,IY,IIZ) + HOURS
 2200 CONTINUE
 2210 XTOTAL(IX,IY,IZ)=0.0
 2220 CONTINUE
 2230 CONTINUE
 3000 CONTINUE
 4000 CONTINUE
 5000 CONTINUE
      GO TO (5100,6000) IOPT(1)+1
 5100 CONTINUE
      DO 5120 IZ=1,NZ
      PRINT 11000,Z(IZ)
11000 FORMAT(1H1,10X,'INCREASE IN MOISTURE (G/M**3) AT Z  = ', F7.0,
     +     ' METERS')
      DO 5110 IX=1,12
```

Figure A4 (continued)

```
      PRINT 11001,(XTOTAL(IX,IY,IZ),IY=1,12)
11001 FORMAT(1H0,10X,12F10.2)
      DO 5105 IY=1,12
 5105 XTOTAL(IX,IY,IZ)=0.
      PRINT 11003
11003 FORMAT(1H0)
 5110 CONTINUE
      PRINT 11002,HOURS
11002 FORMAT(1H0, 10X,*THIS CONDITION OCCURS AN AVERAGE OF *,F7.0,* HOUR
     +S PER YEAR*)
 5120 CONTINUE
      GO TO 20000
 6000 CONTINUE
      DO 6030 IZ=1,NZ
      DO 6020 IL=1,NXLIM
11010 FORMAT(1H1,10X,'NUMBER OF HOURS THAT THE INCREASE IN MOISTURE AT Z
     + = ',F7.0,' METERS EQUALED OR EXCEEDED ', F7.2,' G/M**3')
      PRINT 11010,Z(IZ),XLIM(IL)
      IIZ=IL*NZ+IZ
      DO 6010 IX=1,12
      PRINT 11004,(XTOTAL(IX,IY,IIZ),IY=1,12)
11004 FORMAT(1H0,10X,12F7.1)
      PRINT 11003
      IF(IOPT(3).EQ.1) GO TO 6010
      DO 6025 IY=1,12
 6025 XTOTAL(IX,IY,IIZ)=0.
 6010 CONTINUE
      IF(IOPT(3).NE.1) GO TO  6020
      DO 6012 IX=1,12
      DO 6011 IY=1,12
      XTOTAL(IX,IY,IZ)=XTOTAL(IX,IY,IZ)+AHOURS(IL)*XTOTAL(IX,IY,IIZ)
     +     /NHOURS
      XTOTAL(IX,IY,IIZ)=0.
```

Figure A4 (continued)

```
 6011 CONTINUE
 6012 CONTINUE
 6020 CONTINUE
      IF(IOPT(3).NE.1) GO TO  6030
      PRINT 11005,Z(IZ)
11005 FORMAT(1H1,10X,*INCREASE IN NUMBER OF HOURS OF FOG AT*,F6.0,
     +    *  METERS*)
      DO 6015 IX=1,12
      PRINT 11004,(XTOTAL(IX,IY,IZ),IY=1,12)
      PRINT 11003
      DO 6014 IY=1,12
      XTOTAL(IX,IY,IZ)=0.
 6014 CONTINUE
 6015 CONTINUE
 6030 CONTINUE
      GO TO 20000
 9000 PRINT 12000
12000 FORMAT(1H ,10X,*TOO FEW STABILITY CLASSES IN SUBROUTINE PRISE*)
20000 CONTINUE
      IF(KASE.LT.NCASES) GO TO  5
      END
```

Figure A4 (continued)

```
      SUBROUTINE PRISE(KSTAB,KSTB,UBAR,T,HO,QS,CF,PR),RETURNS(A1)
C     SUBROUTINE PRISE COMPUTES FINAL PLUME RISE USING BRIGGS 1969
C     FORMULAE.  IF UBAR IS LESS THAN 1 M/S THE CALM EQN IS USED FOR
C     STABLE CONDITIONS OR UBAR IS SET EQUAL TO .5 M/S IN UNSTABLE AND
C     NEUTRAL CONDITIONS. INPUT IN METRIC UNITS, QS IN MW. PLUME RISE IS
C     CORRECTED FOR LATENT HEAT USING RESULTS OF COMPARISON WITH A 1-D
C     CUMULUS CLOUD MODEL.
      FB=8.9*QS
      GO TO (100,100,100,10,100,11,12), KSTAB
   10 GO TO (21,21,31,32),KSTB
   11 GO TO (21,21,21,21,31,32),KSTB
   12 GO TO (21,21,21,21,31,32,33),KSTB
   21 IF(UBAR-.5) 22,23,23
   22 U=.5
      GO TO 24
   23 U=UBAR
   24 PR=(1.6/U)*(100*HO*HO*FB)**(1./3.)*CF
      GO TO 200
   31 S=.049/T
      GO TO 40
   32 S=.27/T
      GO TO 40
   33 S=.49/T
   40 CONTINUE
      IF(UBAR-1) 50,60,60
   50 PR=5.0*(FB*FB/(S*S*S))**(1./8.)*CF
      GO TO 200
   60 PR=2.9*(FB/(UBAR*S))**(1./3.)*CF
      GO TO 200
  100 RETURN A1
  200 RETURN
      END
```

Figure A4 (continued)

```
      SUBROUTINE RCPTOR(X0,Y0,XV,YV,XR,YR,CANG,DV,DV2,DR),
     +RETURNS(A)
C     SUBROUTINE RCPTOR DETERMINES IF A RECEPTOR IS IN A PLUME AND
C     COMPUTES THE DISTANCE FROM A VIRTUAL SOURCE POINT IF IT IS. INPUTS
C     INCLUDE POSITIONS OF THE REAL AND VIRTUAL SOURCE AND RECEPTOR, THE
C     COSINE OF 1/2 THE ANGULAR WIDTH OF THE PLUME, AND THE DISTANCE
C     FROM THE REAL TO VIRTUAL SOURCE. IF THE RECPTOR IS NOT IN THE
C     PLUME, THE SUBROUTINE RETURN SKIPS FURTHER CONSIDERATION OF THE
C     RECPTOR.
10000 FORMAT(11X,*RECPTOR*,6F10.0,F10.5,2F10.0)
      D2=(XR-X0)*(XR-X0)+(YR-Y0)*(YR-Y0)
      IF(DV) 20,20,5
    5 CONTINUE
      DR2=(XR-XV)*(XR-XV)+(YR-YV)*(YR-YV)
      IF(DR2-D2) 20,20,10
   10 IF(DR2-DV2)  20,20,15
   15 DR=SQRT(DR2)
      RANG=(D2-DR2-DV2)/(-2*DV*DR)
10001 FORMAT(11X,*RCPTOR COMPUTATIONS *,F10.0,F10.5)
      IF(RANG-CANG) 20,30,30
   20 RETURN A
   30 CONTINUE
      RETURN
      END
```

Figure A4 (continued)

```
      SUBROUTINE DIFFUSE(NS,KSTB,UBAR,     UBC,DR,ZLID,H,Q,ICT,NZ,Z,CHI)
C     SUBROUTINE DIFFUSF PERFORMS DIFFUSION COMPUTATIONS USING A SECTOR
C     AVERAGED GAUSSIAN PLUME MODEL WITH COMPLETE REFLECTION AT GROUND
C     LEVEL.  A REFLECTING LID IS OPTIONAL.  THE SOURCE MAY BE ELEVATED
C     OR AT GROUND LEVEL. THE RELEASE HEIGHT IS ASSUMED TO BE BELOW THE
C     LID.  ALL REFLECTION TERMS CONTRIBUTING LESS THAN .25 PERCENT OF
C     THE DOMINANT TERM TO CHI/Q ARE NEGLECTED. WHEN ZLID/SIGMAZ IS LESS
C     THAN I.5, A UNIFORM VERTICAL CONCENTRATION IS ASSUMED.  TEN LEVELS
C     CAN BE TREATED, IF A LEVFL IS ABOVE THE LID THE CONCENTRATION IS
C     ZERO. THE BASIC SECTOR AVERAGE MODEL IS DESCRIBE IN SECTION 3-3 OF
C     M+AE-1968. TREATMENT OF REFLECTION IS BASED ON SECTION 6.6 OF TEXT
C     BY CSANADY, 1973
      DIMENSION Z(10),CHI(10)
C     OBTAIN SIGMAZ ESTIMATF
      CALL SIGMAZ(KSTB,UBAR,UBC,H,ICT,DR,SZ,SZ2)
10000 FORMAT(11X,*STAB.CLASS,WIND SPEED,RELEASE HEIGHT,ICT,DISTANCE,AND
     + SIGMAZ ARE*,I5,F6.2,F5.0,I5,F7.0,F6.2)
      DNM= -2*SZ2
      COEF=(.0635*NS)/(DR*SZ*UBAR)
C     IS THERE A LID, IF SO GO TO 30
      IF(ZLID) 10,10,30
C     NO LID
C     ELEVATED RELEASE, IF SO GO TO 20
   10 IF(H) 11,11,20
C     COMPUTE CHI/Q FOR GROUND LEVEL SOURCE WITHOUT LID
   11 DO 15 I=1,NZ
      IF(Z(I)) 12,12,13
   12 CHI(I)=2*COEF
      GO TO 15
   13 CHI(I)=2*COEF*EXP(Z(I)*Z(I)/DNM)
   15 CONTINUE
C     GO TO 300 TO COMPUTE CHI
      GO TO 300
```

Figure A4 (continued)

```
C       COMPUTE CHI/Q FOR ELEVATED SOURCE WITHOUT LID
   20 DO 25 I=1,NZ
      IF(Z(I)) 21,21,22
   21 CHI(I)=2*COEF*EXP(H*H/DNM)
      GO TO 25
   22 E1=EXP((Z(I)-H)**2/DNM)
      IF(Z(I)*H/SZ2-2.9957) 24,23,23
   23 CHI(I)=COEF*E1
      GO TO 25
   24 CHI(I)=COEF*(E1+EXP((Z(I)+H)**2/DNM))
   25 CONTINUE
      GO TO 300
C       THERE IS A LID
   30 RO=ZLID/SZ
      RO2=RO*RO
C       IS THERE   UNIFORM CONCENTRATION IN THE VERTICAL IF NOT GO TO 50
      IF(RO-1.5) 40,40,50
   40 DO 45 I=1,NZ
      IF(Z(I)-ZLID) 42,42,41
   41 CHI(I)=0
      GO TO 45
   42 CHI(I)=2.507*COEF*RO
   45 CONTINUE
      GO TO 300
C       IS THE SOURCE ELEVATED, IF SO GO TO 110
   50 IF(H) 55,55,110
C       COMPUTE CHI/Q FOR GROUND LEVEL SOURCE WITH LID
   55 DO 100 I=1,NZ
      IF(Z(I)-ZLID) 59,59,56
   56 CHI(I)=0
      GO TO 100
   59 IF(Z(I)) 60,60,80
   60 IF(1.73-RO) 65,65,70
```

Figure A4 (continued)

```
   65 CHI(I)=2*COEF
      GO TO 100
   70 CHI(I)=2*COEF*(1+EXP(-2*R02))
      GO TO 100
   80 R1=Z(I)/SZ
      R1R0=R1*R0
      E1=EXP(-R1*R1/2)
      IF(R02-R1R0-2.9957) 81,90,90
   81 E1=E1+EXP((Z(I)-2*ZLID)**2/DNM)
      IF(R2+R1R0-2.9957) 85,90,90
   85 E1=E1+EXP((Z(I)+2*ZLID)**2/DNM)
   90 CHI(I)=COEF*E1
  100 CONTINUE
      GO TO 300
C     COMPUTE CHI/Q FOR ELEVATED SOURCE WITH LID
  110 R2=H/SZ
      R2R0=R2*R0
      DO 180 I=1,NZ
      IF(Z(I)-ZLID) 119,119,115
  115 CHI(I)=0
      GO TO 180
  119 IF(Z(I)) 120,120,140
  120 E1=EXP(-R2*R2/2)
      IF(R02-R2R0-2.9957) 121,130,130
  121 E1=E1+EXP((H-2*ZLID)**2/DNM)
      IF(R02+R2R0-2.9957) 125,130,130
  125 E1=E1+EXP((H+2*ZLID)**2/DNM)
  130 CHI(I)=2*COEF*E1
      GO TO 180
  140 R1=Z(I)/SZ
      R1R0=R1*R0
      R1R2=R1*R2
      E1=EXP((Z(I)-H)**2/DNM)
```

Figure A4 (continued)

```
      IF(R1R2-2.9957) 141,145,145
  141 E1=E1+EXP((Z(I)+H)**2/DNM)
  145 IF(R02+R1R2-R1R0-R2R0-2.9957) 146,170,170
  146 ZL2=2*ZLID
      E1=E1+EXP((Z(I)+H-ZL2)**2/DNM)
      IF(R02+R2R0-R1R0-2.9957) 150,151,151
  150 E1=E1+EXP((Z(I)-H+ZL2)**2/DNM)
  151 IF(R02+R1R0-R2R0-2.9957) 155,156,156
  155 E1=E1+EXP((Z(I)-H-ZL2)**2/DNM)
  156 IF(R02+R1R0+R2R0+R1R2-2.9957) 160,161,161
  160 E1=E1+EXP((Z(I)+H+ZL2)**2/DNM)
  161 IF(2*R02+R1R2/2-R1R0-R2R0-2.9957) 165,170,170
  165 E1=E1+EXP((Z(I)+H-4*ZLID)**2/DNM)
  170 CHI(I)=COEF*E1
  180 CONTINUE
C     COMPUTE CHI(Z) FROM CHI(Z)/Q AND Q
  300 DO 310 I=1,NZ
      CHI(I)=CHI(I)*Q
  310 CONTINUE
      RETURN
      END
```

Figure A4 (continued)

```
      SUBROUTINE SIGMAZ(KSTB,UBAR,UBC,H,ICT,DR,SZ,SZ2)
C     SUBROUTINE SIGMAZ COMPUTES AN ESTIMATE OF SIGMA Z USING BRIGGS
C     RELATIONSHIPS. SIGMA Z IS A FUNCTION OF DISTANCE AND STABILITY.
C     FOR HIGH WIND SPEEDS AND COOLING TOWER PLUMES A CORRECTION FACTOR
C     IS ADDED TO SIGMA Z TO ACCOUNT FOR WAKE EFFECTS.
      GO TO (10,11,10,10,11,11,10,12,12,12,12,12,12,12),ICT
   10 GO TO (21,22,23,24,25,26,27),KSTB
   11 GO TO (21,22,23,24,25,26,26),KSTB
   12 GO TO (22,24,25,26),KSTB
C     COMPUTE INTIAL SIGMA Z ESTIMATE
   21 SZ=.2*DR
      GO TO 30
   22 SZ=.12*DR
      GO TO 30
   23 SZ=.08*DR/(SQRT(1+.0002*DR))
      GO TO 30
   24 SZ=.06*DR/(SQRT(1+.0015*DR))
      GO TO 30
   25 SZ=.03*DR/(1+.0003*DR)
      GO TO 30
   26 SZ=.02*DR/(1+.0003*DR)
      GO TO 30
   27 SZ=.012*DR/(1+.0003*DR)
   30 GO TO (35,50,50,35,50,50,50,35,50,50,35,50,50,50),ICT
   35 IF(UBAR-UBC)  50,40,40
C     CORRECT SIGMA Z FOR COOLING TOWER WAKE
   40 SZ2=(SZ*SZ+H*H/6.28)
      SZ = SQRT(SZ2)
      GO TO 100
   50 SZ2=SZ*SZ
  100 CONTINUE
      RETURN
      END
```

DISTRIBUTION

No. of
Copies

OFFSITE

1 ERDA Chicago Patent Group

A. A. Churm

1 Aluminum Company of America
Post Office Box 120
Vancouver, WA 98660

Lyman J. Harris
Northwest Area Power Manager

1 Benton County Public Utility District
Post Office Box 6270
Kennewick, WA 99336

Robert W. Blodgett, Manager

1 Bonneville Power Administration
Post Office Box 3621
Portland, OR 97208

C. Ray Foleen
Deputy Administrator

1 Culp, Dwyer, Guterson & Grader
1300 Hoge Building
Seattle, WA 98104

Gordon Culp

1 Electric Power Research Institute
Post Office Box 10412
Palo Alto, CA 94304

Laura Henning

20 Energy Research and Development Administration
Mail Stop F-309
Washington, DC 20545

W. F. Savage, Chief
Advanced Concepts Evaluation Branch

No. of Copies	
27	ERDA Technical Information Center
1	Nuclear Regulatory Commission Washington, DC 20555
1	Pacific Northwest Utilities Conference Committee Post Office Box 1231 Wenatchee, WA 98801 Howard C. Elmore, Chairman
1	Pacific Northwest Utilities Conference Committee on Engineering and Planning 2730 Northwest 77th Place Portland, OR 97213 David J. Lewis, Consultant
1	Portland General Electric Company 621 Southwest Alder Street Portland, OR 97205 A. J. Porter, Vice President
1	Puget Sound Power and Light Company Puget Power Building Post Office Box 535 Bellevue, WA 98004 John W. Ellis, President
1	Jack Criswell, General Manager Springfield Utility Board 250 North "A" Street, Box 300 Springfield, OR 97477
1	National Academy of Public Administration 1225 Connecticut Avenue NW Washington, DC 20036 R. Kloman
2	Washington State Energy Office 1000 South Cherry Olympia, WA 98504 Larry Bradley

No. of
Copies

15 Energy Facility Site Evaluation Council
820 East Fifth Avenue
Olympia, WA 98504

Roger Polzin

ONSITE

8 ERDA Richland Operations Office

O. J. Elgert
P. W. Gottschalk
R. H. Lindsey/G. L. Liffick
F. R. Standerfer
M. W. Tiernan

Research and Development Programs Division

W. A. Burns (2)

40 Battelle-Northwest

D. B. Cearlock
R. L. Conley
D. W. Dragnich
R. F. Foster
J. J. Fuquay
H. Harty (10)
J. V. Ramsdell (10)
A. E. Reisenauer
W. H. Rickard
C. L. Simpson
J. K. Soldat
R. W. Wallace
D. G. Watson
Technical Information (5)
Technical Publications (3)

2 Washington Public Power Supply System

Rodger Woodruff
J. R. Young